Process Modeling and Planning for Robotic Cold Spray Based Additive Manufacturing

Hongjian Wu

THESE DE DOCTORAT DE L'ETABLISSEMENT UNIVERSITE BOURGOGNE FRANCHE-COMTE

PREPAREE A L'UNIVERSITE DE TECHNOLOGIE DE BELFORT-MONTBELIARD

Ecole doctorale n° 37

Sciences physiques pour l'ingénieur et microtechniques - SPIM

Doctorat de Sciences pour l'Ingénieur

Par

Mr. Hongjian WU

Process Modeling and Planning for Robotic Cold Spray Based Additive Manufacturing

Thèse présentée et soutenue à UTBM Site de Sévenans, le 15 Décembre 2020

Composition du Jury :

Mr. Pasquale Daniele CAVALIERE	Professeur, Université de Salento	Rapporteur
Mr. J Paulo Da Silva BARTOLO	Professeur, Université de Manchester	Rapporteur
Mr. Kondo Hloindo ADJALLAH	Professeur, Université de Lorraine	Examinateur (président)
Mr. Hanlin LIAO	Professeur, UTBM	Examinateur
Mr. Sihao DENG	Maître de Conférences-HDR, UTBM	Directeur de thèse
Mr. Rija Nirina RAOELISON	Maître de Conférences UTBM	Codirecteur de thèse

General introduction

Cold gas dynamic spraying or cold spraying is a newly developed solid-state powders deposition technique that allows conversion of powders into a solid coating on substrates. During the deposition process, metal powders are accelerated by high-pressure gas flow through a convergent-divergent de-Laval nozzle at very high velocities. They remain at a temperature below the melting point and impact on a solid surface that results in strong plastic deformation and thus a coating formation. Nowadays, cold spraying is widely used to prepare various functional coatings, to restore damaged metal components and recently to fabricate freestanding 3D metal components. Industrial robots are widely used due to their high stability and highly accurate motion. The robot offline programming technology allows for reducing burden and difficulties of programming, for improving the accuracy that makes the cold spray additive method viable for complex parts.

Recently, both industrial and academic communities are paying more and more attention to cold spray additive manufacturing, especially for the direct manufacturing of soft metal components. In comparison with other additive manufacturing technologies, many advantages make it unique in fabricating freestanding metal components. For example, cold spray processes can deposit temperature-sensitive materials without phase transformation or grain growth. It also can be used for the fabrication of multi-material and gradient deposits, and its high production efficiency is expected to make breakthrough in the field of large parts rapid manufacturing. Today, the latest developments in the cold spray industry require more new methods and processes to improve its manufacturing accuracy, flexibility and reliability, to be more competitive. Therefore, the work of this thesis aims to research new process implementation to enhance cold spray additive manufacturing. For that purpose, our work will mainly focus on robotized cold spraying processes, simulation, and planning under the following organization:

The first chapter mainly introduces the cold spray technology including its basic principle and applications, and foremost, the basic information of industrial robots. Due to their high performance, the industrial robots have widely used in the field of CS to perform all kinds of spraying tasks. As cold spraying is currently extended to the manufacturing of complex 3D parts, it is necessary to develop an auxiliary system specifically to provide an ideal

spraying/deposition strategy. Developed for such a purpose, the RobotStudio™ tool with its software extension TST is introduced in this chapter.

The second chapter proposes a concept of modular system for designing and implementing a new cold spray additive manufacturing framework. In this study, a new cold spray additive manufacturing system is developed based on the conventional cold spray system. At the same time, various different technology and application will be integrated into our current system. This chapter also focuses on decomposing the current cold spray additive manufacturing system into different modules to understand the physical and functional relationships between the key elements of the entire system. This physical and functional modularity is a useful to promote hybrid additive manufacturing processes. According to the different applications and purposes, the current cold spray additive manufacturing system is divided into five modules: spray module, robot module, in-situ measurement module, inter-process module and post-process module. One of our major objectives is to investigate if the modular system is suitable to revolutionize the cold spray additive manufacturing method.

In the next chapter (chapter 3), a new approach for cold spray process and coating thickness simulation will be developed. Generally, in addition to the development of coating structure and performance, the thickness distribution accuracy is also an important requirement particularly for the manufacturing of complex components by cold spraying. Indeed, meeting the requirements of coating thickness distribution is critical for both longevity and performance of the cold sprayed components. This chapter will address a development of simulation method to assess the coating thickness distribution during a cold spray deposition. Our approach will be based on a three-dimensional geometric model using a Gaussian distribution law. This model considers also the relative deposition efficiency depending on different robot kinematic parameters. The next is the implementation of the 3D geometric coating thickness model into the off-line programming software RobotStudio™ as a module of the software TST, so that it could be coupled with robotic trajectories and processing parameters to simulate coating deposition. The prediction capability of the model will be discussed through comparison with several experimental results.

Chapter 4 investigates the development of stable layer-building strategy to enhance the molding ability of cold spray based on the system we develop in the previous chapter. In practice, a major difficulty of the cold spray deposition is the formation of triangle-like deposition profile that acts as reflexion surface and limits thereby the application of cold spray additive manufacturing. Therefore, a stable layer-by-layer building strategy is a major

milestone for producing complex 3D shapes in an additive way by cold spraying. Using the 3D geometric coating thickness model, a series of simulation verification will be carried out over a combination of different parameters. This work aims to find the suitable combination of parameters and they role in determining the layer geometry, and thus on the component built-up process.

The last chapter (Chapter 5) gives a restitution of the various conclusions that supports this method as a potential general additive manufacturing principle making the cold spray assisted by a 3D strategy model, a real layer-by-layer additive manufacturing process for various 3D complex shape. Current limitations will be also addressed with future prospects. Note that an appendix part provides some theoretical considerations related to topology and 3D geometric transformations we use for the coating simulation model.

Content

List of figures

Chapter 1 Introduction

Chapter 2 Design and implementation of modular framework for CSAM

Chapter 3 Cold spray process modeling and simulation

Chapter 4 Stable layer-building strategy to enhance cold spray based additive manufacturing

Annexes

List of tables

Chapter 1

Introduction

1.1 Cold spray technology

In the mid-1980s, a new spraying technique called cold-gas dynamic spraying or cold spraying (CS) was initially developed by a group of scientists from the Institute of Theoretical and Applied Mechanics of the Siberian Branch of the Russian Academy of Sciences (ITAM of RAS) in Novosibirsk, Russia [1,2]. For the modern manufacturing industry, surface technology is important and necessary because it has specific abilities to provide corrosion protection, wear control, damage repair, fouling protection and temperature/oxidation protection, etc. The sprayed coating has excellence performance including structural homogeneity, high density, high purity, notable cohesive strength, and frequently moderate compressive residual stresses. As an emergent technology, CS has many advantages that makes it uniquely competitive among various thermal spraying technologies [1–4]. For example, being a non-thermal or low-temperature process, CS allows spraying thermally sensitive materials without the risk of melting, oxidation, thermal decomposition, crystallization, grain growth, or phase transformations. In addition, the high speed and energy of sprayed particles can provide high deposition efficiency. Therefore, CS has been applied to prepare various functional coatings [2,5,6] and to restore damaged metal components [7–10] as well as to fabricate freestanding metal parts [9–12]. During the deposition process, the spray gun needs to be precisely controlled to achieve the desired coating thickness or the final shape of the deposit. Thus, industrial robots have been widely used in the field of CS due to their high performance, such as high accuracy, high repeatability, high flexibility, etc.

1.1.1 Principle of cold spray

Generally speaking, CS belongs to the wide family of thermal spray technology. As shown in Figure 1.1, due to its low gas temperature and high particle velocity, CS can be separated from other thermal spray processes [2,4]. Figure 1.2 shows a typical CS system which consists of high-pressure compressed gas sources, power sources, a powder feeder, a spray gun and an industrial robot. The gas source is separated into two different gas lines: one is fed to the gas heater as propellant gas and the other is sent to the powder feeder (carrier gas) to drive the powders into the nozzle. The propellant gas can be heated. The powder feeder can provide continuous and controllable feeding. During a spraying process, metal powders with a size distribution in between 1 and 50 μm are accelerated by high-pressure gas flow through a

convergent-divergent de-Laval nozzle to reach a high velocity (500–1200 m/s) [2,4]. Particles remain at a temperature lower than the melting point and then impact against a solid surface to form a coating [2]. The industrial robot arm is used to perform the motion of the spray gun in order to achieve controllable, safe and accurate spraying path.

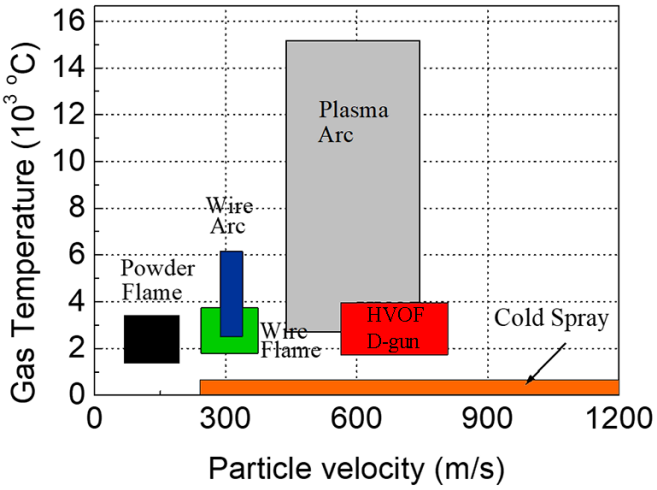

Figure 1.1 Different thermal spraying techniques with different particle velocity and gas temperature.

There are two types of operating parameters in CS: the process parameters and the parameters related to the robot motion. The process parameters generally include the feedstock data and the gas condition [13–15]. These parameters govern the in-flight behaviour of the particles as well as their deformation during the collision onto the substrate. The second category of parameters refer specifically to the kinematic parameter of the spray gun which is in fact controlled by the industrial robot via a robot trajectory programming [16–20]. In the following section, these parameters will be illustrated in details.

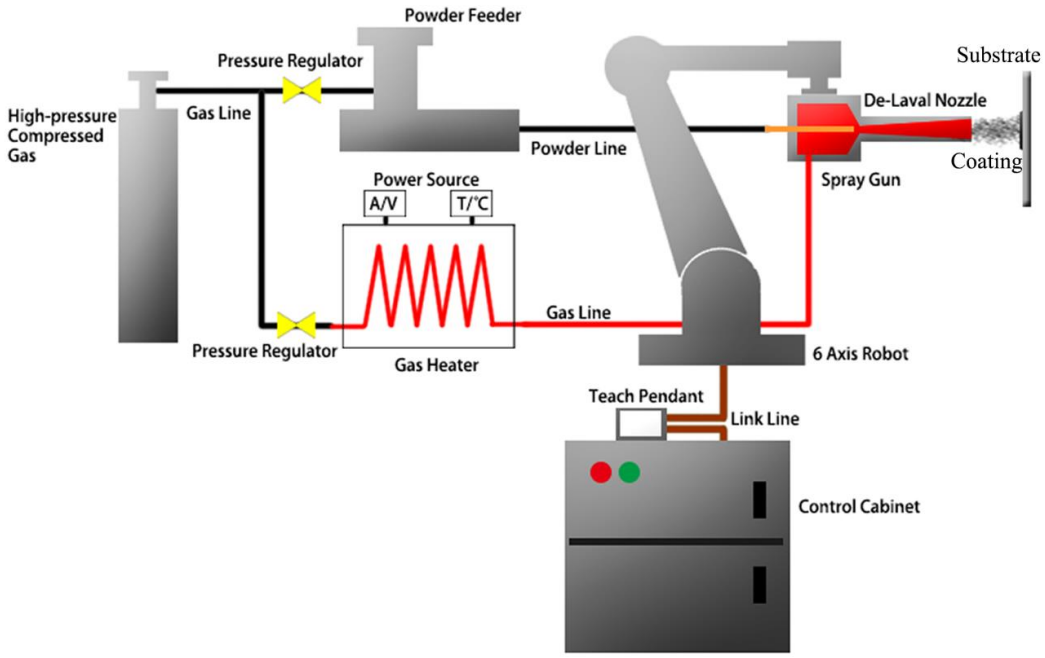

Figure 1.2 Schematic diagram of the CS system.

1.1.2 Spraying parameters in cold spray

Many publications have described the relationship between the spraying parameters and the coating characteristics as well as the coating structures [1,4,14]. Only when the pre-set spraying parameters permit the sprayed particles to reach the material-related critical speed, the particle/substrate or interparticle interfaces form a dense coating [21,22].

Generally, the propellant in CS can be air, argon, nitrogen, or helium. The gas nature has a particularly important role on the particle acceleration. Different gas sources affect the particle acceleration and impact velocity due to their different average molar mass [23–25]. For example, helium gas leads to higher increases in the particle velocity due to its lower molar mass [23]. Normally, the gas temperature and pressure refer to the parameters of the propelling gas. In CS, the maximum gas temperature is about 900°C [26]. The temperature setting is mainly determined according to the sprayed material. For example, the spraying temperature for pure copper powder is generally set in between 400-600 °C [27,28].

Since the temperature of the working gas is significantly lower than the melting point of the material, there will be no oxidation and phase change. The optimal temperature setting can not only conducive to the increase of the particle speed and the deposition efficiency, but also minimizes the effect of high temperatures on the material performance and the substrate. The

working gas pressure of CS is generally set in between 1.5~3.5MPa [24,26]. The working gas expands from the high pressure at the nozzle inlet to normal pressure, resulting in a supersonic airflow which varies with the nozzle structure and size, working gas type, gas pressure and temperature, powder particle size and density and other factors.

1.1.3 Kinematic parameters in cold spray

As mentioned above, industrial robots are widely used in field of CS due to their high stability and high accuracy of manipulation and motion, leading to the fact that the coating quality is affected directly by the robot kinematics [17–20]. Therefore, the CS kinematic parameters are actually a series of parameters manipulated and controlled by the robot. Figure 1.3 illustrates the general process of spraying gun motion, and the involving kinematic parameters are listed below:

- Spray trajectory
- Relative speed between nozzle and substrate
- Spray distance
- Spray angle
- Scanning step
- Over-length

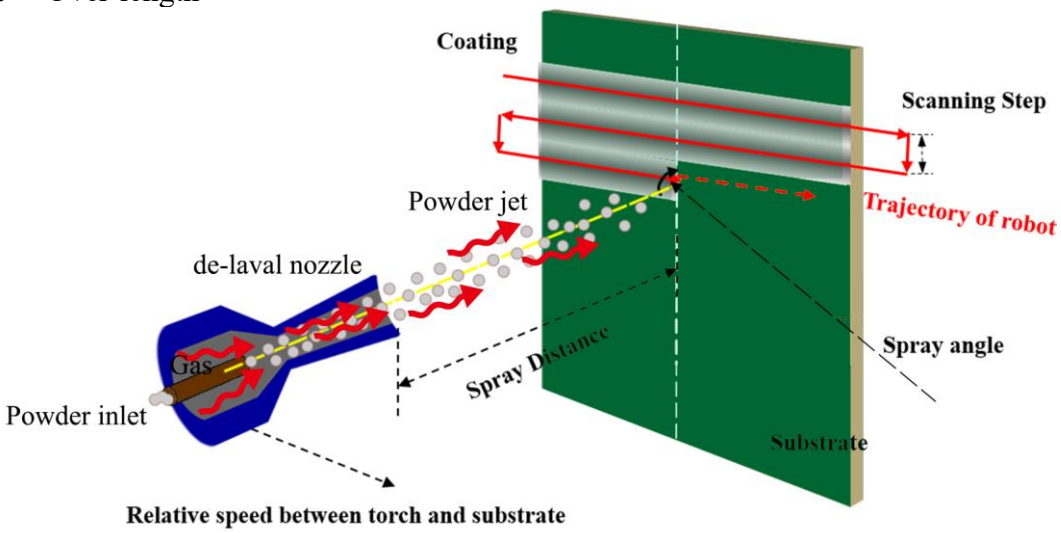

Figure 1.3 Kinematic parameters in the cold spraying process.

1.1.3.1 Spray trajectory

The spray trajectory, also called spray path, is a point set of spraying targets that are connected to each other by robotic programming. The aim of spray trajectory planning is to enable the coating to cover the entire object surface uniformly. Spray trajectory not only influences the coating thickness and distribution, but also the property of coating, especially the coating anisotropy[16,29–31]. Therefore, it is very important to plan the spraying path before spraying. With the increase of complex workpiece geometry, path programming has evolved from the initial manual manner to the current computer-aided automatic programming based on different algorithms [16,18,32], especially the usage of robot offline programming technology that improves the capability and reliability of path planning.

1.1.3.2 Nozzle traverse speed

The nozzle traverse speed is the moving speed of the robot in relation to the substrate. The relative moving speed between the nozzle and the substrate is referred to as nozzle traverse speed. The nozzle traverse speed equals to the moving speed of the robot. It is one of the most important parameters that can influence the mass distribution and the coating thickness [19,20,33]. The faster the nozzle travels, the fewer the deposited particles. Correspondingly, the coating thickness will also decrease in a certain period of time. In addition, the slower the nozzle moves, the longer the heating source exposition on the same area of the substrate surface, that leads to the deterioration of the coating quality because of local over-heating and residual stress [34–36].

In order to obtain a desired coating with uniform thickness and performance, appropriate and stable nozzle traverse speed is required. Generally, the effective moving speed of a robot during a deposition cannot be maintained at the predefined value due to the factor of inertia and motor performance. For this reason, influences of the inertia of the nozzle setup and performance limitation on the robot speed should be eliminated in spraying processes. Nowadays, some studies have been performed to improve the stability of robot performance by kinematic optimisation [37,38].

1.1.3.3 Spray distance

The spray distance or standoff distance is the distance in between the nozzle and the

substrate surface, which will affect the particle final states reaching the substrate, and thereby the coating thickness and deposition efficiency [18].

Generally speaking, there exists a critical velocity of particle for a given material. Only the sprayed particles reaching a velocity higher than this critical value can adhere on the substrate to form a coating. As shown in Figure 1.4, the spray distance will directly influence the flight duration of particles from the nozzle exit to the substrate, and definitely affects the acceleration of particles [33,39]. There is an optimum distance for an optimum deposition efficiency [3,33]. Therefore, an appropriate value of spray distance should be defined and keep constant during the operating process.

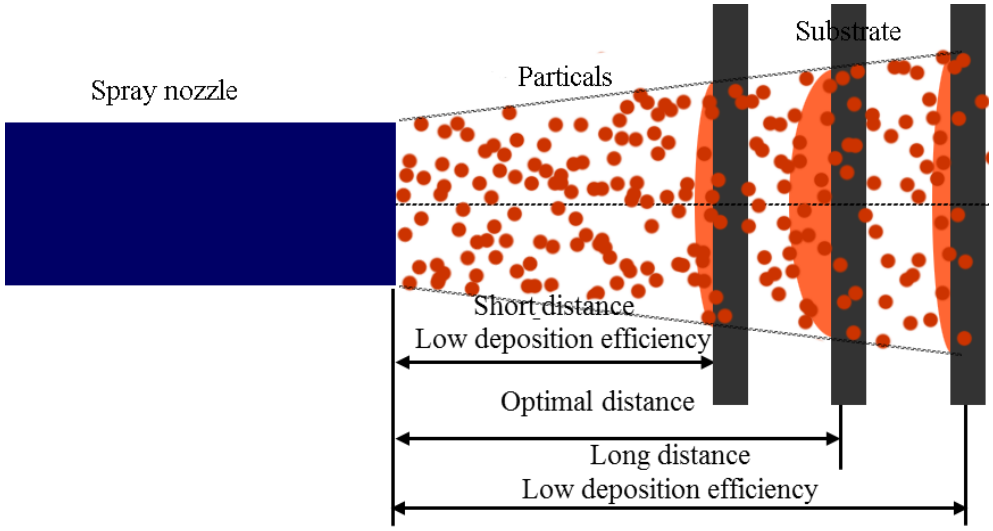

Figure 1.4 Influence of spray distance.

1.1.3.4 Spray angle

The spray angle is the angle between the nozzle and the surface of the substrate (Figure 1.5). Generally, in the CS process, the nozzle should be kept perpendicular to the substrate surface to have a maximum deposition efficiency. In Li.et al.'s report [40], the spray angle has little effect on the deposition efficiency in the angle range of 80-90°.

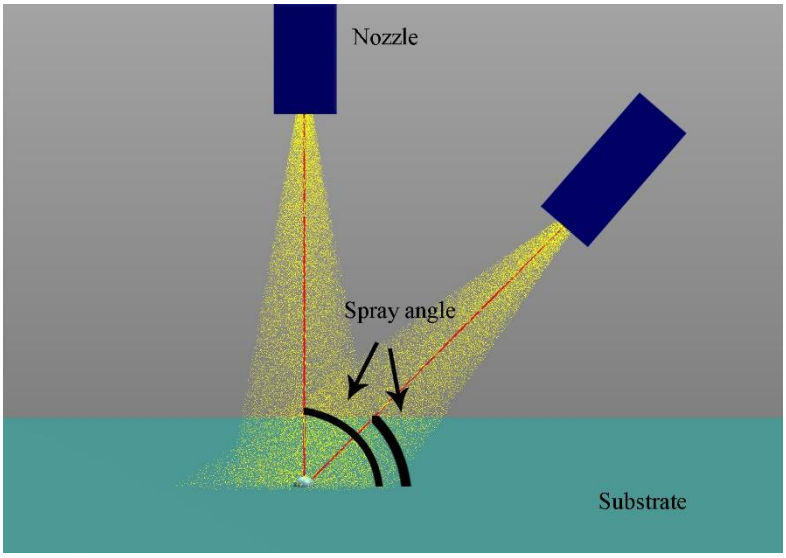

Figure 1.5 Schematic of spray angle.

In any case, it is certain that the inclined spray angle increases the particle loss and decreases the deposition efficiency due to the particle rebound during the impact on the substrate. The porosity of the coating will increase if the spray angle decreases from 90°. Therefore, the most active manner is that the spray angle should be kept at about 90°, that is easier to achieve for a plane surface. However, if the robot axes will reach their rotation limit at a certain point on the workpiece, especially for the workpiece with a complex shape, the robot has to compromise the spray angle to obtain a smoother scanning speed and coating quality. This has been proved to be feasible [40]. The spray angle between 90° and 45° is considered acceptable by striking a balance between deposition efficiency and the coating quality.

1.1.3.5 Scanning step

The scanning step refers to the interval between two successive scanning tracks when a coating is deposited by a multi-track trajectory (Figure 1.6). It is the key factor for the flatness and the thickness of a coating. The optimal value of the scanning step can result in a uniform coating. If the scan step is too small, the coating surface roughness will become rather low. If the scan step is too large, the flatness of coating will be decreased and the coating thickness distribution will become uneven. Besides, different scanning steps will lead to the different distribution of the track-to-track profile, thereby affecting the distribution of residual stress and pores [41,42].

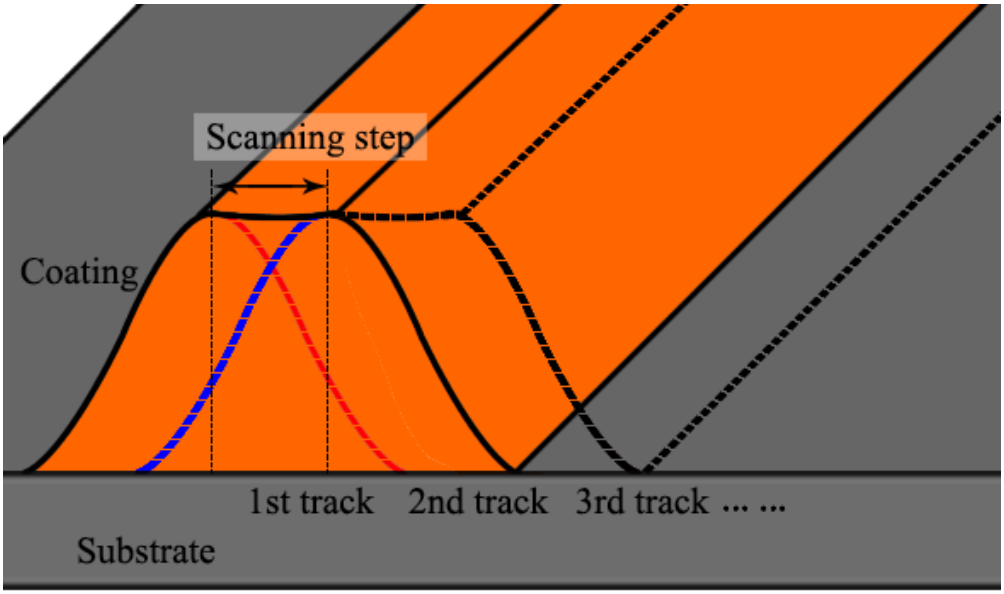

Figure 1.6 Schematic of scanning step.

1.1.3.6 Over-length

Generally, in the spraying processes, a round-trip alternating path is always used to scan the entire surface, such as the commonly used zig-zag path, as shown in Figure 1.7. Here, a part of the trajectory that exceeds the boundary of the workpiece is a parameter called over-length. When changing the scanning direction in between two successive passes, the robot will go through a process of deceleration and re-acceleration in order to overcome its own inertia and the weight of the nozzle. Therefore, it is necessary to reserve a certain over-length to allow the robot to re-reach the predefined speed to ensure a constant robot speed in the surface area of the substrate. It is required to avoid unnecessary waste of materials by choosing an appropriate value of over-length.

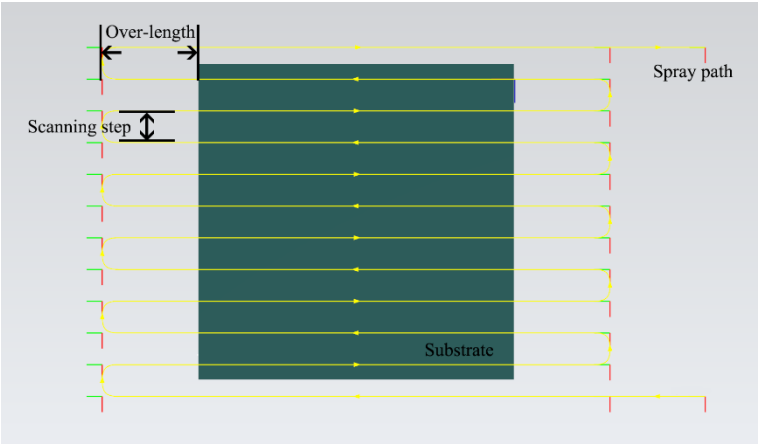

Figure 1.7 Commonly used zig-zag path in CS.

1.1.4 Applications of cold spray

As mentioned above, CS is a newly developed solid-state deposition technique that allows conversion of powders into a solid coating structure without local melting, phase transformation, grain growth, etc. Nowadays, CS has been widely applied as a coating technology in a broad range of industries, including aerospace, automotive, energy, medical, marine and other fields [2,9,10] .

CSed deposits provide effective protection against high temperature, corrosion, erosion, oxidation and chemicals [4]. For example, the CSed Al-5% Mg coating is a viable corrosion coating on ZE41A-T5 magnesium [43]. The Ni-20Cr cold-spray coating is very useful in developing high-temperature oxidation resistance for T22 and SA 516 boiler steels [44]. With the development of CS technology, the fundamentals of the process are now better understood and more available equipment has been developed to better perform this manipulation. Except for preparing various functional coatings, CS can be used for reconstruction or repair of damaged metal components or to fabricate free-standing metal components [9,10,45]. In the next parts, CS based repairing and additive manufacturing will be introduced respectively.

1.1.4.1 Cold spray repair

With the rapid development of modern industrial sectors, many long-term important components suffer from varying degrees of damage due to corrosion, collision, wear, fatigue, or other reasons. They have to be removed from service. However, replacing or producing a new part will likely lead to high costs and time-consuming, that would encourage companies to renew the damaged components instead of replacing them. As a result, developing economically sustainable and highly reliable maintenance services and repair strategies are paid more attention.

Nowadays, there are several types of metal manufacturing technology that have been used for the remanufacturing of parts, like laser metal deposition (LMD) [46,47] and selective laser melting (SLM) [48,49], as well as laser beam build-up welding [50,51], etc. However, among these techniques, high-power electron beams or high-frequency laser radiations are used for heating or melting materials but can lead to unsatisfactory results such as oxidations, grain growth, residual thermal stresses, and phase transformations.

Except for preparing various functional coatings, CS can be used for reconstruction or

repair of damaged metal components, especially in the aircraft industry. Compared to other repair methods (laser beam build-up welding, metal inert gas welding, and laser cladding), CS enables the recovery of defective areas without thermally affecting the base material and is proven as a cost-effective repair process [9,10]. To date, it has been successfully applied to repair various damaged components due to its capability to avoid any thermal damage to the underlying substrate material, and unique ability to retain the original properties of the feedstock powder.

Typical examples are restorations of a mechanically damaged gas turbines of an aircraft [52], reconditioning the housings of oil pumps on aircraft engines [53], refurbishment of a damaged aluminium hydraulic valve body [54] and worn aluminium mold [45], etc. In a recent work, a special spiral trajectory was developed for repairing damaged parts with cold spray [29]. Figure 1.8 shows this spiral trajectory and a repaired coupon. The specific trajectory is composed of two opposite spirals, one for entering and the other exit, which ensures the stable movement of the robot during repair, and thus provides a uniform coating. This method can match the coating with the original damaged defect shape to avoid excessive material deposition and to reduce post-processing work. In this work, the spiral trajectory included various nozzle traverses speed in inverse proportion to the crater depth to produce a homogenous deposit and to save feedstock.

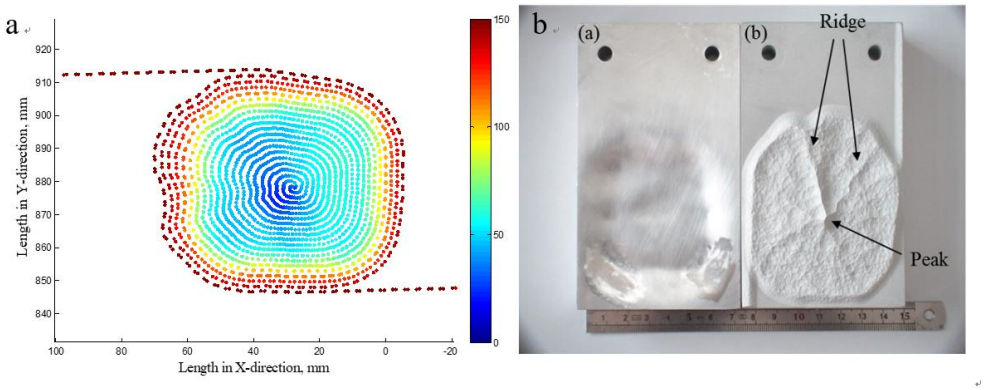

Figure 1.8 (a) Nozzle traverse speed distribution along the spiral trajectory; (b) The original and CS repaired damaged workpiece.

1.1.4.2 Cold spray based additive manufacturing

Additive manufacturing (AM), also called rapid manufacturing or 3D printing, is the general term for a series of technologies that build 3D objects by adding materials layer by layer (whether the material is plastic, metal, concrete or human tissue). In 1981, the Nagoya

Municipal Industrial Research Institute came up with an idea of 3D printing inspired by a photo-hardening polymer technology [55]. Note that the term 3D printing began to be used around 1993 when the Massachusetts Institute of Technology developed the first powder bed process using inkjet print heads [56].

AM uses the gradual accumulation of materials to manufacture solid parts, which is different from traditional material removal-cutting technology. What AM technology has in common is the use of computers, 3D modeling software (computer-aided design or CAD), special machinery and equipment, and layering materials. Once the CAD sketch is generated, the AM device reads the data from the CAD file and lays down or adds successive layers of liquid, powder, sheet material or other materials in a layer-by-layer manner to create a 3D object [57]. As the development of AM, technology practitioners have put forward the concepts of narrow and generalized AM (Figure 1.9 [58])). Narrow sense AM is a series of technologies characterized by the combination of different energy sources and CAD/CAM technology, layering and accumulating materials, such as selective laser melting (SLM) [59,60] and selective laser sintering (SLS) [61], as well as wire and arc additive manufacturing (WAAM) [62], etc. The generalized AM is a relatively broad technology group, which is based on the accumulation of materials and aims to directly manufacture parts of various sizes. Such a typical process is thermal spraying, physical vapor deposition (PVD) [63] or electro-chemical deposition [64], etc. In addition, according to the type and method of processing materials, AM can be divided into metal forming, non-metal forming, and bio-material forming.

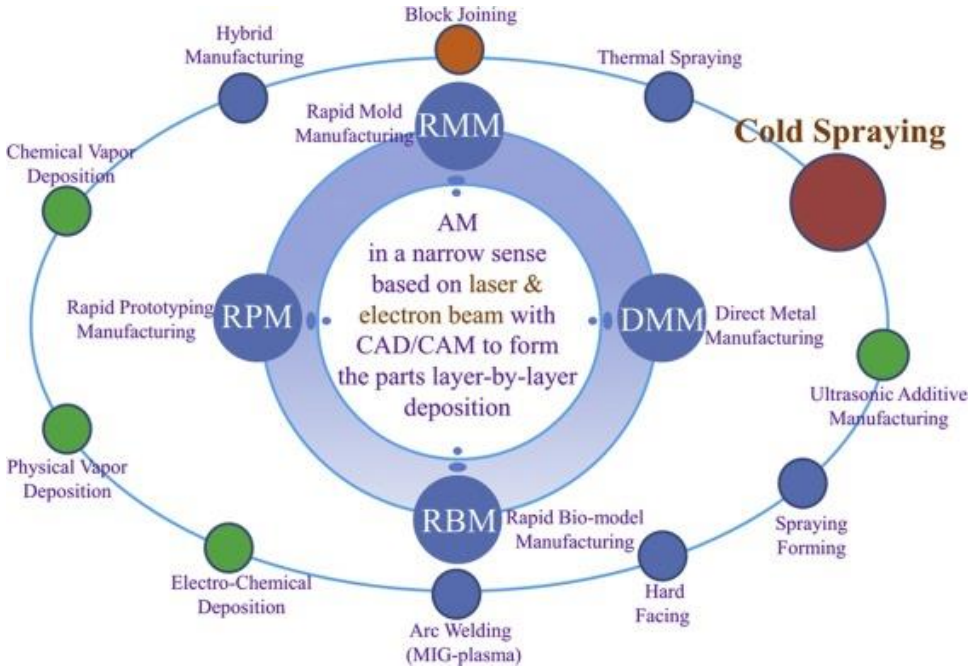

Figure 1.9 AM in the broad and narrow sense [58].

Nowadays, metal-related AM technology has become the focus of the global industry. CS has attracted much attention because of its great potential in solid-state forming metal components. In fact, this technology now is regarded as a potentially competitive AM due to the ability to build 3D objects when the CS gun is attached to a robot. Nowadays, with the development of technology, it has gradually occupied its place in the field of AM. In comparison with other AM technologies, many advantages make it unique in fabricating freestanding metal components. For example, CS processes can deposit temperature-sensitive materials without phase transformation or grain growth. Moreover, CS can be used for the fabrication of multi-material and gradient deposits, and its high production efficiency is expected to make breakthrough in the rapid manufacturing of large parts. To date, some companies or research institutions have intensively invested in the CSAM process and have achieved various results. For example, General Electric company (GE) builds large amounts of components for aviation's jet engines by using the CSAM system. They also used two robots to produce large metal components for the first time, where one robot held the component and moved it to a precise position, while the other one held the spray gun to spray materials on the component [65]. Titomic company has adopted the CS process to spray titanium or titanium alloy materials onto a scaffold to produce a load-bearing structure [66]. There is no doubt that CSAM will be more widely used in the field of direct metal manufacturing and will eventually develop and innovate in the direction of commercialisation.

All the CS applications, especially CS based repair and AM, require precise control of the kinematic parameters during the spraying process. These parameters not only ensure the feasibility of CS based applications, but also the quality of the CSed deposits, including geometry and mechanical properties. Therefore, the application of industrial robots in CS is particularly important. The next section will introduce industrial robots in detail.

1.2 Industrial robot

Generally, a robot is a machine capable of carrying out a complex series of actions automatically. It is often used to replace humans to complete a certain task, especially in those repetitive and dangerous tasks that humans are not suitable for, or are unable to do because of the size limitations or even those extreme environments such as outer space or deep ocean. Nowadays, many different kinds of robot have been developed affecting the way people live and work, such as industrial robots, mobile robots, collaborative robots, biomorphic robots,

military robots and so on. Among these categories, industrial robots are currently the most widely used and most mature one.

Since the United States developed the world's first industrial robot in 1962, industrial robot technology and its products have developed rapidly, and are now widely adopted in the field of industrial manufacturing and processing [67]. Typical applications of industrial robots include welding, painting, packing, assembly, stacking, product inspection and testing, which are accomplished with high efficiency and precision. As long as the process is well programmed and prepared, productivity can be improved largely by robots.

In the field of CS and thermal spraying, a spray gun is usually attached to a robot's end-effector to deposit materials on the substrate surface. Stable and precisely control on CS parameters is important and necessary for a desirable coating. Robot-assisted CS system allows the precision and stability performance that manual operating cannot meet. Last but not least, industrial robots can protect operators without potential harm resulting from the extreme working environment such as high temperature, noise, dust.

Commonly used industrial robots include FUNUC Robots, MOTOMAN Robots, ABB Robots and KUKA Robots, etc. In this thesis, all spraying processes are performed by an ABB IRB2400-16 robot. In this section, Multi-axis robot system, as well as its basic performance, will be introduced.

1.2.1 Multi-axis robot system

The Multi-axis robot system is an automatically controlled, reprogrammable, multipurpose manipulator with three or more axes. Generally, the number of axes for a simple manipulator such as a CNC machine is in between 2 and 3, and in between 3 and 6 for the programmable robots [67]. Besides, the degree of freedom is equal to the number of axes. Therefore, multi-axis robot system with greater number of axes can perform more complex actions and tasks. Figure 1.10 shows a typical 6-axis robot system which mainly consists of two parts including the manipulator and its controller system.

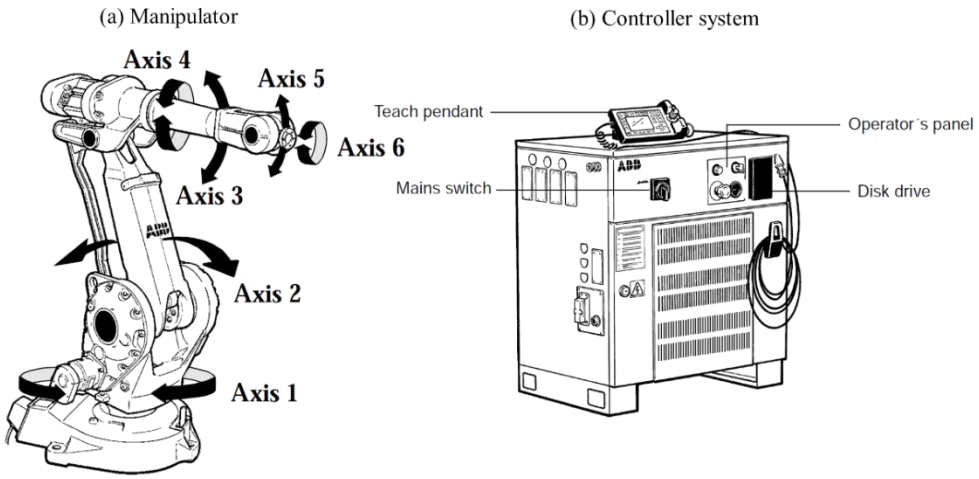

Figure 1.10 ABB IRB 2400 consisting of (a) manipulator with 6 axes and (b) controller system.

The manipulator is the six-axis robot body. As shown in Figure 1.10 (a) [68], Axis 1, located at the robot base, allows the robot to rotate from left to right; Axis 2 is the axis powering the movement of the entire lower arm, which allows the lower arm of the robot to extend forward and backward; Axis 3 allows the upper arm to raise and lower as well as to reach behind the body, extending the robot's work envelope; Axis 4 allows rotating the upper arm in a circular motion; Axis 5 is responsible for the pitch and yaw motion, allowing the wrist of the robot arm, to tilt up and down; Axis 6 is responsible for a twisting motion. It allows rotating freely with a capacity of more than a 360-degree rotation in either clockwise or counter-clockwise direction. There is a flange on the sixth axis, which can be used to attach tools like welding devices, spray guns, grinding and deburring devices, grippers and so on.

In addition, the controller system contains a control cabinet and its electronics, which are mainly used to control the manipulator, external axes and other peripheral equipment, etc. As shown in Figure 1.10 (b), a teach pendant connected with the control cabinet is used to display robot status, to control and program robot motion. Operators can use the joystick or buttons on the teach pendant to move the robot with a defined speed. Besides, robot programs prepared on the PC can also be synchronized to the robot control system via the disk drive shown in Figure 1.10 (b), and displayed on the screen of teach pendant. In the following section, basic performances of multi-axis robot system will be presented in detail.

1.2.2 Robot technical specification

1.2.2.1 Degree of freedom

Degree of freedom refers to the freedom of movement of a rigid body in three-dimensional space. Specifically, the body is free to change its position forward or backward (surge), up or down (heave), left or right (sway) in three perpendicular axes, combined with changes in orientation through rotation about three perpendicular axes, often termed yaw (normal axis), pitch (transverse axis), and roll (longitudinal axis) [66]. In a mechanic context, the number of degrees of freedom is equal to the total number of independent displacements or aspects of motion, and can also be regarded as the number of axes. A typical industrial robot used in CS or in thermal spray has a six degree of freedom (Figure 1.10).

1.2.2.2 Robot coordinate systems

The coordinate system is important for any industrial robot to perform a proper motion. Generally, the coordinate system as defined by geometry includes Cartesian Coordinate System, Polar Coordinate System, Cylindrical, or Spherical Coordinate Systems. Industrial robots with 6 degrees of freedom mostly use the Cartesian Coordinate System. Figure.1.11 shows five coordinate systems used in robot system, including world coordinates, base coordinates, tool coordinates, user coordinates and object coordinates [69]. The detailed definitions are as follows:

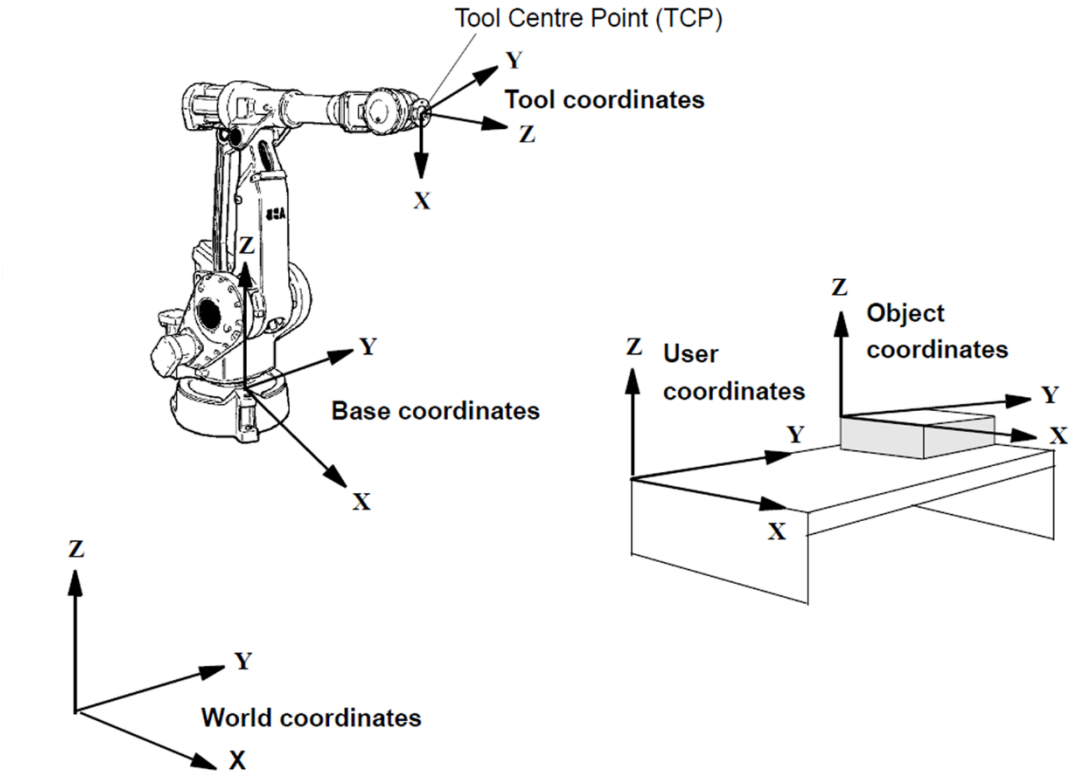

Figure 1.11 Coordinate systems of industrial robot.

The world coordinate system defines a reference to the floor which is the starting point for the other coordinate systems. People often use the origin of the robot base as world coordinate system. Therefore, the world coordinate system generally equals to the base coordinate system.

Base coordinate system is the base framework attached to the base of the robot. Itdefines the position of the base relative to the world coordinate system.

The tool coordinate system is freely definable. It is attached to the end of arm of tooling. When no tool has been installed on the robot, the origin of the coordinate system is at the center of the robot's sixth axis flange. The origin of the tool coordinate system is called Tool Center Point (TCP) and is used for tools. In CS applications, especially in AM or repair, TCP needs to be redefined, and its position is usually defined at the impact point on the substrate, which is located on the projection line from the nozzle outlet, considering the pre-set spray distance. Besides, there are two different programming ways for the use of TCP. If the spray gun is attached to the robot, TCP will be defined as being held by the robot and moving with the robot during the spraying process. If the spray gun is fixed at an appropriate position while the substrate or the formed part attaches to the robot, TCP will not be defined as being held by the robot and kept stationary at the defined position.

The user coordinate system specifies the position of a fixture or a workpiece manipulator. It can be defined as a movable user coordinate system if a work object is placed on an external mechanical unit. The object coordinate system specifies how a workpiece is positioned in a fixture or a workpiece manipulator.

1.2.2.3 Working envelop

A robot's work envelope refers to the working volume which can be reached by the center of the end effector of the Robot arm. In other words, it is the maximum overall area within which the robot arm can move. Figure 1.12 displays the working envelop of ABB IRB 2400/16 robot [68]. This shape is created when the robot reaches forward, backward, up and down. So, the robot's range of movement depends on the different robot properties such as length/diameter of each joint component. What is more, the working envelope is important for a particular application. For CS applications, the trajectory and the robot's motion should be controlled within the limits of the working envelop.

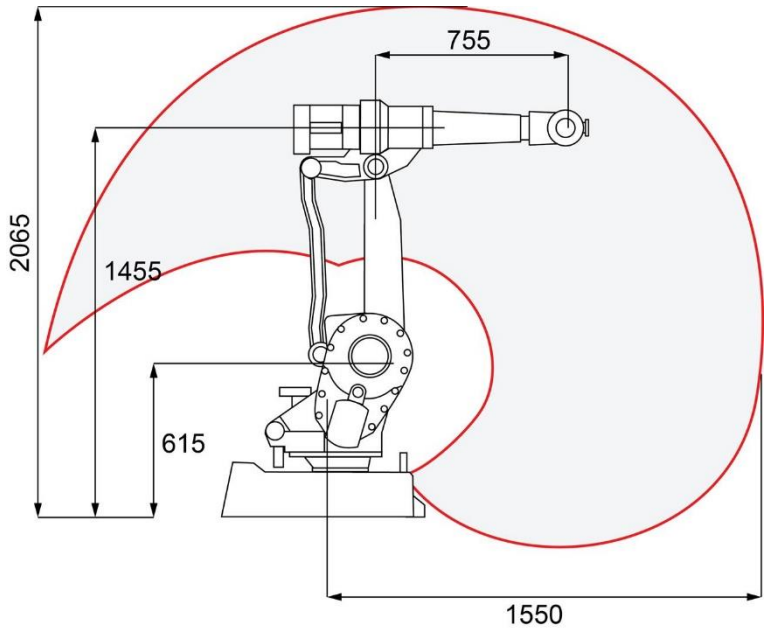

Figure 1.12 Working envelop of ABB IRB 2400/16 robot.

1.2.2.4 Payload

Robot payload or carrying capacity is the weight a robot arm can lift, that is based on the size of the robot and the power of the actuator. Therefore, it is very important to consider the robot application when determining the maximum payload. For safety reasons, the total weight,

including the tools installed on the end effector of the robot cannot exceed the maximum payload of the robot. It should be noted that the maximum payload is not a constant value and depends on the size of the tool, or exactly, the position of the tool's gravity centre.

As shown in Figure 1.13, it illustrates the maximum weight permitted for load mounting on the mounting flange at different positions of a robot IRB 2400/16 from ABB Company [68], where L is the distance in X-Y plane from Z-axis to the gravity centre. The maximum own moment of inertia on the total handling weight also should be considered. These parameters can be found in advance in the corresponding Robotics Technical Manual.

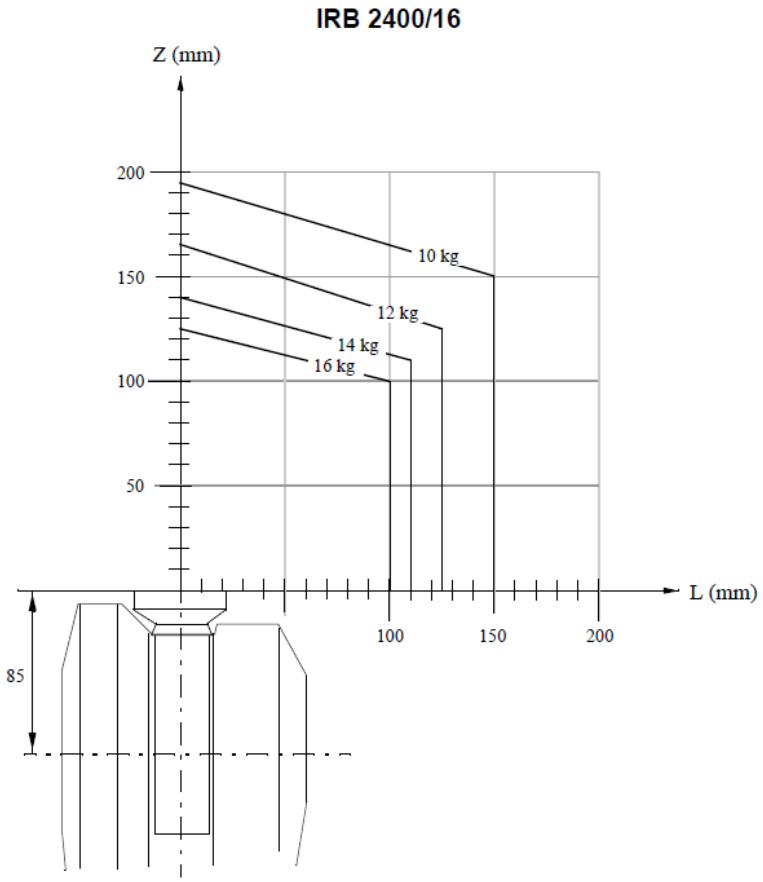

Figure 1.13 Payload of ABB IRB 2400/16 robot.

1.2.2.5 Speed

The robot speed mentioned here refers to the linear speed of the TCP moving around in the world coordinate system frame. Similarly to the other robot specifications, the robot speed is a very important characteristic for evaluating the robot performance, depending on the size, power, and other features of the robot. Ordinarily, the robot speed and the rotation speed of

each axis have their limits. If the distance for acceleration or deceleration is not enough, the robot could not reach the predefined speed. However, the constant or smooth motion of the robot is very important for lots of applications including spraying, painting and welding, etc. The robot speed that deviates from the predefined value cannot ensure product quality. Therefore, it is very important to ensure a constant robot speed concerning robot kinematics.

Actually, in CS, different nozzle traverse speeds are applied according to the desired coating thickness and the specific application. For example, the nozzle traverse speed is chosen from 40 mm/s up to 200 mm/s [33] generally to achieve a full coating deposition. Sometimes, a nozzle traverse speed [70] as high as 500 mm/s is used to obtain the single-particle deposition on the substrate, which is used for the study of bonding mechanism and particle deformation behavior. However, during CS, the path direction constantly changes to cover the entire surface of the substrate. Especially when performing some complex spraying path, the robot speed cannot maintain a constant predefined speed. As a result, it is essential to optimize the robotic kinematics parameters or to find a compromise between robot speed and spray angle.

1.2.2.6 Joint motion

The desired angles or positions of the end-effector motion is achieved by moving all the robot joints. The motion state of each axis of the robot can be described through three indicators: joint position, joint velocity, and joint acceleration. For the joint position, it represents the value of axis rotation at a given time, with a unit of degree. Normally, each axis of the robot has its corresponding rotation limit. Table 1.1 lists the axis motion specification of robot ABB IRB 2400/16 [68]. It can be found that axis 6 permits the largest range of motion, while axis 3 permits the smallest range. The joint position of each axis decides the TCP position and orientation within the working envelop. A smooth changing of the joint position within its rotation limit is conducive to a better axis motion performance. Otherwise, it will cause the axis servo motor to spend more energy to complete the robot motion, that will cause more fluctuations of the TCP speed.

The joint speed is the angular speed of an axis with a unit of degree per second (°/s). It is defined by the derivative of the joint position with respect to time. As another variable to evaluate the axis performance, the joint speed represents how fast an axis rotates, whose limit is based on the servomotor performance. As shown in Table 1.1, each axis of the robot has its corresponding joint speed. And axis 6 has the maximum axis speed, that is, this axis has the

most sensitive motion performance. Similarly, a sudden changing of the joint speed will increase the load on the control system and will probably reach the limit of the drive system.

Table 1.1 Axis motion specification of robot ABB IRB 2400/16.

Axis	**Range of Movement,**	**Maximum axis speed, /s**	**Maximum axis acceleration, /s²**
1	+180 to -180	150	298.734
2	+110 to -100	150	84.959
3	+65 to -60	150	356.740
4	+200 to -200	360	638.927
5	+120 to -120	360	637.599
6	+400 to -400	450	830.221

In addition. the joint acceleration is to evaluate how joint speed varies, with a unit of °/s2. Generally, the greater the acceleration of the joint, the faster the response of the axis to the corresponding command, and the higher the accuracy. However, the servo motor must provide greater power to obtain the larger joint acceleration that is required to achieve the desired speed, and this has a certain impact on the mechanical longevity of the system. In other words, lower joint acceleration or sustained joint acceleration can reduce mechanical wear. Moreover, the three indicators of the joint are related to each other. In order to improve the robot performance and maintain the TCP speed, it is important to make sure that all the joint positions are within limits. Besides, the joint speed of all axes is constant or smoothly changes.

1.2.3 Robot programming

Compared to traditional machines, the main advantage of industrial robots is their programmability. Robots can perform arbitrary sequences of predefined motions. In CS applications, the main task of the industrial robot is to execute the spraying trajectory with high precision. The planning and generation of the spraying trajectories are based on the shape of the workpiece to be sprayed and different operating parameters. Thus, an efficient and proper programming method is necessary for trajectory generation and post-analysis.

Currently, the methods of robotic programming involve the on-line teaching [71] and off-line programming [16,19]. The choice of the method to use mainly depends on the type and

complexity of the project. Most robot programming uses an online teaching method, which is appropriate and efficient for certain simple tasks. However, for those complex movements that require higher accuracy, offline programming should be used to define the robot's movement in order to perform tasks that cannot be accomplished by on-line teaching method. In this section, these two methods of robotic programming will be presented.

1.2.3.1 On-line programming technique

Industrial robots generally consist of three parts: a controller, a robot arm, and a teach pendant [67,68]. The teach pendant is the remote controller of the robot, which is equipped with a user operation interface software and buttons, moving handles, touch screen, etc. The operator controls the robot to complete the specified actions through these human-computer interaction functions. This process is called online programming or teaching programming. Traditionally, it is the most commonly used robotic programming method in most industries.

In general, the tool and its assembly are first installed on the end-effector of robot (wrist). A Tool Center Point (TCP) should be defined based on the tool and the task, that is usually located at the end of the tool or at the point of contact. The operator uses the manual control on the teach pendant to control the robot and moves the TCP to the desired position, and then stores the information of the position in a series of motion commands (including the position and orientation of the TCP). After storing all target points and robot motion commands, the corresponding trajectory program can be then tested. It is worth mentioning that industrial robots have good position repeatability, that is, after teaching, the robot can run the same program repeatedly, and the accuracy of returning to the same spatial position point can reach the level of ten microns to hundreds of microns.

The advantages of this programming method are its low learning cost and easy use. In the process of online programming process, operators are required to perform on-site operations in the working unit of the robot. However, since this method requires many manually operated robot movements, the programming process will be tedious and time-consuming. Depending on the complexity of the task, this may take days or even weeks. In addition, the robot needs to leave the production line during online programming so the production will be interrupted.

Generally, online robot programming requires experienced engineers to debug on-site and run the program repeatedly to achieve the desired effect. For CS, the working range of the spray gun, the nozzle travel speed, the spray distance and the spray angle, etc, need to be considered

for the programming. However, for tasks that require high complexity and accuracy as well asrepeated modifications, the online programming method may not be suitable. Thus, the next section will introduce the second programming method, called offline programming method, which aims to handle complex programming tasks.

1.2.3.2 Off-line programming technique

Robot offline programming refers to "virtual" programming of the robot on the computer (PC) through related software tools [72,73]. Programmers need to use CAD models to offer a more scientific programming strategy. This process includes creating CAD models, robot path planning, creating motion programs, and robot motion simulation. When using this method for programming, there is no need to stop the robot in production, so it will not hinder the production operations.

With the development of robot technology and the continuous expansion of its application fields, offline programming technology has gradually become a popular programming method, which is mainly used to complete some complex programming tasks. Currently, this technology has been widely used in welding, laser cutting, thermal spraying, CNC machining and other fields, to deal with some complex programming tasks. In conclusion, the robotic off-line programming technology provides a complete solution for industrial robots, from trajectory generation, parameter selection to process simulation and trajectory optimization. The trajectory of the robot can be generated by using the geometric data of the workpiece to ensure the accuracy of the trajectory, and at the same time provides more optimization strategies while reducing also the occurrence of collision accidents.

Robot offline programming technology is even more essential in CS application. First of all, an accurate and reasonable spray trajectory is a necessary condition for ideal coatings. The robot offline programming technology can provide optimized spraying path and reliable programming [16,19]. In addition, for complex shapes, online programming is difficult to complete with the correct definition of the trajectory point. During the spraying process, it must ensure that the spraying direction is perpendicular to the surface of the workpiece, and at the same time it must ensure also that the coating can evenly cover the entire surface of the workpiece. Offline programming is an accurate programming method based on the CAD model. This allows the robot to easily adjust the tool operation direction and the starting pose of the robot to avoid the singularity state and obtain the most optimized path.

In addition, CS is not only used to prepare various functional coatings on the surface of various complex parts as a coating technique, but also to repair various damaged metal components as a repair technology, and to fabricate freestanding metal parts as an AM technology. Since many applications are no longer just a process of producing simple coatings, Computer-aided design (CAD) and Computer-aided manufacturing (CAM) are needed to provide the ideal spray strategy, including generating trajectories, simulating the process and collision detection. Robot offline programming technology can be used as a new production capacity and modernization application to provide desirable solutions in the process. The next section will introduce application software used for offline programming.

1.3 Robot off-line programming software

Robot offline programming technology requires the application of related software systems, called robot offline programming software [72]. Many robot manufacturers have developed their own robot offline programming systems compatible with their robots. The software operator can create a three-dimensional virtual scene of the entire actual workstation and uses the related functions provided by the software to accomplish many programming tasks that cannot be completed by online programming. As shown in Figure.1.14, this is a typical case of cooperation between multirobot using offline programming technology.

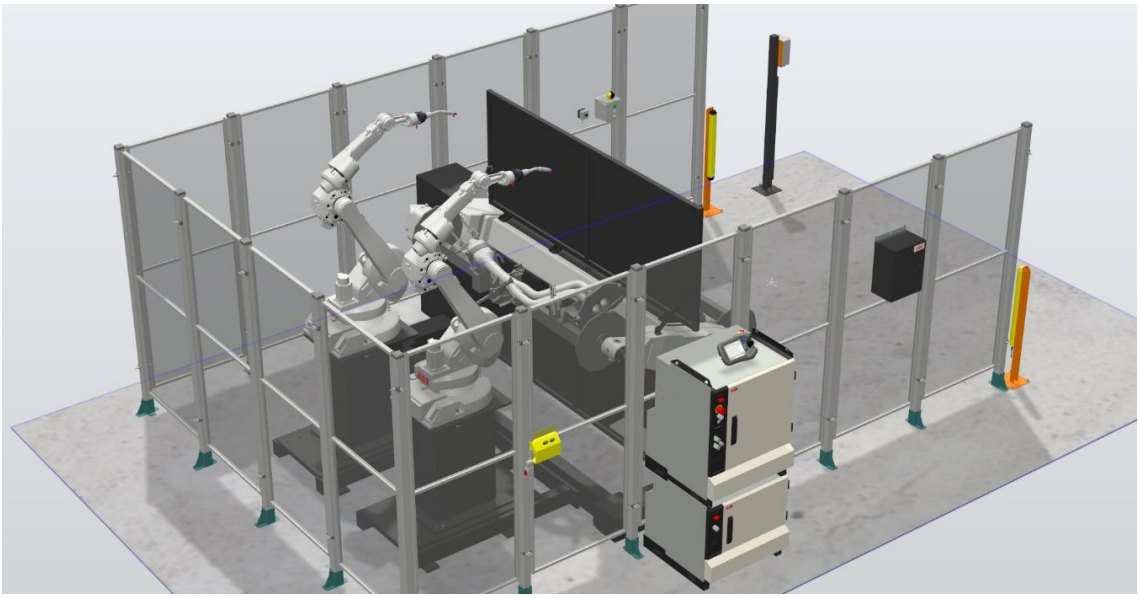

Figure 1.14 An example of robot cooperation using robot offline programming software.

Nowadays, there is various robot offline programming software used in the world. For example, RobotStudio™ is a powerful off-line programming software developed by Asea

Brown Bovrie Ltd (ABB) that enables very realistic simulations of robot motion[69]; RobotMaster [74] is an offline programming software developed by Hypertherm Robot Software Co that is compatible with most robot brands on the market, including KUKA, ABB, Fanuc, Motoman, Panasonic, etc. and integrates advanced functions including robot programming, simulation and code generation functions. In the following section, we will introduce RobotStudio™, which is the offline programming software used for the studies in this thesis.

1.3.1 RobotStudio™

RobotStudio ™ is a commercial software provided by ABB company. It is specifically developed for performing robotic tasks including programming, trajectory simulation, and collision detection, etc. RobotStudio™ is based on ABB Virtual Controller technology, which is the same as a software embedded and running in real robots [69]. The technique makes it possible to graphically create a virtual robotic site like the real site. Therefore, users can use the software to specify the robot's motion, automatically form executable code and then synchronize it to the actual robot. RobotStudio ™ provides the ability to design the robot program in a computer with a learning programming method. The advantages of RobotStudio ™ are as below:

All types of robot models of ABB products are available in the Robot system library.

Commonly used geometric models such as STL, IGES, STEP, ASCII, ACIS and CATIA can be imported directly into RobotStudio ™ as digital components for modeling.

Robotic programming and simulation including the detection of collisions in the graphic environment ensure the safety of the operator and the equipment.

The program is designed and created in a computer so that it can be prepared in advance even though the robot is still in production.

RobotStudio™ provides an interface for users to personalize development according to specific requirements.

Figure 1.15 shows the general process of programming using RobotStudio™, which is suitable for various industrial applications, including CS.

- Generally, the first step is to establish a virtual workstation with the same configuration as the actual spray shop, including the same type of robot, spray gun and tools, and the

same placement between the various elements. The advantage of the virtual robot workstation is that it can truly reflect the actual spraying process. In addition, it is convenient to change the spraying procedure at any time and observe whether the various components interfere with each other, thereby preventing collisions between the equipment effectively.

- Then, the CAD model of the workpiece to be processed is imported into the corresponding virtual robot workstation and is placed in the operation position.
- After that, a tool coordinate system should be defined, known as the tool centre point (TCP), to specify the tool's centre point position and its orientation.
- Then, a workpiece coordinate system, also called workobject, is used to define workpiece origin and coordinate orientation. Each position is specified in the workobject coordinate. This means that even if a fixture or workpiece is moved, only the workobject coordinate system needs to be redefined, then all the defined points will be revised accordingly. Besides, if a tool is replaced, the original program can still be used, unchanged, by making a new definition of the tool.
- The next step is to create a robot trajectory with the help of CAD files.It is easier and more accurate to obtain and define a target point position, which will result in a trajectory with higher precision.
- After generating the robot trajectory, simulation can be carried out through the function of the simulation module in Robotstudio. According to the results of the simulation, the robot trajectory and the process strategy can be adjusted in the feedback loop to achieve the desired result.
- Once the trajectory of the robot is confirmed, the corresponding program can be downloaded to the actual robot system for calibration, testing and application.

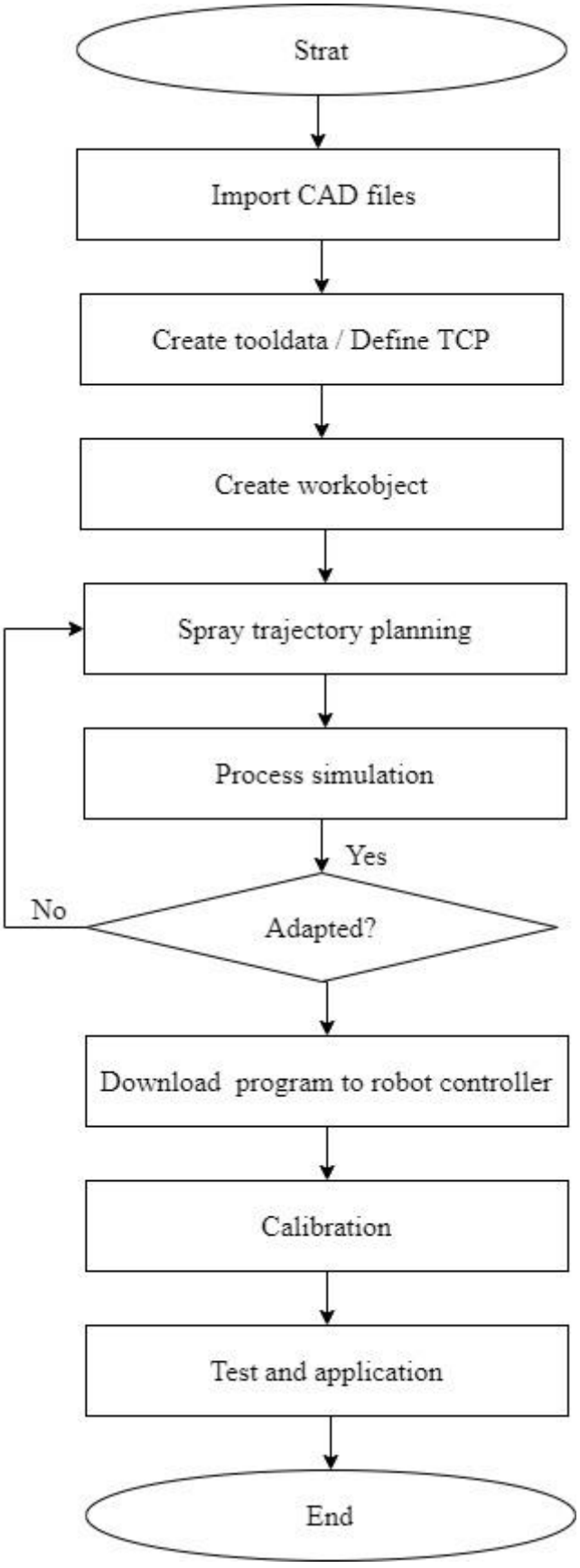

Figure 1.15 Procedure of an off-line programming.

1.3.2 Necessity of auxiliary system for cold spray application

Generally, RobotStudio™ or other offline programming software can meet the needs of general applications. Operators can generate an appropriate trajectory according to the CAD model of the workpiece. For example, the trajectory can be easily created on a curved intersection or an edge of the workpiece for the application of welding or cutting. As for CS process, the trajectory consists of paths separated by the constant scan step to guarantee that the coating covers the entire surface of the substrate. Besides, for the purpose of high coating quality, several operating parameters including spray angle and spray distance must be constant. The nozzle should be perpendicular to the substrate surface to ensure high deposition efficiency.

However, it is not easy to create parallel spray paths on curved substrate surfaces, which is time-consuming and lacks precision even under off-line programming software. Moreover, CS based additive repair or manufacturing is no longer a process of producing simple coatings but requires more and advanced and complicated paths to meet various spraying tasks. Exactly, CS repair needs to generate a trajectory that matches the original damaged defect shape in order to avoid excessive material deposition and reduce post-processing work, and CSAM needs to create a shaping path adapting CS characteristics. Obviously, the basic function including trajectory generation in RobotStudio™ cannot meet the above-mentioned cases.

Therefore, in order to satisfy the specific requirements of the new application in the CS, it is necessary to develop software based on the off-line programming platform to provide the appropriate spray strategy quickly and precisely. RobotStudio™ allows the developers to develop different kind of custom applications or Add-Ins as a new feature in its application. LERMPS (Laboratoire d'Etudes et de Recherches sur les Matériaux, les Procédés et les Surfaces) has developed an add-in application program named Thermal Spray Toolkit (TST) in the framework of RobotStudio™ [16,20]. In the next part, the main functions of TST will be briefly presented.

1.3.3 Thermal Spray Toolkit (TST)

TST is a RobotStudio™ based extension software developed for the generation of trajectory in thermal spray applications, and all its functions are also suitable for CS. Figure 1.16 shows the four basic modules of TST.

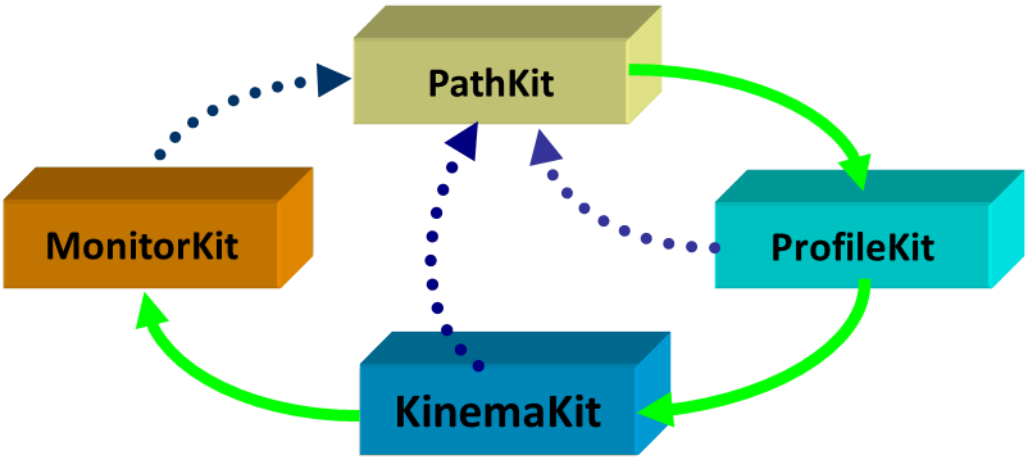

Figure 1.16 Modules in Thermal Spray Toolkit (TST)

Here, PathKit enables the creation of robotic trajectories according to the geometry of workpiece. In this module, one method is presented using orthogonal planes to cut the substrate surface, then a series of scanning curves can be generated. Meanwhile, the normal vector is calculated to define the orientation of the nozzle on every point of the curves. PathKit uses this method to generate robot trajectories for thermal spraying in the offline programming software RobotStudio™ [75,76]. It can automatically and quickly generate trajectories according to the shape of the workpiece that meets the required operating parameters (as shown in the Figure 1.17).

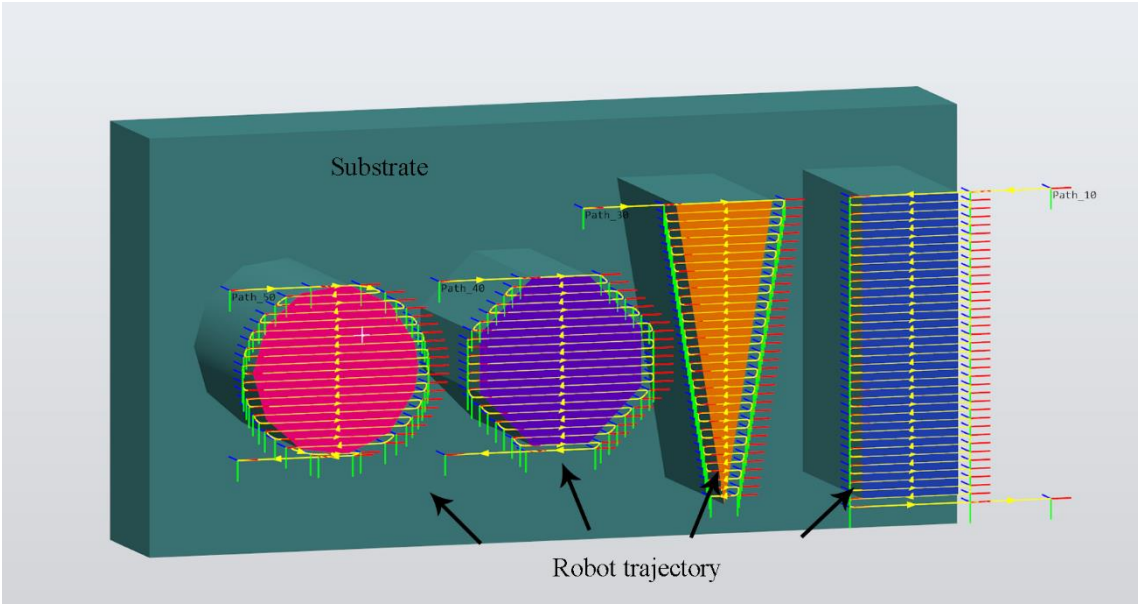

Figure 1.17 Spray trajectory generation under PathKit.

ProfileKit module is developed for the purpose of the coating deposition simulation. Currently, a coating thickness model based on the numerical method was developed and was

used to predict the coating thickness and distribution. Combining with the robot kinematic parameters, the coating profile is simulated with an asymmetric Gaussian distribution curve. Thus, the suitable coating thickness can be obtained within the required tolerances.

A concept called 'flatness' is added to illustrate the homogeneity of coated thickness, and the relevant simulated coating thickness and flatness result can be displayed on the graphic interface [31]. As shown in Figure 1.18, they are the user interfaces of ProfileKit 2D and ProfileKit 3D respectively [19]. According to the calculation and simulation results, the spraying strategy including the robot trajectory and operating parameters can be adjusted with iteration in the feedback loop to achieve the desired coating thickness distribution.

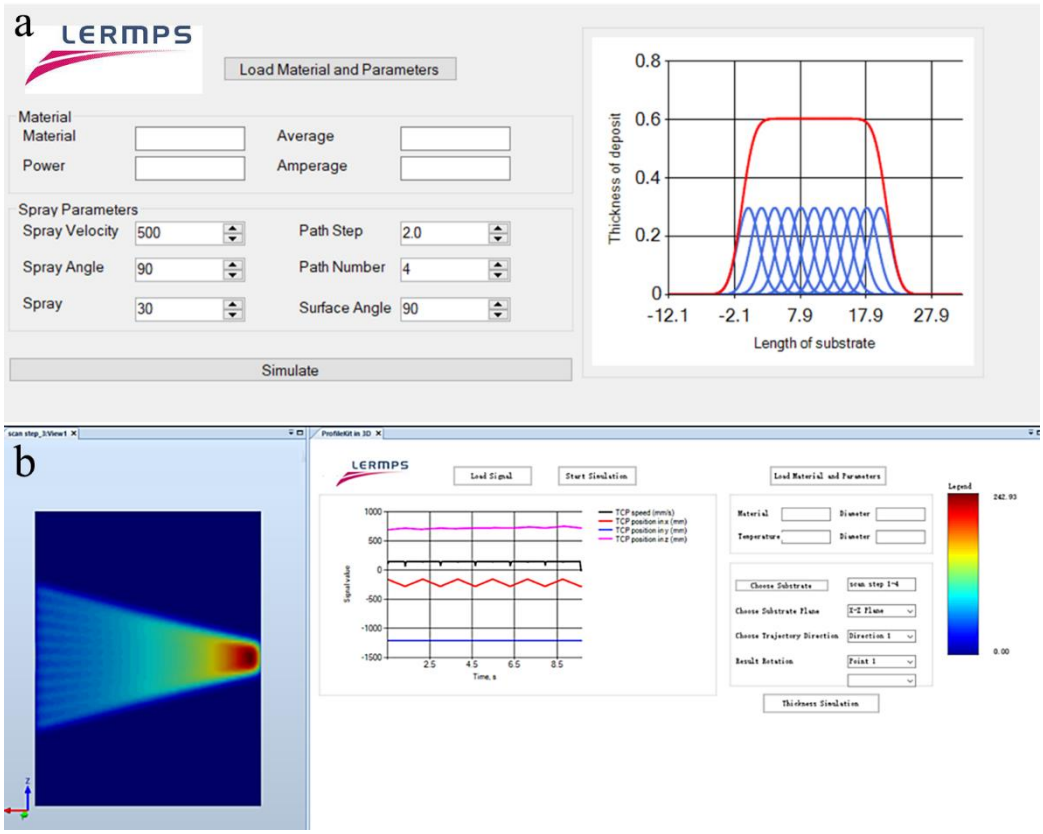

Figure 1.18 (a) the user interface of ProfileKit of coating profile simulation in 2D. (b) the user interface of ProfileKit of coating thickness simulation in 3D.

MonitorKit monitors the speed and trajectory of the robot by communicating with the operating robot. It is able to evaluate the path accuracy, which can provide evidence for trajectory optimisation.

KinemaKit is used to optimize the kinematics parameters in the spraying process by collecting and analysing various signal data of the robot's motion. The signal data Mainly includes TCP position and orientation and the position of each axis versus time, etc. Kinematic

analysis method is useful for the optimised mounting method of spray nozzle on the robot [37]. Besides, the optimal placement of the workpiece in the robot workspace is selected through robotic kinematic analysis method to optimize the robot's trajectory [38].

1.4 Conclusion and objectives

CS is a newly developed solid-state material deposition technique. It is widely used to prepare various functional coatings on the component surface, or restore damaged metal components or to fabricate freestanding 3D metal components. With the continuous development of CS technology and its expansion of application fields, people need to handle more and more complex tasks requiring high precision. Nowadays, due to the high performance of industrial robots, they have been widely used in the field of CS to perform all kinds of spraying tasks. In CS, the nozzle is moved by the robot to scan on the surface of the workpiece, and thus to form a coating. All kinematic parameters, including spray angle, spray distance and nozzle traverse speed, etc, can be stably and accurately controlled.

In addition, robot offline programming technology allows to reduce the burden and difficulty of programming, to improve the accuracy, and to make CS available for more complex parts. Since CS is no longer a single process of producing simple coatings, it is also used to repair various damaged parts or to manufacture complex 3D parts, so that it is necessary to develop an auxiliary system specifically for CS to provide an ideal spraying strategy, including generating trajectories, process simulation and collision detection. Therefore, in this chapter, RobotStudio™ and its extension software TST are introduced based on the robot’s application in CS.

Today, the latest developments in the CS industry require more new methods and processes to improve its manufacturing accuracy, flexibility and reliability, for more competitiveness. Therefore, the subject of the thesis concerns robotized CS process simulation and planning in order to enhance the ability of CS in the application of AM or remanufacturing.

The present work is mainly composed of the following three parts:

1. Firstly, based on the conventional CS system, a new robotized CS system framework is designed for modern CS applications.

2. Secondly, a new approach using a geometric 3D model is developed and integrated into the ProfileKit of TST for CS process simulation.

3. Thirdly, a novel spray strategy is proposed to elaborate freeform 3D objects with acceptable precision.

References

[1] R.C. Dykhuizen, M.F. Smith, Gas dynamic principles of cold spray, Journal of Thermal Spray Technology. 7 (1998) 205–212.

[2] A. Moridi, S.M. Hassani-Gangaraj, M. Guagliano, M. Dao, Cold spray coating: review of material systems and future perspectives, Surface Engineering. 30 (2014) 369–395.

[3] T. Stoltenhoff, H. Kreye, H.J. Richter, An analysis of the cold spray process and its coatings, Journal of Thermal Spray Technology. 11 (2002) 542–550.

[4] V.K. Champagne, The cold spray materials deposition process, Elsevier, 2007.

[5] X. Xie, C. Chen, Y. Ma, Y. Xie, H. Wu, G. Ji, E. Aubry, Z. Ren, H. Liao, Influence of annealing treatment on microstructure and magnetic properties of cold sprayed Ni-coated FeSiAl soft magnetic composite coating, Surface and Coatings Technology. 374 (2019) 476–484.

[6] L. Ajdelsztajn, J.M. Schoenung, B. Jodoin, G.E. Kim, Cold spray deposition of nanocrystalline aluminum alloys, Metallurgical and Materials Transactions A. 36 (2005) 657–666.

[7] V. Champagne, D. Helfritch, Critical assessment 11: structural repairs by cold spray, Materials Science and Technology. 31 (2015) 627–634.

[8] A.W. James, G.P. Wagner, B.B. Seth, Cold spray repair process, 2002.

[9] S. Yin, P. Cavaliere, B. Aldwell, R. Jenkins, H. Liao, W. Li, R. Lupoi, Cold spray additive manufacturing and repair: Fundamentals and applications, Additive Manufacturing. 21 (2018) 628–650.

[10] R.N. Raoelison, C. Verdy, H. Liao, Cold gas dynamic spray additive manufacturing today: Deposit possibilities, technological solutions and viable applications, Materials & Design. 133 (2017) 266–287.

[11] H. Wu, X. Xie, M. Liu, C. Verdy, Y. Zhang, H. Liao, S. Deng, Stable layer-building strategy to enhance cold-spray-based additive manufacturing, Additive Manufacturing. (2020) 101356.

[12] C.J. Huang, H.J. Wu, Y.C. Xie, W.Y. Li, C. Verdy, M.-P. Planche, H.L. Liao, G. Montavon, Advanced brass-based composites via cold-spray additive-manufacturing and its potential in component repairing, Surface and Coatings Technology. 371 (2019) 211–223.

[13] R.P. Singh, U. Batra, Effect of Cold Spraying Parameters and Their Interaction an Hydroxyapatite Deposition., Journal of Applied Fluid Mechanics. 6 (2013).

[14] H. Assadi, T. Schmidt, H. Richter, J.-O. Kliemann, K. Binder, F. Gärtner, T. Klassen, H. Kreye, On parameter selection in cold spraying, Journal of Thermal Spray Technology. 20 (2011) 1161–1176.

[15] S. Grigoriev, A. Okunkova, A. Sova, P. Bertrand, I. Smurov, Cold spraying: From process fundamentals towards advanced applications, Surface and Coatings Technology. 268 (2015) 77–84.

[16] S. Deng, Robot offline programming and real-time monitoring of trajectories: development of an add-in program of robotstudio™ for the thermal spraying, in: Graduate School of "Physics for Engineers and Microtechnology," University of Technology of Belfort-Montbéliard France, 2006.

[17] D. Fang, Diagnostic et adaptation des trajectoires robotiques en projection thermique, PhD Thesis, Université de Technologie de Belfort-Montbeliard, 2010.

[18] Z. Cai, Programmation robotique en utilisant la méthode de maillage et la simulation thermique du procédé de la projection thermique, PhD Thesis, 2014.

[19] C. Chen, Research and realization of assistant off-line programming system for thermal spraying, PhD Thesis, Belfort-Montbéliard, 2016.

[20] S. Deng, Programmation robotique hors-ligne et contrôle en temps réel des trajectoires: développement d'une extension logicielle de" Robotstudio" pour la projection thermique, PhD Thesis, Besançon, 2006.

[21] H. Assadi, F. Gärtner, T. Stoltenhoff, H. Kreye, Bonding mechanism in cold gas spraying, Acta Materialia. 51 (2003) 4379–4394.

[22] T. Schmidt, F. Gärtner, H. Assadi, H. Kreye, Development of a generalized parameter window for cold spray deposition, Acta Materialia. 54 (2006) 729–742.

[23] X. Suo, S. Yin, M.-P. Planche, T. Liu, H. Liao, Strong effect of carrier gas species on particle velocity during cold spray processes, Surface and Coatings Technology. 268 (2015) 90–93.

[24] S. Yin, M. Meyer, W. Li, H. Liao, R. Lupoi, Gas flow, particle acceleration, and heat transfer in cold spray: a review, Journal of Thermal Spray Technology. 25 (2016) 874–896.

[25] M. Grujicic, C. Tong, W.S. DeRosset, D. Helfritch, Flow analysis and nozzle-shape optimization for the cold-gas dynamic-spray process, Proceedings of the Institution of Mechanical Engineers, Part B: Journal of Engineering Manufacture. 217 (2003) 1603–1613.

[26] T. Schmidt, H. Assadi, F. Gärtner, H. Richter, T. Stoltenhoff, H. Kreye, T. Klassen, From Particle Acceleration to Impact and Bonding in Cold Spraying, J Therm Spray Tech. 18 (2009) 794. doi:10.1007/s11666-009-9357-7.

[27] H.-K. Kang, S.B. Kang, Tungsten/copper composite deposits produced by a cold spray, Scripta Materialia. 49 (2003) 1169–1174.

[28] The effects of heat treatment on the mechanical properties of cold-sprayed coatings, Surface and Coatings Technology. 261 (2015) 278–288. doi:10.1016/j.surfcoat.2014.11.017.

[29] C. Chen, S. Gojon, Y. Xie, S. Yin, C. Verdy, Z. Ren, H. Liao, S. Deng, A novel spiral trajectory for damage component recovery with cold spray, Surface and Coatings Technology. 309 (2017) 719–728. doi:10.1016/j.surfcoat.2016.10.096.

[30] Z. Cai, T. Chen, C. Zeng, X. Guo, H. Lian, Y. Zheng, X. Wei, A Global Approach to the Optimal Trajectory Based on an Improved Ant Colony Algorithm for Cold Spray, Journal of Thermal Spray Technology. 25 (2016) 1631–1637. doi:10.1007/s11666-016-0468-7.

[31] Z. Cai, S. Deng, H. Liao, C. Zeng, G. Montavon, The Effect of Spray Distance and Scanning Step on the Coating Thickness Uniformity in Cold Spray Process, Journal of Thermal Spray Technology. 23 (2014) 354–362. doi:10.1007/s11666-013-0002-0.

[32] A. Frutos, Numerical analysis of the temperature distribution and Offline programming of industrial robot for thermal spraying, 2009.

[33] A new approach to simulate coating thickness in cold spray - ScienceDirect, (n.d.). https://www-sciencedirect-com.ezproxy.utbm.fr/science/article/abs/pii/S0257897219311429?casa_token=cML6QAKhIa0AAAAA:v12Geei3OQ6OIrwVUOYOEGrm4S4nXKkeW7uoUMW_gXtqK9f-GS7f7ZkL9qnqW1Ppw0ViekHvtw0 (accessed August 13, 2020).

[34] T. Suhonen, T. Varis, S. Dosta, M. Torrell, J.M. Guilemany, Residual stress development in cold sprayed Al, Cu and Ti coatings, Acta Materialia. 61 (2013) 6329–6337. doi:10.1016/j.actamat.2013.06.033.

[35] W. Li, K. Yang, D. Zhang, X. Zhou, Residual Stress Analysis of Cold-Sprayed Copper Coatings by Numerical Simulation, Journal of Thermal Spray Technology. 25 (2016) 131–142. doi:10.1007/s11666-015-0308-1.

[36] V. Luzin, K. Spencer, M.-X. Zhang, Residual stress and thermo-mechanical properties of cold spray metal coatings, Acta Materialia. 59 (2011) 1259–1270. doi:10.1016/j.actamat.2010.10.058.

[37] C. Chen, H. Liao, G. Montavon, S. Deng, Nozzle Mounting Method Optimization Based on Robot Kinematic Analysis, J Therm Spray Tech. 25 (2016) 1138–1148. doi:10.1007/s11666-016-0429-1.

[38] S. Deng, H. Liang, Z. Cai, H. Liao, G. Montavon, Kinematic Optimization of Robot Trajectories for Thermal Spray Coating Application, J Therm Spray Tech. 23 (2014) 1382–1389. doi:10.1007/s11666-014-0137-7.

[39] C. Chen, Y. Xie, C. Verdy, R. Huang, H. Liao, Z. Ren, S. Deng, Numerical investigation of transient coating build-up and heat transfer in cold spray, Surface and Coatings Technology. 326 (2017) 355–365. doi:10.1016/j.surfcoat.2017.07.069.

[40] G. Wkh, L. Wkh, R. Dqg, Effect of Spray Angle on Deposition Characteristics in Cold Spraying, (n.d.) 6.

[41] Anisotropic response of cold sprayed copper deposits - ScienceDirect, (n.d.). https://www-sciencedirect-com.ezproxy.utbm.fr/science/article/pii/S0257897217312665?casa_token=-sMDWp6W5BEAAAAA:ENgNN_1Fqy2kxZCmzNwKc0r9R_Y8Irgv3Qj1-m79ScvIzhl2wY71qcmV8R5kMp3UXuSn-RthfCU (accessed August 13, 2020).

[42] F.-I. Trifa, Modèle de dépôt pour la simulation , la conception et la réalisation de revêtements élaborés par projection thermiquePplication au cas de l'alumine-rutile (Al2O3-13%TiO2) projetée à la torche atmosphérique à plasma d'arc, thesis, Besançon, 2004. http://www.theses.fr/2004BESA2023 (accessed August 13, 2020).

[43] B.S. DeForce, T.J. Eden, J.K. Potter, Cold Spray Al-5% Mg Coatings for the Corrosion Protection of Magnesium Alloys, Journal of Thermal Spray Technology. 20 (2011) 1352–1358. doi:10.1007/s11666-011-9675-4.

[44] N. Kaur, M. Kumar, S.K. Sharma, D.Y. Kim, S. Kumar, N.M. Chavan, S.V. Joshi, N. Singh, H. Singh, Study of mechanical properties and high temperature oxidation behavior of a novel cold-spray Ni-20Cr coating on boiler steels, Applied Surface Science. 328 (2015) 13–25. doi:10.1016/j.apsusc.2014.12.033.

[45] J.C. Lee, H.J. Kang, W.S. Chu, S.H. Ahn, Repair of Damaged Mold Surface by Cold-Spray Method, CIRP Annals. 56 (2007) 577–580. doi:10.1016/j.cirp.2007.05.138.

[46] B. Graf, S. Ammer, A. Gumenyuk, M. Rethmeier, Design of experiments for laser metal deposition in maintenance, repair and overhaul applications, Procedia Cirp. 11 (2013) 245–248.

[47] T. Petrat, B. Graf, A. Gumenyuk, M. Rethmeier, Laser metal deposition as repair technology for a gas turbine burner made of inconel 718, Physics Procedia. 83 (2016) 761–768.

[48] I. Kelbassa, P. Albus, J. Dietrich, J. Wilkes, Manufacture and repair of aero engine components using laser technology, in: Pacific International Conference on Applications of Lasers and Optics, Laser Institute of America, 2008: pp. 208–213.

[49] V.G. Smelov, A.V. Sotov, A.V. Agapovichev, Research on the possibility of restoring blades while repairing gas turbine engines parts by selective laser melting, in: IOP Conference Series: Materials Science and Engineering, 2016: p. 012019.

[50] S. Nowotny, S. Scharek, E. Beyer, K.-H. Richter, Laser beam build-up welding: precision in repair, surface cladding, and direct 3D metal deposition, Journal of Thermal Spray

Technology. 16 (2007) 344–348.

[51] I.L. Shitarev, V.G. Smelov, A.V. Sotov, Repair of a gas turbine blade tip by impulse laser build-up welding, in: Applied Mechanics and Materials, Trans Tech Publ, 2014: pp. 96–99.

[52] K. Ogawa, D. Seo, Repair of Turbine Blades Using Cold Spray Technique, Advances in Gas Turbine Technology. (2011). doi:10.5772/23623.

[53] Special features of reconditioning the housing of a Caterpillar diesel oil pump by gas-dynamic spraying: Welding International: Vol 30, No 1, (n.d.). https://www.tandfonline.com/doi/abs/10.1080/09507116.2015.1030152 (accessed August 13, 2020).

[54] C.A. Widener, M.J. Carter, O.C. Ozdemir, R.H. Hrabe, B. Hoiland, T.E. Stamey, V.K. Champagne, T.J. Eden, Application of High-Pressure Cold Spray for an Internal Bore Repair of a Navy Valve Actuator, Journal of Thermal Spray Technology. 25 (2016) 193–201. doi:10.1007/s11666-015-0366-4.

[55] A. Su, S.J. Al'Aref, History of 3D Printing, in: 3D Printing Applications in Cardiovascular Medicine, Elsevier, 2018: pp. 1–10.

[56] C.A.G. Lengua, History of Rapid Prototyping, in: Rapid Prototyping in Cardiac Disease, Springer, 2017: pp. 3–7.

[57] I. Gibson, D.W. Rosen, B. Stucker, Additive manufacturing technologies, Springer, 2014.

[58] W. Li, K. Yang, S. Yin, X. Yang, Y. Xu, R. Lupoi, Solid-state additive manufacturing and repairing by cold spraying: A review, Journal of Materials Science & Technology. 34 (2018) 440–457.

[59] Q. Jia, D. Gu, Selective laser melting additive manufacturing of Inconel 718 superalloy parts: Densification, microstructure and properties, Journal of Alloys and Compounds. 585 (2014) 713–721.

[60] X. Yan, R. Lupoi, H. Wu, W. Ma, M. Liu, G. O'Donnell, S. Yin, Effect of hot isostatic pressing (HIP) treatment on the compressive properties of Ti6Al4V lattice structure fabricated by selective laser melting, Materials Letters. 255 (2019) 126537.

[61] S.F.S. Shirazi, S. Gharehkhani, M. Mehrali, H. Yarmand, H.S.C. Metselaar, N.A. Kadri, N.A.A. Osman, A review on powder-based additive manufacturing for tissue engineering: selective laser sintering and inkjet 3D printing, Science and Technology of Advanced Materials. (2015).

[62] T.A. Rodrigues, V. Duarte, R.M. Miranda, T.G. Santos, J.P. Oliveira, Current Status and

Perspectives on Wire and Arc Additive Manufacturing (WAAM), Materials. 12 (2019) 1121. doi:10.3390/ma12071121.

[63] D.M. Mattox, Handbook of physical vapor deposition (PVD) processing, William Andrew, 2010.

[64] J.-P. Kruth, M.-C. Leu, T. Nakagawa, Progress in additive manufacturing and rapid prototyping, CIRP Annals-Manufacturing Technology. 47 (1998) 525–540.

[65] Brothers In Arms: These Robots Put A New Twist On 3D Printing | GE News, (n.d.). https://www.ge.com/news/reports/brothers-arms-robots-put-new-twist-3d-printing (accessed August 13, 2020).

[66] Titomic - Industrial Scale Additive Manufacturing, 3D Printing, Titanium, Innovative, Melbourne, Australia, (n.d.). https://www.titomic.com/ (accessed August 13, 2020).

[67] Unimate - The First Industrial Robot, Robotics Online. (n.d.). https://www.robotics.org/joseph-engelberger/unimate.cfm (accessed August 13, 2020).

[68] Product specification - IRB 2400, (n.d.) 60.

[69] M.M. Dalvand, S. Nahavandi, Teleoperation of ABB industrial robots, Industrial Robot: An International Journal. (2014).

[70] S. Yin, X. Wang, X. Suo, H. Liao, Z. Guo, W. Li, C. Coddet, Deposition behavior of thermally softened copper particles in cold spraying, Acta Materialia. 61 (2013) 5105–5118.

[71] A. León, E.F. Morales, L. Altamirano, J.R. Ruiz, Teaching a robot to perform task through imitation and on-line feedback, in: Iberoamerican Congress on Pattern Recognition, Springer, 2011: pp. 549–556.

[72] Y. Nagatsuka, K. Inoue, Device, method, program and recording medium for robot offline programming, 2012.

[73] S. Deng, Z. Cai, D. Fang, H. Liao, G. Montavon, Application of robot offline programming in thermal spraying, Surface and Coatings Technology. 206 (2012) 3875–3882.

[74] Robotmaster, Wikipédia. (2020). https://fr.wikipedia.org/w/index.php?title=Robotmaster&oldid=171099309 (accessed August 13, 2020).

[75] S. Deng, H. Liao, C. Coddet, Robotic trajectory autogeneration in thermal spraying, May, 2005.

[76] S. Deng, H. Liao, C. Zeng, C. Coddet, New Functions of Thermal Spray Toolkit, A Software Developed for Offline and Rapid Robot Programming, Thermal Spray 2006: Building on 100 Years of Success. (2006) 15–18.

Chapter 2

Design and implementation of modular framework for CSAM

2.1 CSAM system

2.1.1 Introduction

Generally, a CSAM system is developed based on the conventional CS system. Most traditional CS systems are focused on the application of wear or corrosion-resistant coatings, but the CSAM system is designed to produce freeform components and to restore damaged parts with a retention of the inherent coating ability. However, a CS system involves some obvious limitations. For example, the process is relatively simple, straightforward but not precise enough, and it is difficult to complete high-precision and complex manufacturing. Besides, there is a lack of accurate and effective simulation methods to guide the entire spraying process. To date, the desired coatings are basically provided by trial and error method. In addition, it is difficult to adjust the operating parameters in real-time, because the response time of the spray system is relatively long. In practice, the optimal spray parameters are usually kept constant during the spraying process, while the growth of the coating is only affected by the kinematic parameters such as the nozzle scanning speed, the spray angle and the spray distance. However, the lack of effective monitoring and intervention measures makes it difficult to control deviations and disturbances in actual spray process.

Recent advances in CS industry call for new process implementation to improve manufacturing accuracy and flexibility. To respond to this challenge, a concept of modular system is presented in this study to design and implement a new CSAM framework that can cope with many different types of products, processes, machines, and persons. The proposed CSAM system aims to integrate multiple technologies to improve the efficiency and responsiveness of the production system, as well as the reliability and quality in the production process. In addition, based on the smart manufacturing concept of Industry 4.0 [1,2], a novel approach is proposed to bring the perception and the decision-making abilities into the traditional CS system.

In the field of industry, modularization is a way to expand the capabilities of systems by building them from different subsystems (or modules) that use direct physical links or indirect event-driven methods to interconnect functional modules to achieve coupling between each other [3,4]. This concept can explain not only the structure of the entire system, but also the relationship and role of each critical element. The advantage of modularization is that it is easy to manage, maintain and upgrade, and thus to build a stable production system. It also enables

to develop and integrate new functional modules according to new development demand. In addition, to meet both the requirements of controlling production and quality, it is also necessary to integrate advanced computing and online monitoring systems, to adapt to and use the current intelligent manufacturing environment.

2.1.2 Framework structure

The current CSAM system is designed and organized as an open framework system, as shown in Figure 2.1. According to the different applications and purposes, the system is divided into five modules: spray module, robot module, in-situ measurement module, inter-process module and post-process module. However, it needs to be reminded that with the continuous development of requirements and technology, new system modules can be added and existing modules can be updated. The relationship between the modules and their main tasks provide relevant information on current and potential applications of the entire manufacturing system. Therefore, the next part will discuss current system modules. It should be reminded that these modules do not run independently, but are coupled to each other through direct physical links or indirect decentralized and event-driven manners.

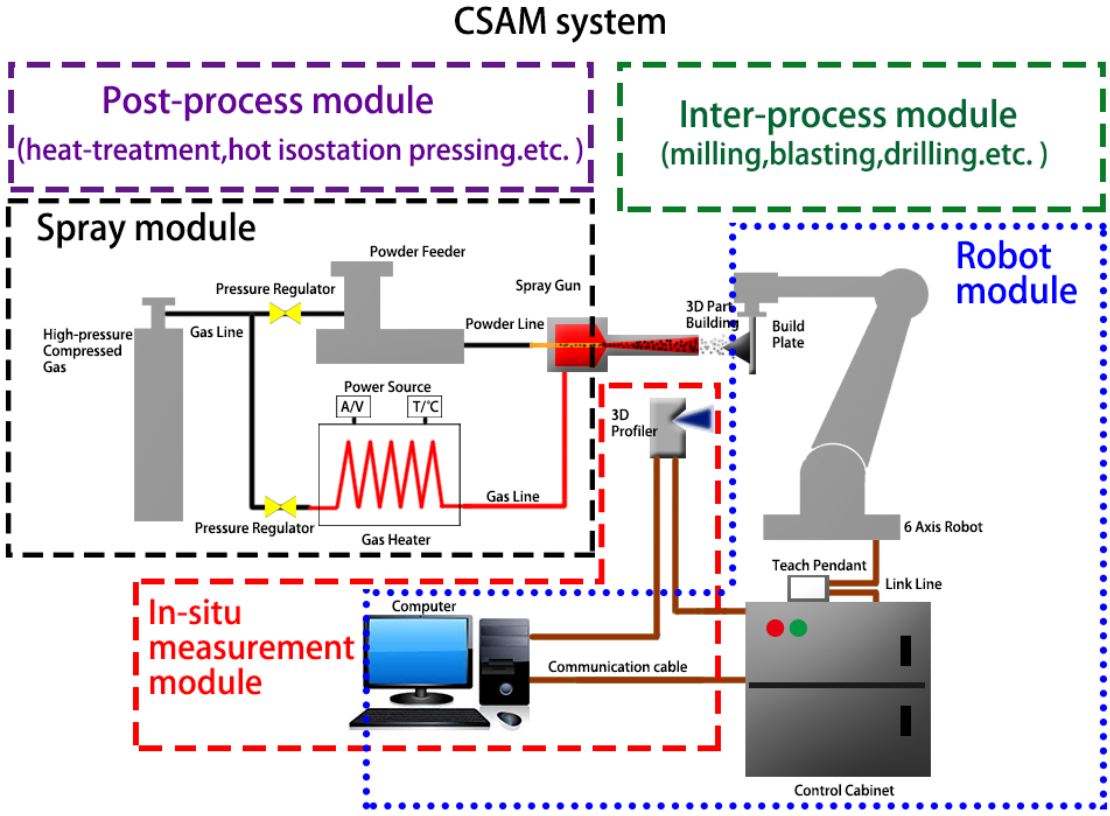

Figure 2.1 Schematic diagram of the CSAM system.

2.1.2.1 Spray module

There are two types of CS systems that are widely used in general production. One is a low-pressure portable CS system [5,6], and the other is a high-pressure CS system [5,7]. The former device is simple and easy to perform, suitable for on-site repairs. Besides, it usually obtains the coating by controlling the movement of the spray gun manually but has lower accuracy. The latter uses a robotic arm to control the spray gun movement, that enables achieving arbitrary nozzle trajectories on various complex surfaces with high precision. Compared with low-pressure portable CS systems, the high-pressure CS system has a higher upper limit of adjustable spray parameters, and can be used for more material applications with high-performance.

In this study, the CSAM system is based on a homemade CS system. As showed in Figure 2.1, the apparatus consists of high-pressure compressed gas sources, power sources, a powder feeder, a spray gun with a de Laval nozzle. The gas source can be air, argon, nitrogen, or helium. It is separated into two different gas lines: one is fed to the gas heater as propellant gas and the other is sent to the powder feeder as powder carrier gas. The main gas-flow is heated to set temperatures by the gas heater while the other one is used for powder transportation. The powder feeder can provide continuous and controllable feeding. With the help of the de-Laval nozzle, the gas is accelerated to supersonic velocity and carries powders to reach the critical velocity for bonding.

Generally, several factors affect the performance of the spraying process, such as powder materials, spraying parameters, but the design of the nozzle has the most significant influence. As we all know, the acceleration of particles in the supersonic gas jet is critical for the successful deposition of the material. Many literatures have presented the theory behind nozzle design for supersonic flow applications [8–12].

Figure 2.2 Different nozzle for CSAM.

Firstly, the commonly used CS nozzle materials are mainly metals, including stainless steel, tool steel and super-hard alloy metals, but sometimes sintered tungsten carbide materials are also used. The disadvantage of using metal materials is that the high-temperature resistance is poor.

Secondly, the working gas in the CS process is usually heated to a higher temperature, that makes it easy a powder sticking on the nozzle internal wall, especially in the "throat" of de Laval nozzle (clogging) when spraying some low melting point metal materials. This is disadvantageous due to the long spraying time required in AM.

Thirdly, the common nozzle cross-sectional shapes are round, rectangular and oval. The exit diameter of ordinary nozzles is generally in the range of 4-10 mm, so the minimum width of the spraying track is often limited to the length of the nozzle. Tabbara et al. [8] studied the effects of different nozzle cross-sectional shapes on particle distribution and velocity at the outlet, including circular, elliptical and rectangular nozzles. Xinkun SUO et al. [9] studied the influence of different basic size parameters of a rectangular nozzle on the distribution and velocity of magnesium (Mg) particles. Their studies have shown that the particle flow characteristics during acceleration are related to the final geometry of the coating, and both shape and size of the nozzle affect both number and size distribution of particles in the powder

jet.

Lastly, the particles tend to spread in the nozzle acceleration channel resulting in a wider outlet flow that makes it difficult to produce a narrow single-pass coating deposition. Therefore, new developments of spray module may rely on increased accuracy and spatial resolution by using micro-nozzles or other structural nozzles.

2.1.2.2 Robot module

The robot module involves an industrial robot arm (ABB IRB 2400 as used in this study), a robot control cabinet and a computer. It is the most automated module in the whole system. As mentioned above, Industrial robots are widely used in the field of CS due to their high performance, such as high accuracy, high repeatability, high flexibility; and low complexity such as low operating condition, ease of use, low maintenance requirement.

Generally, the most common role of an industrial robot in CS is to hold the spray gun to spray materials while the substrate is fixed in the workshop as shown in Figure 2.3 (a). However, this configuration may be not appropriate for CSAM. First, the spray gun is connected with many pipes, for example, powder line, gas line and signal cables. Intense movement of these pipes with the robot would affect the stability of the powder feeding and the signal output. Secondly, the large and heavy spray gun as well as the connected pipes will limit the robot motion, its speed, acceleration, actuator torque and work range. And most importantly, this configuration does not permit the substrate or formed part to displace in between the different processes.

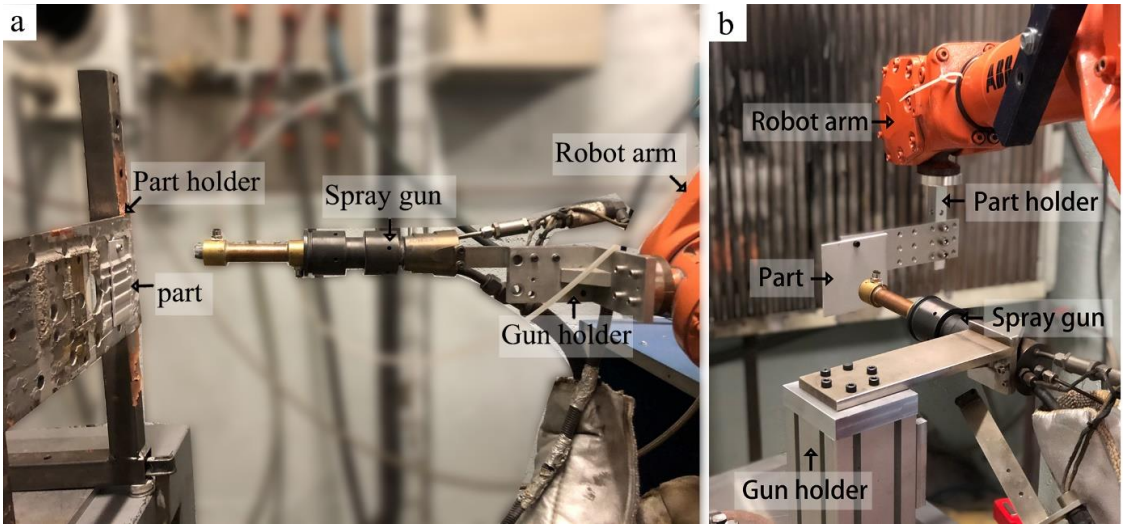

Figure 2.3 Different configuration manner: (a) the robot holds the spray gun; (b) the spray gun is fixed.

In the proposed CSAM system, the spray gun is fixed at an appropriate position while the substrate or the formed part is attached to the robot's end-effector (Figure 2.3 (b)). As the spraying equipment remains stationary, spraying conditions will be more stable. The robot arm performs not only the relative movement in between the substrate and the spray nozzle, but also the displacement of the formed part in between different processes. In addition, CSAM process can benefit from the high performance of the robot. The robot can be programmed via online teaching on-site or offline planning on the computer to perform high-precision spray trajectories for fabricating complex geometries.

The robot can also combine other technologies to fulfil the agile AM process, for example, the on-line monitor module which allows the robot to adjust the spray trajectory according to the deposition strategy in this study. Moreover, another idea is to combine the CSAM with subtractive manufacturing technologies by moving the formed part between these processes. In this case, the robot will enhance the role of the carrier to achieve the hybrid CSAM process.

2.1.2.3 In-situ measurement module

The in-situ measurement module mainly includes a 3D scanning system with a 3D scanner and corresponding software, and a computer. Normally, the 3D scanner can be optical, laser, or contact. In this study, a high-speed 3D laser profiler (LJ-V7060, Keyence, Japan) is used to perform contour scanning, data acquisition and processing, which is connected to the robot control cabinet via a computer. And the system adopts a link port to ensure the reliable high-speed communication (as shown in Figure 2.4).

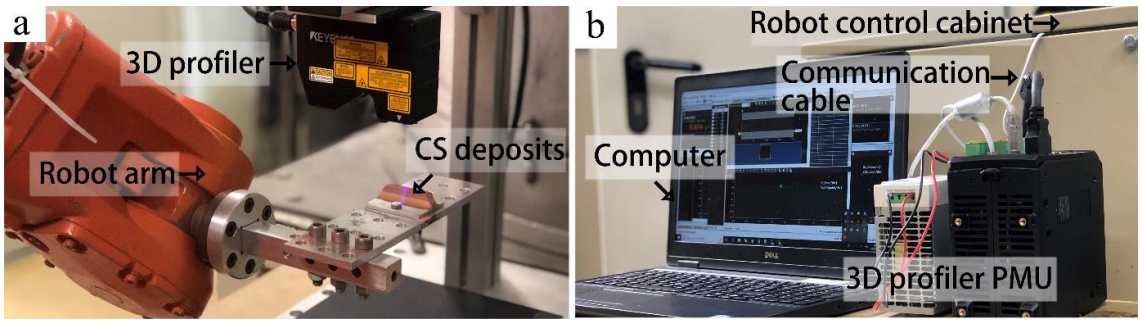

Figure 2.4 (a) CS deposits scanning via the 3D profilometer; (d) data collection and process.

Firstly, the 3D scanning system can be used for CAD modeling. In the process of robot offline programming, it is often necessary to assist the programmer through the CAD model of the workpiece to create the spray target points and to define the spray trajectory. Especially for some complicated workpieces, the corresponding CAD data is indispensable. Here, the 3D

scanning system can be used for reverse engineering modeling of complex models. The geometric data can be used for offline programming in conventional or repair CS.

Secondly, the 3D scanning system can also be used to monitor the process of CS coating deposition. As mentioned before, the spray parameters are normally kept constant during the spraying process while the coating deposition is only affected by the robotic kinematic parameters. Many studies have focused on the modeling of CS to reveal the relationship between operating parameters and as-sprayed coatings. The model is generally used to predict the coating thickness and properties so that the optimal spray strategy can be achieved. However, this method is only helpful for strategic planning in CSAM, but it cannot solve the model deviations and disturbances in the actual spray process. Here, the 3D scanner system can be used to measure, record and treat the data in the AM process. The 3D scanner measures the morphology of deposited coatings online and transfers the data to the robot controller. Then, the obtained results can be used to compare with the theoretical model to give the adaptive adjustment of the robot trajectory. These functionalities can give the robot more sensations which enable accurate and stable manufacturing. The key to this objective is an early detection, diagnosis, and correction of processing errors.

Thirdly, the 3D scanning system can be used for measuring the coating thickness. Normally, coating-thickness is an essential indicator to monitor and control. The 3D scanner can be used as a non-destructive measurement tool to scan the final coating after spraying to obtain information such as thickness, roughness, and even the geometry as a quality control in AM process.

2.1.2.4 Inter-process module

With the rapid development in recent years, the CS process has become a mature and relatively independent metal manufacturing process. However, in CSAM applications, the CS process alone cannot guarantee the material properties and geometric accuracy of the final part. To be precise, during the CS process, due to the inertial effect of the robot movement, the speed of the spray gun will be reduced when changing the direction, resulting in uneven coating distributions.

In addition, the physical processes involved in coating deposition are very complex. The stability of powder feeding and the structure of the substrate will also affect the quality and profile of the coating. The formed poor coating structure will affect the subsequent spraying

process, leading to greater and greater deviations in the quality and geometric accuracy of the coating. Therefore, the concept of hybrid manufacturing is proposed to compensate for the inherent limitations of a single process of CS.

The inter-process module is dedicated to the analysis and realization of combinations of CSAM processes and processes 'X', such as milling, drilling or other processes, which are characterized by a strong interaction with the actual CSAM process. This module will allow the combinations of CSAM with other subtractive manufacturing processes, thus becoming a hybrid AM process. Figure 2.5 illustrates the envisioned implementation in the future. When the surface undulation of the coating becomes larger or the monitored deposits no longer meet the expectations during the additive manufacturing by CS, the milling cutter will permit optimal conditions for coating deposition with desirable accuracy and reliable shape control. More investigations on the hybrid CSAM should be strongly encouraged. Future research will focus on integrating and coordinating more technologies into the inter-process module to enhance the accuracy and feasibility of the CSAM system.

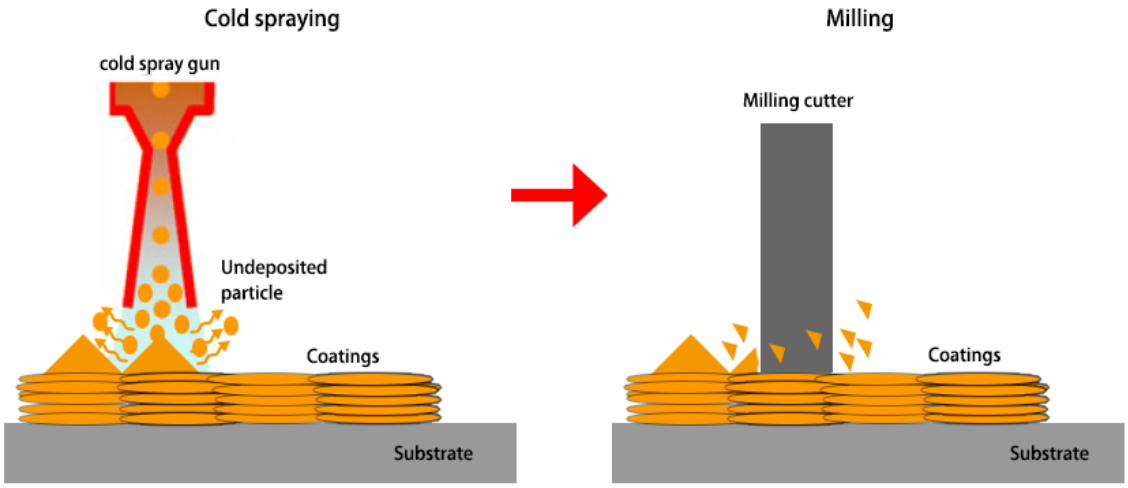

Figure 2.5 (a) Schematic representation of CS+milling process.

2.1.2.5 Post-process module

Generally speaking, CSed parts require extensive post-processing to overcome rough surface finishing. Besides, CS deposits normally have high tensile strength but very low ductility which results from the enhanced work hardening effect.

The post-heat-treatment enables to improve mechanical performance by eliminating work hardening effect, reducing the defects and achieving a proper metallurgical bonding. Some

researches about the improvement of cold-sprayed coating via heat treatment were reported [13–19]. Heat treatment can effectively change the microstructure of many kinds of CSed coatings, like Cu [14,17], Al [15,16], stainless steel coatings [18,19] and Inconel 718 [20], etc. Meanwhile, some necessary performance tests are required to check if the product is qualified in terms of failure mechanisms, residual stress, microstructure, microhardness, mechanical properties, etc.

Therefore, the post-process module is designed to improve the CSed deposits to reach the desired properties and/or geometry. The design and implementation of the post-treatment process should depend on the material and its application. For example, CSed Cu coatings usually anneal at quite moderate temperatures between 400 and 600 °C. In RZ Huang et al. 's report [17], after heat treatment of 500 °C, the interface between Cu particles disappeared and the grain of Cu coating became very uniformed and fine.

In addition, Hot isostatic pressing (HIP) [21] or friction stir welding [22] also enables to improve mechanical performance by reducing the defects and achieving a proper metallurgical bonding. Figure 2.6 illustrates the principle of HIP, which compresses materials by applying high temperature of several hundreds to 2000 °C and isostatic pressure of several tens to 200MPa at the same time. P. Petrovskiy et al [14] encapsulated HIP to reduce the porosity and to improve the mechanical properties of cold-sprayed Ti6Al4V deposits. In Tom Peat et al.'s work [23], WC-CoCr and Al2O3 reinforced MMC coatings were CSed on AISI316 and friction stir process. The results revealed that the particles were significantly refined and the particle distribution was improved over the as-deposited coatings.

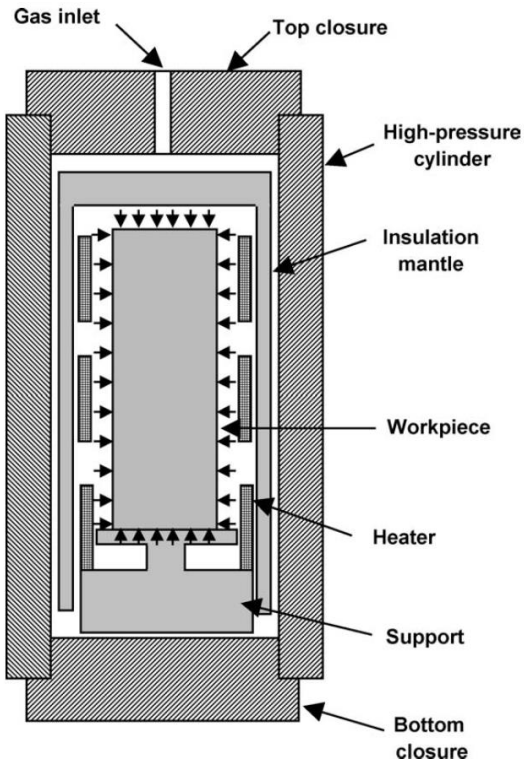

Figure 2.6 Schematic representation of common HIP process [21].

2.1.3 Manufacturing Procedure

Figures 2.7 shows the standard manufacturing procedure based on the current CSAM system. The figure also illustrates the information flow and the transmitted data between sub-systems.

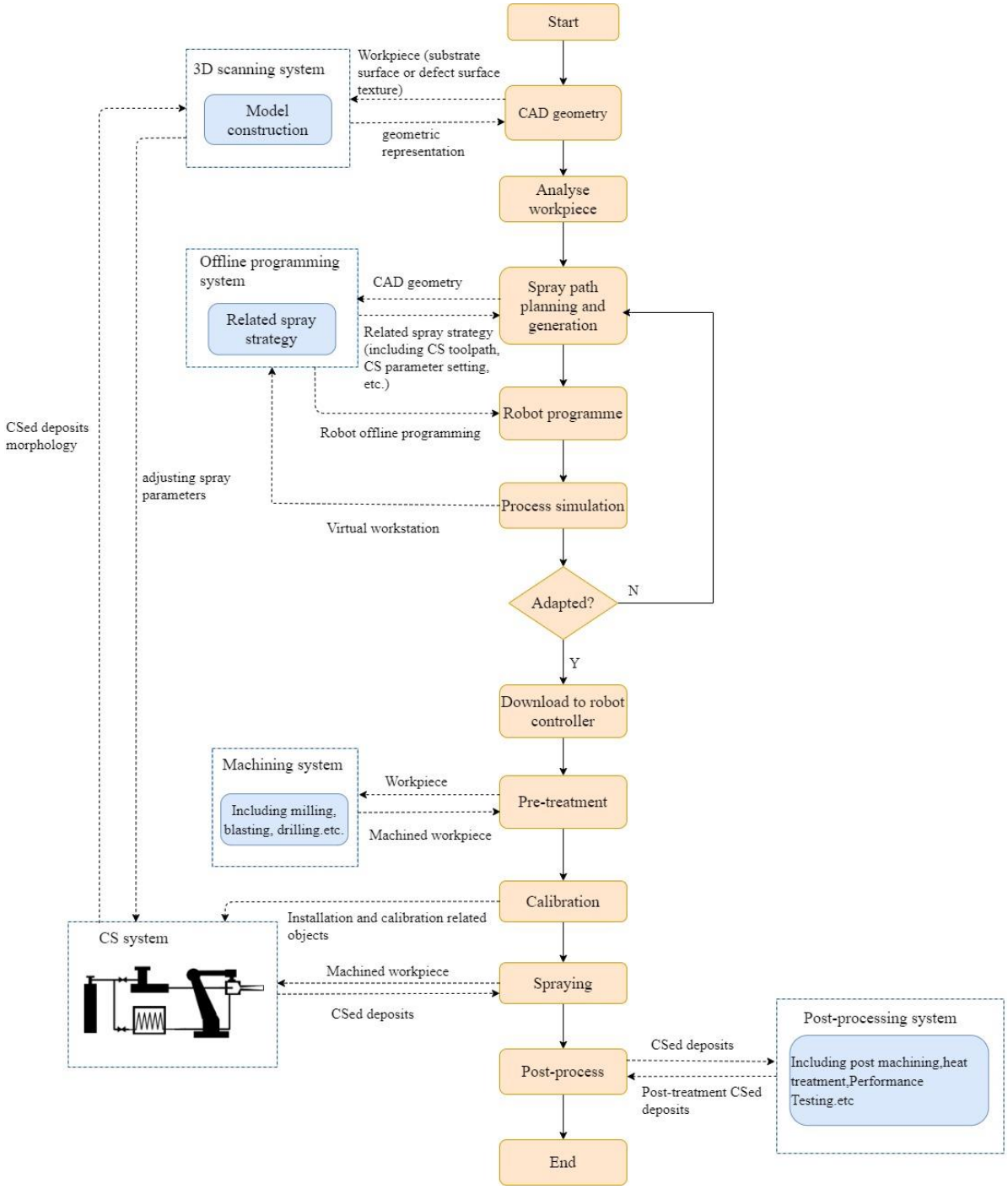

Figure 2.7 Flowchart of CSAM process.

Since the CSAM is no longer a process of producing simple coatings, Computer-aided design (CAD) and Computer-aided manufacturing (CAM) are indispensable to develop the ideal spray strategy, including trajectories generation, programming and process simulation. Whether it is spraying a coating on a complex surface, a filling material to a damaged contour, or a building a freestanding shape component, the corresponding CAD model is a necessity. Therefore, the first step is to acquire 3D geometric model. If there is no original CAD model

available, it must create one by using CAD software such as Catia (Dassault Systèmes) [24], SolidWorks (Dassault Systèmes) [25], Pro/Engineer [26] (Parametric Technology Corporation), etc. If the workpiece is too complicated to be recreated by CAD software, the acquisition of a geometric model, called reverse engineering, should be considered. The geometric information of the workpiece can be obtained by the 3D scanner. The 3D model can then be rebuilt from these measured data. This method is particularly effective for complex workpieces without CAD files.

The next step is to analyse the workpiece and formulate effective related manufacturing strategies. Robot offline programming technology is used as a new AM production capacity and modernization application to provide desirable solutions in the process. In this study, RobotStudio™, an off-line programming software developed by Asea Brown Bovrie Ltd (ABB), is used as the unique CAM software of current CSAM, which can provide graphical simulation of the robot and its work cell, kinematic models of the robot, motion planning and programming for manufacturing process. Therefore, the related spray strategy will be elaborately planned in the offline programming software, including tool path and kinematic parameter settings, etc.

After generating the related spraying strategy, the robot motion program can be created according to the planned CS tool path. The dynamic simulation of the spraying process can be carried out under the offline programming system. Through simulation and analysis, if the expected result is achieved, the generated robot program can be synchronized to the robot controller system to proceed with the next step. If not, the related spraying strategy can be adjusted with iteration in the feedback loop to achieve the desired result.

Then, the workpiece will be pre-processed (including blasting or others machining) and fixed at an appropriate position in the work spot. After a series of tests and calibrations, the CS process can be implemented. In addition to depositing materials during this process, the 3D scanning system will also be used to monitor the growth process of the coating in real-time. A complete scanning process includes the following sub-programs: creating a connection, running spray program, sending scan request, receiving returned data, judging the validity of the data, diagnosis and decision making, returning feedback information, and saving data.

In practice, after launching the spray program, the robot takes the substrate in front of the nozzle to perform the spraying. When the predefined number of cycles is reached, the spray program is interrupted and the contour scan module is activated. At this time, the robot arm

moves to the measurement window of the 3D profiler, then the robot program sends a trigger signal to the 3D profiler for scanning. The computer will receive and analyse the scanning results so that the decision-making algorithm could compare the real coating profile with the theorical model to decide the compensation value of the robot motion. The adjustment parameters of the robot trajectory will be sent back via the feedback subroutine to modify the current spray process (as shown in Figure 2.7). This approach is also applicable to many AM processes and enables the closed-loop control as well as the real-time parameter optimization to realize stable and high-accuracy AM.

After spraying, the post-processing will be carried out to improve the CSed deposits to reach the desired performance as well as precision. The desired shape and precision can be obtained after the post-machining on CSed deposits and some necessary performance tests. Here, the material characterization will be inclusive of failure mechanisms, residual stress, microstructure, microhardness, mechanical properties, etc. Meanwhile, according to materials and performance requirements, suitable heat treatment solutions will be proposed and formulated to improve the performance of the as-sprayed deposit.

2.2 Manufacturing strategy

CS is a special powder solid deposition technology. It is very important to fully consider its characteristics such as overspray and spray resolution, as well as multiple-layer deposition and edge effects, and propose appropriate manufacturing strategies. At present, many researchers have proposed some clever and effective strategies for CASM [27–30]. J. Pattison et al.[27] proposed a triangular tessellation scheme to create thick coatings or vertical walls (Figure 2.8). Besides, they also presented the fabrication of complex components containing embedded devices (Figure 2.9).

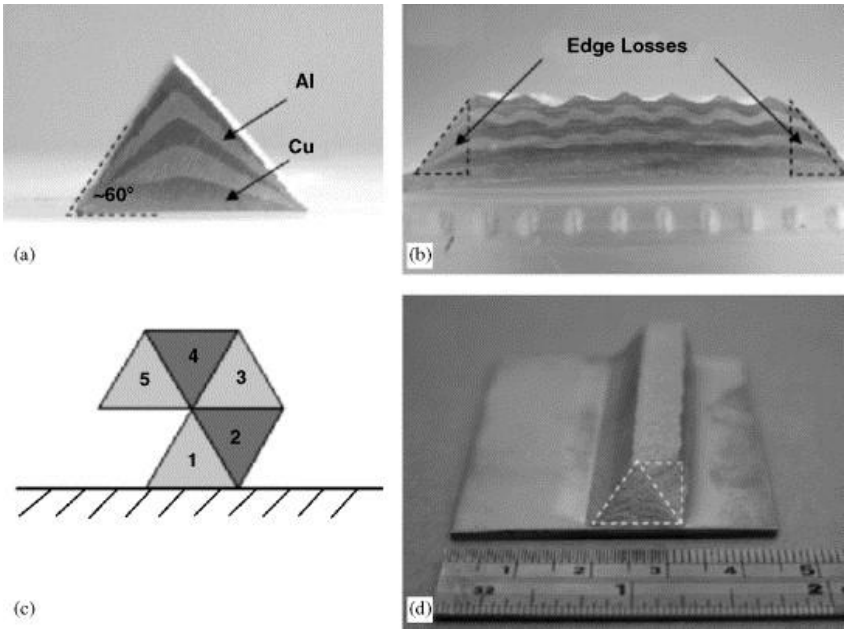

Figure 2.8 Triangular tessellation scheme for the production of primitive shapes [27].

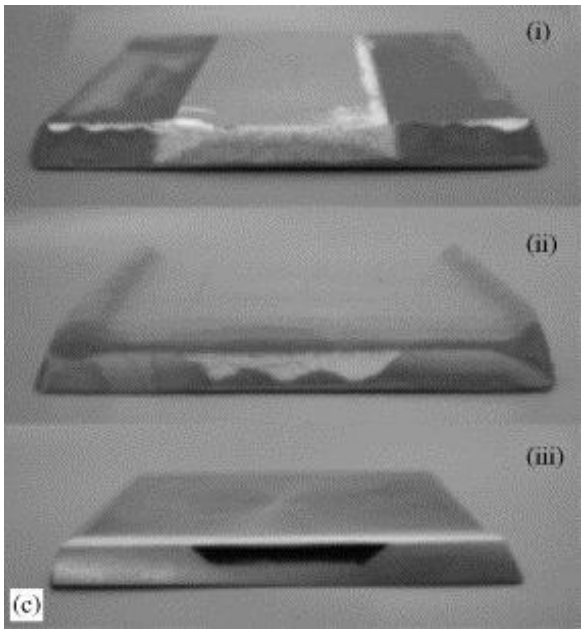

Figure 2.9 titanium component constructed with an internal channel, prepared by dissolving aluminum [27].

Lynch et al. made a significant prowess by combining the CS deposition with design and topology shape structural optimisation [30]. As shown in Figure 2.10, they proposed reliable design guidelines, from the design of the three-dimensional structure to the use of topology optimization technology and control of the nozzle trajectory for various kind of spray paths, and finally to the obtained blank and further processing to form the final shape of the bracket. In addition, they also considered the design of removable 3D support, which is very consistent

with the current mainstream 3D printing technology processing ideas.

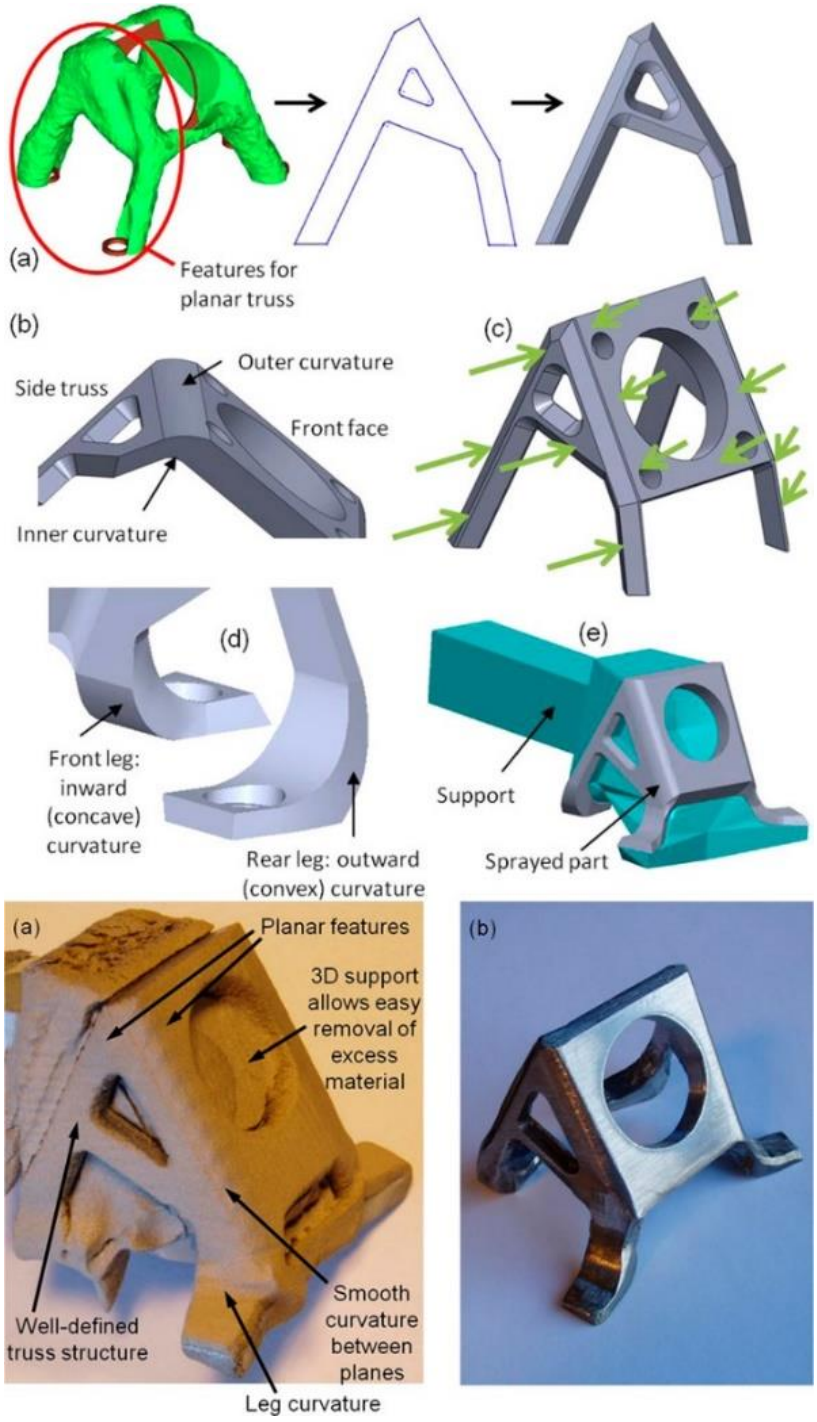

Figure 2.10 Schematic of the fabrication process of a part manufactured using CS and topology optimization technology [30].

As shown in Figure 2.11, Yannick Cormier et al. [31] used a specially designed mask to fabricate array structure that is a pyramidal fin array used for a compact heat exchanger. Their research suggests that CSAM can consider using different specially designed masks to prevent the deposition of redundant materials to allow only the deposition of the desired pattern.

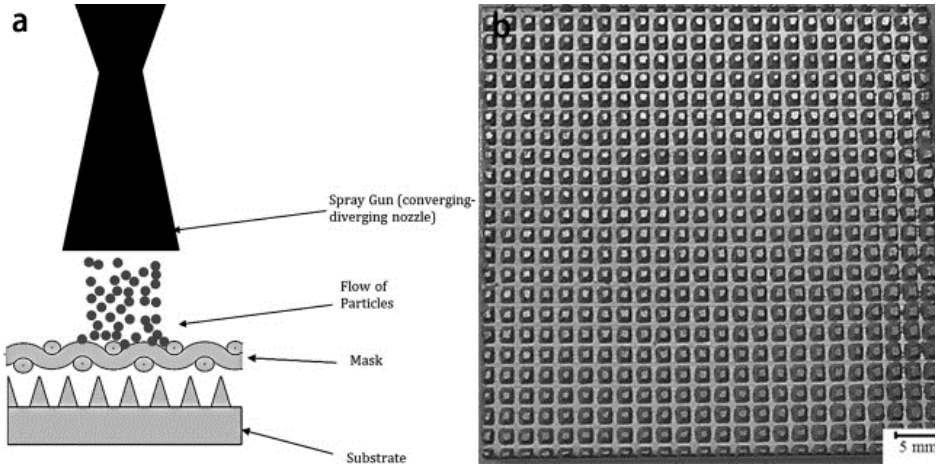

Figure 2.11 Schematic of the fabrication process of CSAM pyramidal fin arrays heat sink [31].

Based on the above discussion, improving the accuracy, reliability and ability of CS based AM or remanufacturing requires more advanced strategies with higher efficiency and more agility. This study also suggests that more research on spray strategies should be engaged. Therefore, in the next part, some manufacturing strategy for the current CSAM system will be presented.

2.2.1 Process simulation for prediction and optimization

With the continuous development of CSAM, the sprayed materials, sprayed objects and application fields are also continuously expanding. Faced with different spraying conditions, how to obtain the best spraying strategy and parameters in the shortest time is the key to realize the actual benefits of CSAM. Therefore, from the production and design concept, it is necessary to transform the design and manufacturing concept based on simulation and experience. Through advanced simulation technology, it can provide predictions of spraying results and optimize the spraying parameters to quickly and effectively guide the manufacturing process and to avoid cost waste caused by repeated trials.

In this study, the robot offline programming system, RobotStudio ™, is used for CSAM process simulation. In addition, the software Thermal Spray Toolkit (TST) [32] is used to enhance the functionality of the RobotStudio ™. As shown in Figure 2.12, a corresponding virtual workstation should be first established, which has the same configuration as the actual spray system, including the same type of robot, spray gun and tools, and the same placement in between the various elements. The advantage of the virtual robot workstation is that it can

truly reflect the actual spraying process. In addition, it is convenient to change the spraying procedure at any time and observe whether the various components interfere with each other, thereby preventing collisions between the equipment effectively.

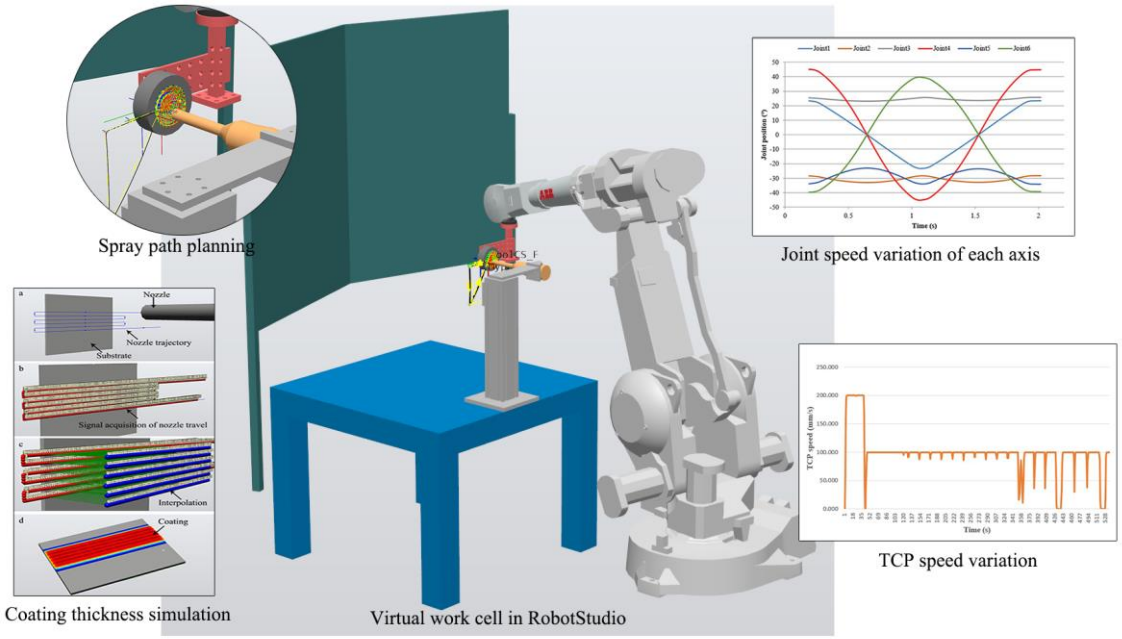

Figure 2.12 CSAM processing with RobotStudio ™.

During the process simulation, trajectory issues and speed issues are two crucial issues, especially in CSAM. Through the trajectory simulation module, it can be observed whether there is divergence in between the expected and the actual robot trajectories. Then, the spray trajectory will be adjusted and decided. Sometimes, even if the spraying target or spraying trajectory conforms to the robot's motion range due to the problem of the configuration of each robot axis, singular points will appear during the robot's motion resulting in preventing the spraying trajectory program from continuing. At this moment, the analyser module of RobotStudio™ can be used to record and analyse the position of each axis, so as to re-adjust the configuration of each axis.

Besides, the real TCP speed can be recorded by the analyser module. And the robot movement data including TCP position and orientation versus time can also be recorded in real-time by the monitoring module of TST. As we all know, the actual TCP movement is important to guarantee the desired coating shape or coating profile. For the purpose of effective CSAM, it is of great importance to determine the dependence of operating parameters such as spray angle, nozzle traverse speed, scanning step and standoff distance on the coating thickness

distribution.

In this study, a 3D model of the coating profile based on Gaussian distribution was developed and integrated into the off-line programming software RobotStudio™ as a module in the software TST. It enables the coating thickness simulation based on the operating parameters in the spray process, robot trajectory and robot kinematic data obtained by process simulation. More detail of the principle and entire development process will be presented in Chapter 3.

2.2.2 Spray method for stable layer building

One of the most crucial issues in fabricating components by AM is to enable controllable and stable layer building. However, in the CSAM, the triangular-like profile is a typical shape produced by continuous spraying. CS single-track changes gradually from a thin coating with high deposition efficiency to a triangle-like profile with low deposition efficiency. This CS unique characteristic and constraint would be reflected throughout the process, thereby limiting the application of CSAM to a certain extent.

In this study, the topology technique is proposed to enhance stable layer building. As shown in Figure 2.13, by changing the spray direction (tilting the nozzle), material deposits on the aside surface of the previous thin coating (<0.5mm) to compensate for the thickness difference in between the middle and side of the deposit. Then, the setting of the best parameters for stable layer construction can be found by using the developed simulation codes. In this way, the volume can be formed via the layer-by-layer manner.

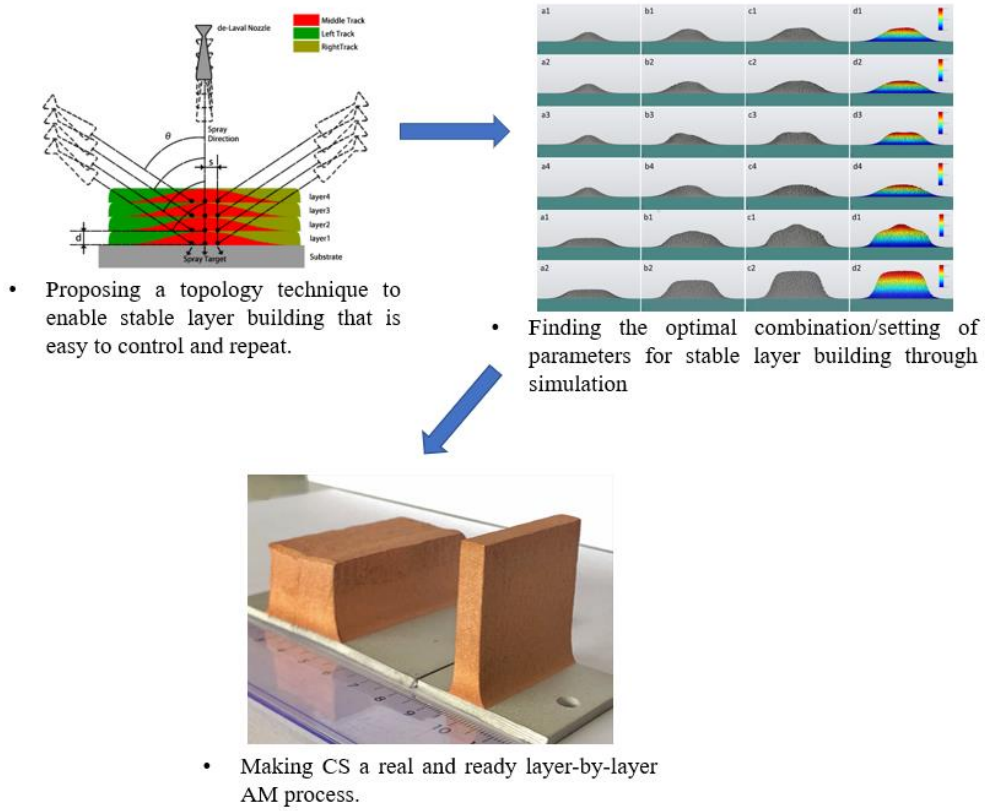

Figure 2.13 Scheme of layer-by-layer CSAM process.

Currently, the CSAM process adopts a six-axis robot arm to hold the substrate for spraying. In this case, the substrate is tilted instead of the nozzle. This method is closer to the AM principle and it is easy to improve repeatability and subsequent process control, making CS a real layer-by-layer AM process. More background principles and the entire development process will be introduced in detail in Chapter 4.

2.2.3 Online measurement and monitoring

As mentioned above, the 3D scanning system can be used to online monitor the process of CS coating deposition. In actual practice, as the CS deposits height increases, the morphology of the component and its mechanical properties are significantly affected. However, stable layer building is a key issue in AM process. In the current CSAM system, the morphology of layers is measured in real-time with the help of the 3D profiler. The in-situ measurement of layer morphology through conventional spraying and topological technology are shown respectively in Figure 2.14 (a) and (b).

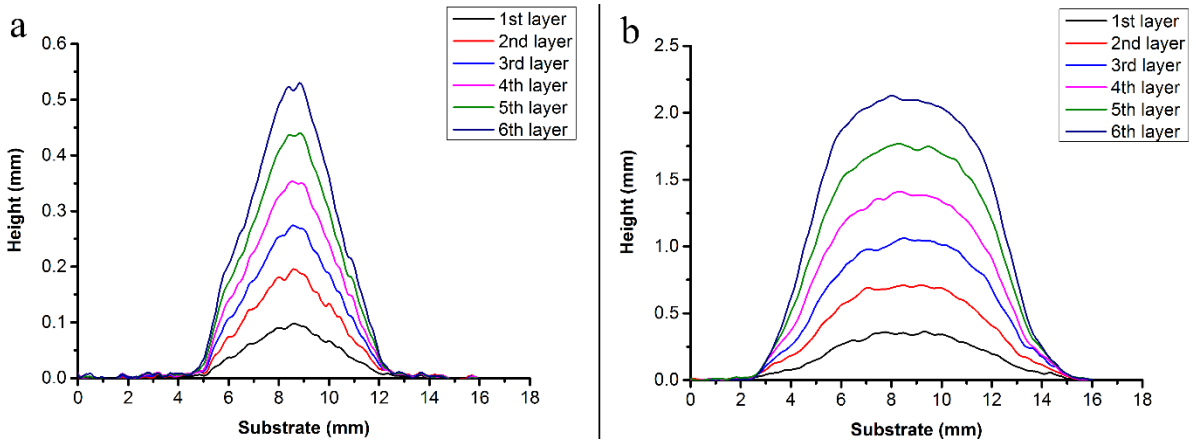

Figure 2.14 Measuring the layer morphology in real-time: (a) by normal spraying; (b) by topology technique.

The advantage of this method is that it helps to understand the characteristics of single track under different spraying parameters, and provides a basis for proposing more effective spraying strategies by storing, processing and analysing the collected data. Besides, the motion parameters are modified according to the feedback of the measurement results, including the spraying angle and spraying distance.

By adjusting the robot motion, it is possible to compensate for the shape formed by spraying and stabilize the fabrication in a pre-set way. As shown in Figure 2.15, a preliminary attempt was made to adjust the deposits to the desired shape using an online adaptive control method. In the future, the system can decide whether and where to machine the part according to the scanning results, and then continue spraying to achieve a hybrid additive.

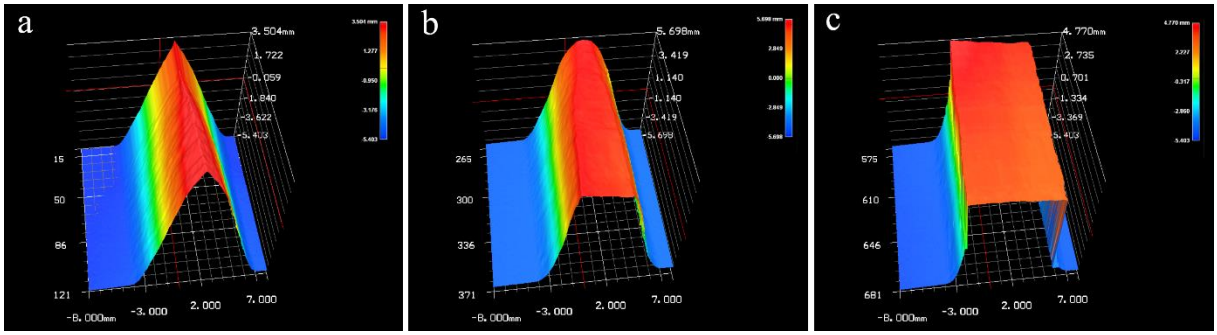

Figure 2.15 (a) result of normal spraying; (b) result of the current spraying strategy (with deviations and disturbances); (c) result of on-line adaptive control.

2.3 Conclusion

In this chapter, the new CSAM system is presented based on the traditional CS system. Here, the modular framework is proposed for the implementation of a new process to enhance CS based AM. It is revealed that modular system is suitable to revolutionize the CSAM method and conduction. The elemental composition of the current system is introduced. The relationship between the modules and their main tasks provide relevant information on current and potential applications of the entire manufacturing system. Besides, the newly added online adaptive control module provides a feasible and practical method for the traditional CS industry to implement AM through a smarter and more flexible manufacturing method to improve product quality and system reliability. However, to fully exert the potential of CSAM, efforts are still required to integrate and coordinate more technologies. Future research will focus on improvements for each component of the framework and on developing more spray strategies for CSAM.

References

[1] C.J. Bartodziej, The concept industry 4.0, in: The Concept Industry 4.0, Springer, 2017: pp. 27–50.

[2] A. Rojko, Industry 4.0 concept: background and overview, International Journal of Interactive Mobile Technologies (IJIM). 11 (2017) 77–90.

[3] M. Sharp, B.A. Weiss, Hierarchical modeling of a manufacturing work cell to promote contextualized PHM information across multiple levels, Manufacturing Letters. 15 (2018) 46–49.

[4] H. Seol, C. Kim, C. Lee, Y. Park, Design process modularization: concept and algorithm, Concurrent Engineering. 15 (2007) 175–186.

[5] A. Kay, J. Karthikeyan, Advanced cold spray system, 2003.

[6] R. Maev, V. Leshchynsky, E. Strumban, Portable, low pressure cold spray systems for industrial applications, in: The Cold Spray Materials Deposition Process, Elsevier, 2007: pp. 217–231.

[7] Review of Relationship Between Particle Deformation, Coating Microstructure, and Properties in High-Pressure Cold Spray | SpringerLink, (n.d.). https://link-springer-com.ezproxy.utbm.fr/article/10.1007/s11666-017-0575-0 (accessed August 31, 2020).

[8] H. Tabbara, S. Gu, D.G. McCartney, T.S. Price, P.H. Shipway, Study on process optimization of cold gas spraying, Journal of Thermal Spray Technology. 20 (2011) 608–620.

[9] X.K. Suo, T.K. Liu, W.Y. Li, Q.L. Suo, M.P. Planche, H.L. Liao, Numerical study on the effect of nozzle dimension on particle distribution in cold spraying, Surface and Coatings Technology. 220 (2013) 107–111.

[10] A.P. Alkhimov, V.F. Kosarev, S.V. Klinkov, The features of cold spray nozzle design, Journal of Thermal Spray Technology. 10 (2001) 375–381.

[11] W.-Y. Li, H. Liao, H.-T. Wang, C.-J. Li, G. Zhang, C. Coddet, Optimal design of a convergent-barrel cold spray nozzle by numerical method, Applied Surface Science. 253 (2006) 708–713.

[12] W.-Y. Li, H. Liao, G. Douchy, C. Coddet, Optimal design of a cold spray nozzle by numerical analysis of particle velocity and experimental validation with 316L stainless steel powder, Materials & Design. 28 (2007) 2129–2137.

[13] K. Spencer, M.-X. Zhang, Heat treatment of cold spray coatings to form protective intermetallic layers, Scripta Materialia. 61 (2009) 44–47.

[14] P.S. Phani, D.S. Rao, S.V. Joshi, G. Sundararajan, Effect of process parameters and heat treatments on properties of cold sprayed copper coatings, Journal of Thermal Spray Technology. 16 (2007) 425–434.

[15] M.R. Rokni, C.A. Widener, V.K. Champagne, G.A. Crawford, S.R. Nutt, The effects of heat treatment on 7075 Al cold spray deposits, Surface and Coatings Technology. 310 (2017) 278–285.

[16] A.C. Hall, D.J. Cook, R.A. Neiser, T.J. Roemer, D.A. Hirschfeld, The effect of a simple annealing heat treatment on the mechanical properties of cold-sprayed aluminum, Journal of Thermal Spray Technology. 15 (2006) 233–238.

[17] R. Huang, M. Sone, W. Ma, H. Fukanuma, The effects of heat treatment on the mechanical properties of cold-sprayed coatings, Surface and Coatings Technology. 261 (2015) 278–288.

[18] B. Dikici, H. Yilmazer, I. Ozdemir, M. Isik, The effect of post-heat treatment on microstructure of 316L cold-sprayed coatings and their corrosion performance, Journal of Thermal Spray Technology. 25 (2016) 704–714.

[19] A.-M. Bandar, P. Vo, R. Mongrain, E. Irissou, S. Yue, Effect of heat treatment on the microstructure and mechanical properties of stainless steel 316L coatings produced by cold spray for biomedical applications, Journal of Thermal Spray Technology. 23 (2014) 641–652.

[20] W. Sun, A. Bhowmik, A.W.-Y. Tan, R. Li, F. Xue, I. Marinescu, E. Liu, Improving microstructural and mechanical characteristics of cold-sprayed Inconel 718 deposits via local induction heat treatment, Journal of Alloys and Compounds. 797 (2019) 1268–1279.

[21] M.H. Bocanegra-Bernal, Hot Isostatic Pressing (HIP) technology and its applications to metals and ceramics, Journal of Materials Science. 39 (2004) 6399–6420. doi:10.1023/B:JMSC.0000044878.11441.90.

[22] R.S. Mishra, Z.Y. Ma, Friction stir welding and processing, Materials Science and Engineering: R: Reports. 50 (2005) 1–78.

[23] T. Peat, A. Galloway, A. Toumpis, P. McNutt, N. Iqbal, The erosion performance of cold spray deposited metal matrix composite coatings with subsequent friction stir processing, Applied Surface Science. 396 (2017) 1635–1648.

[24] CATIA, Wikipédia. (2020). https://fr.wikipedia.org/w/index.php?title=CATIA&oldid=174497863 (accessed September 9, 2020).

[25] https://wwww.solidworks.com/, SOLIDWORKS. (n.d.). https://wwww.solidworks.com/ (accessed September 9, 2020).

[26] Pro/ENGINEER | PTC, (n.d.). https://www.ptc.com/en/products/creo/pro-engineer

(accessed September 9, 2020).

[27] R.N. Raoelison, C. Verdy, H. Liao, Cold gas dynamic spray additive manufacturing today: Deposit possibilities, technological solutions and viable applications, Materials & Design. 133 (2017) 266–287.

[28] S. Yin, P. Cavaliere, B. Aldwell, R. Jenkins, H. Liao, W. Li, R. Lupoi, Cold spray additive manufacturing and repair: Fundamentals and applications, Additive Manufacturing. 21 (2018) 628–650.

[29] J. Pattison, S. Celotto, R. Morgan, M. Bray, W. O'neill, Cold gas dynamic manufacturing: A non-thermal approach to freeform fabrication, International Journal of Machine Tools and Manufacture. 47 (2007) 627–634.

[30] M.E. Lynch, W. Gu, T. El-Wardany, A. Hsu, D. Viens, A. Nardi, M. Klecka, Design and topology/shape structural optimisation for additively manufactured cold sprayed components: This paper presents an additive manufactured cold spray component which is shape optimised to achieve 60% reduction in stress and 20% reduction in weight, Virtual and Physical Prototyping. 8 (2013) 213–231.

[31] Y. Cormier, P. Dupuis, B. Jodoin, A. Corbeil, Net shape fins for compact heat exchanger produced by cold spray, Journal of Thermal Spray Technology. 22 (2013) 1210–1221.

[32] S. Deng, Z. Cai, D. Fang, H. Liao, G. Montavon, Application of robot offline programming in thermal spraying, Surface and Coatings Technology. 206 (2012) 3875–3882.

Chapter 3

Cold spray process modeling and simulation

3.1 Introduction and state of the art

As mentioned in the previous chapters, CS is a newly solid-state material deposition technology which can prepare a variety of functional coatings for many applications in surface technology. The CSed coating has received more and more attention due to its low porosity, high adhesion strength, and low particle oxidation that makes this technology potentially very competitive in the manufacturing industry for durable products [1]. In particular, high deposition rates and efficiencies make this surface technology efficient for AM and structural repairing [2,3]. In practice, various spray coatings for complex components such as turbine blades and vanes also require a good distribution of coating thickness. Indeed, meeting the requirements of coating thickness distribution is critical for the performance and the in-service life of components. Traditionally, the desired coating thickness has been provided by trial and error method. In this process, there are many methods for assessing the coating thickness, such as destructive tests or direct mechanical measurements. However, they are all performed after spraying that mostly makes those approaches time-consuming and expensive.

Nowadays, in order to simplify and speed up the coating development, simulation technology for CS processes was proposed and developed, particularly for component-based simulations that concern coating-thickness distributions, heat and stress distributions. For example, Ju et al. [4] developed a continuous micro mechanic model for depicting the interplay relating heat, solidifying pattern and stress/strain curve, so that thermo-mechanic actions and residual stress can be forecasted in spraying processes. Liu et al. [5] studied the heat and mechanic behaviors of plasma sprayed coatings during the manufacturing process by developing a 3D multilayer model.

Generally speaking, the objective of coating thickness simulation is to optimize the robot trajectory so that the coating can be evenly deposited on the surface of the substrate or variably deposited on different regions of a specified surface, e.g. coating turbine blades requiring diverse coating thicknesses. To date, there has been a series of studies focusing on the coating deposition model in cold spray [5–9]. Duncan et al. [8] optimized the robot path by creating the

required coat thickness over the surface. They proposed a flow rate distribution function to describe the behavior of the nozzle, and the coating deposition was represented by mass, which was measured by multiplying a mass flow rate and working time with a flow rate distribution formula. Based on the model proposed by Duncan, Kout et al. [7] aimed at searching a successive time-dependent array of nozzle configuration for creating the desired coating thickness. The difference of the newly proposed method was that the coating deposition was represented by its height which was calculated by multiplying the volume flow rate with flow rate distribution formulae.

However, none consider the actual robot kinematic parameters in their model, such as the spray distance and the spray angle, which are key factors affecting the deposition efficiency (DE). Sadovoy et al. [10] developed a self-constant model based on mass conservation principle. This model considers the effects of the actual processing parameters and spraying conditions. However, it only involves the influence of the spray angles as a single processing parameter on the coating profile. The effect of other processing parameters, e.g., spray distances and nozzle travel speeds were not investigated. Cai et al. [11] used a symmetric Gaussian distribution curve to characterize the single-coat profile. They proposed a concept of flatness to illustrate their homogeneity coating thickness. However, they did not explain the flatness of the coating in the case of 3 dimensions. To fix this problem, C. Chen et al. [9] proposed a numeral model of the single coat profile to discuss the effects of gun turn angle, nozzle pass speed, and scanning step on the cold sprayed coating thickness distribution. However, their model excluded the impact of spray distance.

Wiederkehr et al. [12] reported a method to obtain a 3D flow distribution model by testing coating profiles. However, the analysis was limited to the case of flat surfaces and did not involve other more complex shapes such as a curved surface. Djurić et al. [13] presented a self-consistent way for counting the mass rate distribution function, efficiency, and cone angle during spraying. They simulated the space mass flux distribution generated out of the nozzle by developing a spraying deposition model. However, no typical applications were shown to

validate the model in their report. In Stepanenko's [14] report, a method was developed to compute feed rate control laws, which can provide production of uniform coating-thickness or coating-thickness variation predefined laws. Hansbo et al. [15] proposed a spraying cone model to optimize the coating-thickness for rotationally symmetric components. However, this model was not validated for a layer by layer process on complex components where concave surface features may exist. Chen et al. [16] used an FEA (finite element analysis) model to simulate transient coating accumulated processes and heat evolutions during cold spraying. However, using finite element analysis or numerical methods to simulate the coating deposition process, such as ANSYS and MATLAB, always requires meshing the part, and then calculating the coating thickness and assigning the final result to each node of the grid. As the nozzle moves, the coating thickness of each node will be continuously updated. Therefore, such an approach must be based on the same dimension and a continuous grid and cost much computation. For the substrates with a large radius of curvature or discontinuous surface regions, it would not be suitable.

Based on this review, it is easy to conclude that most of the coating-thickness simulations mainly focus on the development of coating-thickness models. The experimental process is generally an operation of numerical model superposition for which it is difficult to show the behaviour of coating stack and the macroscopic appearance of final coating distributions intuitively. The calculation of the coating thickness should not be just a simple addition of specific numerical value because the physical processes involved in coating deposition are very complex. The deposition efficiency impacted by the different parameters should not be ignored. More notably, there are still no effective ways to simulate and predict the coating thickness distribution on complex surfaces with a ‘shadow effect’. Shadow effect means that some convex features on the substrate obstruct the flight path of particles to other convex or concave shapes, which is illustrated in Fig. 3.1.

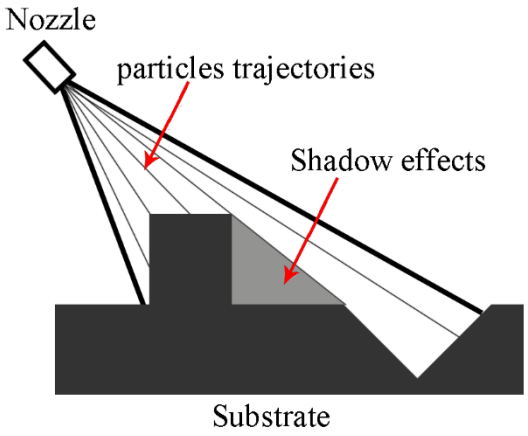

Figure 3.1 Coating condition of shadow effect.

In this study, a new approach was developed and added to the off-line programming software for simulating coating thickness in CS, especially for the prediction of shadow effects. This method uses a numerical model of coating profile based on Gaussian distribution to construct a real-time evolving 3D profile geometric model on the coating substrate. The coating profile model includes the facts of various spray parameters, such as nozzle traverse speed, spray angle and spray distance. Afterward, the coating thickness model was integrated into the off-line programming software RobotStudio™ as a module in the software Thermal Spray Toolkit (TST) [17]. It enables the coating thickness simulation based on the operating parameters in the spray process, robot trajectory and robot kinematic data obtained by process simulation, and then displayed on the graphic interface of RobotStudio™. According to the results of the simulation, the robot trajectory, operating parameters and spray strategy can be adjusted with iterations in the feedback loop to achieve the desired coating thickness distribution. Both numerical and experimental verifications were presented in this chapter. The results show that this proposed method has a reliable prediction accuracy.

3.2 Coating profile model

3.2.1 Single coating profile modelling

The model describing the feedstock jet distribution out of the nozzle is essential for the

calculation of the coating-thickness distribution. According to the central limit theorem, the averages of random variables can be considered as normally distributed when the amount of variable is sufficiently large. Thus, in cold spray process, the coating-thickness distribution also known as coating profile can be expressed by a Gaussian approximation according to the following equation [9,11]:

$$\varphi = \zeta(\theta)\zeta(s)\int_0^T \left(\int \frac{A\zeta(v)}{\sigma\sqrt{2\pi}} e^{-\left(\frac{(x-\mu_x)^2}{2\sigma^2}+\frac{(y-\mu_y)^2}{2\sigma^2}\right)} dxdy\right)dt \qquad \text{Eq. 3-1,}$$

where A is the amplitude factor in relation to the feedstock flow rate obtained from experimental result, σ is the standard deviation of the coating profile, (μx, μy) is the centre coordinate of the coating profile on the substrate surface. ζ(θ), ζ (s) and ζ (v) are deposition efficiencies depending on the spray angle, the spray distance, and the nozzle traverse speed, respectively. The values of each variable are obtained through experiments for a certain powder/substrate material system and spray parameters.

The model proposed by Chen [9] which was illustrated in 2-dimensional polar coordinates is a typical representative case. In this study, the model is described in a 3-dimensional Cartesian coordinate system. As shown in Figure 3.2, the nozzle is defined as a point in the Cartesian coordinate system. The angle of incidence, i.e. spray angle, is θ (on X-Y plane). In the YZ plane, the spray cone in the Cartesian coordinate system is divided into a series of rays with a constant interval angle. Exemplary rays are dash lines in Figure 3.2. For perpendicular spraying, the coating profile is conical and symmetric with respect to the central line of the nozzle. Thus, the spray length at the same deflection angle is constant. For example, at the deflection angle ψ as indicated in Figure 3.2, the spray length AB has the same value as ab, and the angle in between these two rays is γ. Due to the fact that mass distribution out of the nozzle is constant, it can be assumed that the spray length at each deflection angle is constant during inclination. For example, when the XY plane rotates around the x-axis (now the spray angle is β on the X1-Y1 plane), as indicated in Figure 3.2, the spray length AB has the same value as CD.

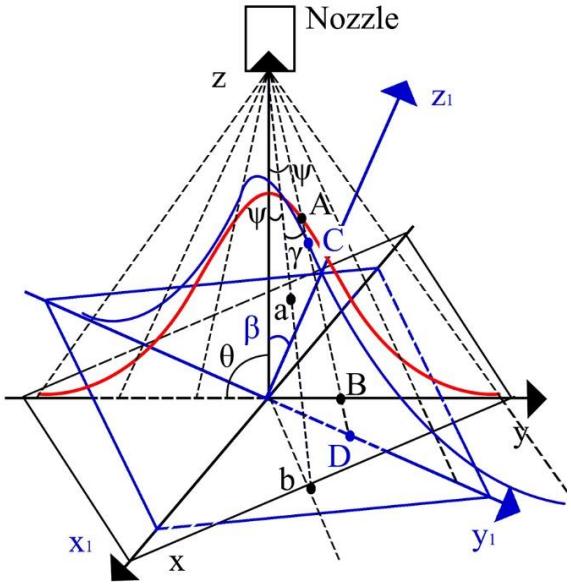

Figure 3.2 Schematic of single coating profile model on X-Y plane (red line) and X1-Y1 plane (blue line). θ and β are the spray angle on X-Y plane and X1-Y1 plane respectively. a is the angle between Z axis and Z1 axis. ψ is the deflection angle (the angle between Z axis and ab line, as well as AB line). γ is the angle between ab line and AB line.

In computer graphics and computational physics applications, an object can be represented by a three-element vector which is typically used to describe a position, normal and Euler rotation. In addition, a transformation (rotation and translation) can be described by a matrix from a three-element vector and a quaternion. Related knowledges can refer to Annexes behind. In order to express the coating profile model in a 3-dimensional graphics environment while maximally preserving the characteristics of the spraying, the following assumptions are proposed in this study.

Firstly, powders are ejected from the nozzle and deposited on the surface of the workpiece during the motion of the nozzle. Therefore, these particles can be considered as a finite number of rays sharing the same starting point. As shown in Figure 3.3 (a) and Figure 3.3 (d), a specific point at a certain distance above the surface of a body is created to represent the outlet of the nozzle. Then from this point, many straight rays are created. These rays are obtained by rotation and symmetric operation of the centreline, which is the vertical line from the starting point to

the body surface. The rays will intersect the substrate to create intersections. In this way, it will be possible to determine the effective area for generating the coating profile on any shape of the substrate.

Secondly, a single coating profile consists of a finite number of cylinders with the same diameter, and the height of each cylinder equals the value of the corresponding Gaussian function. As shown in Figure 3.3 (b) and Figure 3.3 (e), based on the intersection, circles will be created and stretched in the opposite direction of the ray to form a cylinder. The distance stretched is equal to the spray length. The smaller the radius of the cylinder is, the higher the accuracy of the simulation results will be. However, the calculation will be time-consuming. This study uses a cylinder with a radius of 0.02 mm.

Thirdly, the cylinders are established only where the rays touch. Therefore, the coating profile can be in a myriad of shapes, even non-continuous. As shown in Figure 3.3 (c) and Figure 3.3 (f), a number of regular cylinders is composed as a single coating profile model. Although it is created based on the Gaussian model, its final profile is determined by the shape of the substrate.

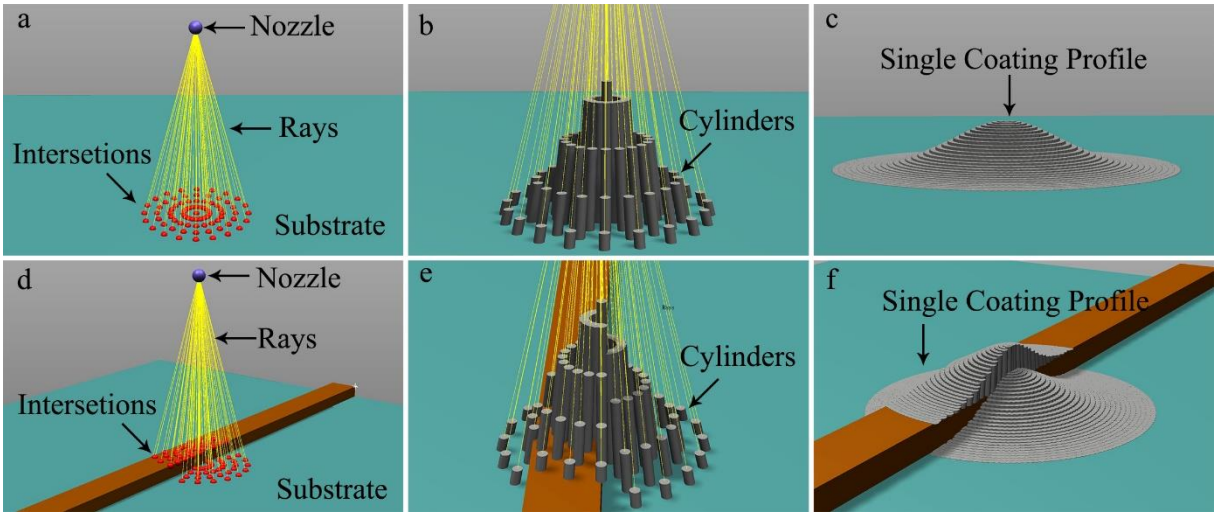

Figure 3.3 (a) Creation of rays and intersection on a flat; (b) Creation of cylinders on a flat; (c) Single coating profile model on a flat; (d) Creation of rays and intersection on a non-planar; (e) Creation of cylinders on a non-planar; (f) Single coating profile model on a non-planar.

3.2.2 Continuous coating profile model

Normally, a set of continuous random variables can be discretized according to certain rules. In order to simulate the deposited coatings on the substrate during the nozzle motion, we assume that the continuous coating profile is a collection of single coating profiles. Figure 3.4 shows the schematic of the coating thickness distribution model. By selecting the appropriate distance between two discrete points, it can create the coating distribution model deposited on the substrate under the traveling of the nozzle. An appropriate distance value is important for the thickness simulation result due to the fact that a large distance value can lead to a less accurate result and a small one can lead to excess computation. Based on the results of trial and error, as long as the distance is less than σ, a continuous coating profile close to the actual situation can be obtained. In this study, the distance between two discrete points was set to σ/2.

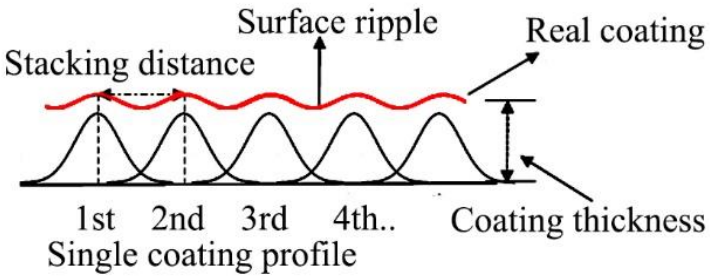

Figure 3.4 Schematic of coating thickness distribution model.

In three-dimensional graphic environment, a continuous coating profile model can be created based on the principle of creating a single coating profile model. As shown in Figure 3.5, the first single coating profile will be created on the substrate, Then the second single coating profile will be created on the substrate and overlap with the first single coating profile, and so forth. Finally, by selecting a stacking appropriate distance, continuous coating topography can be created on any topographic substrate, such as on a flat surface in Figure 3.5 (b), curved surface in Figure 3.5 (c) and complex surface in Figure 3.5 (d).

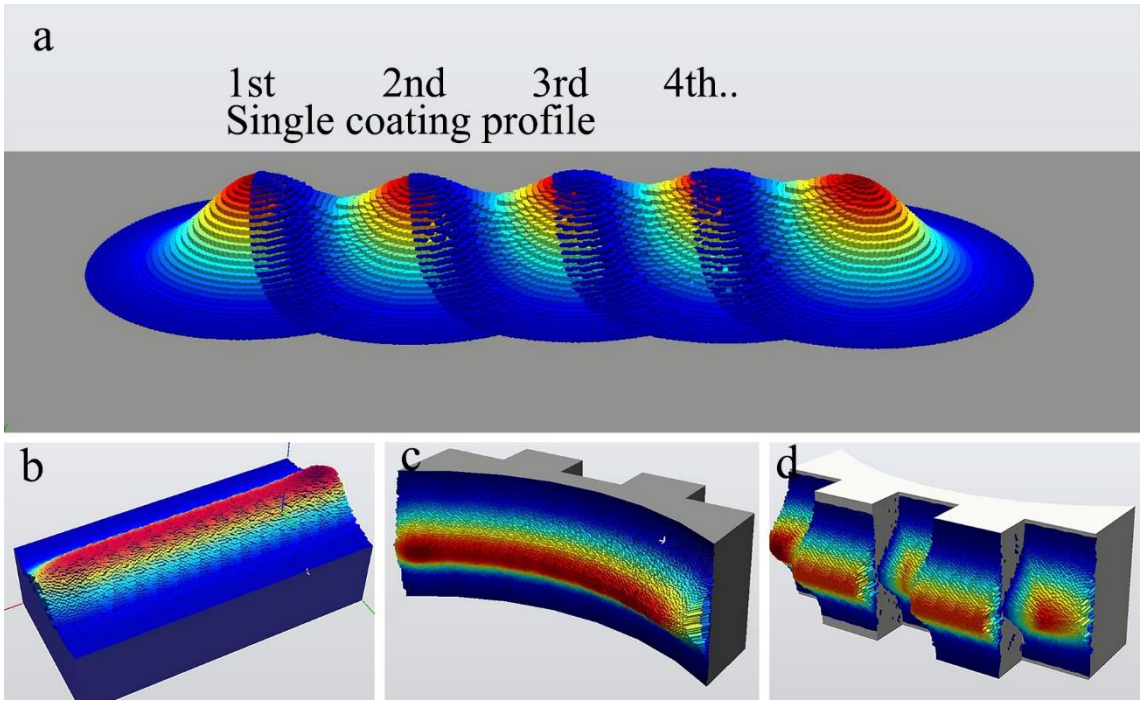

Figure 3.5 (a) Discrete single coating profile with overlaps; (b) Continuous single coating profile on a flat; (c) Continuous single coating profile on a curved surface; (d) Continuous single coating profile on a complex surface.

3.3 Effects of operating parameters on coating thickness

Generally, the CS operating parameters can be classified into several categories: the energy parameters, powder injection parameters and kinematic parameters. Among these parameters, the kinematic parameters are controlled by the robot, such as the speed of the torch, spray distance, scanning step, etc., which directly affect the accuracy of the as-sprayed coating shape or coating profile. Obviously, it is of great importance to determine the dependence of operating parameters such as spray angle, nozzle traverse speed, scanning step and standoff distance on coating thickness distribution. Normally, they change the coating profile and thickness by affecting the deposition efficiency. Gilmore et al. [18] defined it as the rate of the mass of the deposited particles to the overall mass of the spray particles. In practice, deposition efficiency is a systematic variable, and the factors influencing the whole process are very complicated. Among them, the deposition behaviors and deposition mechanisms of particle play an important

role. Nowadays, substantial research has been carried out to understand the deposition of particles. For example, Assadi et al. [19,20] proposed that the occurrence of bonding can be illustrated by shear instability. Li et al. [21] examined the effects of spray angle and particle size on the critical velocity. Prisco [22] described the relation between maximized deposition efficiency and the particle velocity and heat of impact in the cold spray process through a developed mathematical model. In order to study the effects of the spray operating parameter on coating thickness and to validate the proposed coating thickness modeling, the experimental study on cold spray was carried out. The detailed process will be introduced in the next section.

3.3.1 Experimental details

In this study, the relative deposition efficiency and peak correction factor based on experiments are used to characterize the coating profile model under different operation parameters, including spray angle, spray distance and nozzle traverse speed. Experiments were performed by using the CSAM system that was presented in Chapter 2. The pure 7075Al powder with a near-spherical morphology was used to spray on Al substrates. The microstructure of powder and the particle size were displayed in Figure.3.6 a and Figure.3.6 b respectively. High-pressure compressed air was used as the propellant gas with a temperature of 550 °C and a pressure of 2.8 MPa. Compressed argon was used as the powder carrier gas. A coating deposited by single nozzle path was made to study the effects of the spray angle, the spray distance and the nozzle traverse speed on a single coating profile. Hence, three groups of tests were carried out: the first one was for testing the effects of spray angle; the second one was for testing the effects of nozzle traverse speed; the third one was for testing the effects of spray distance. Table 3.1 lists the detailed description of operating parameters. A profile meter (LJ-V7000, Keyence, Japan) was used to measure the individual spray pass thickness after spraying.

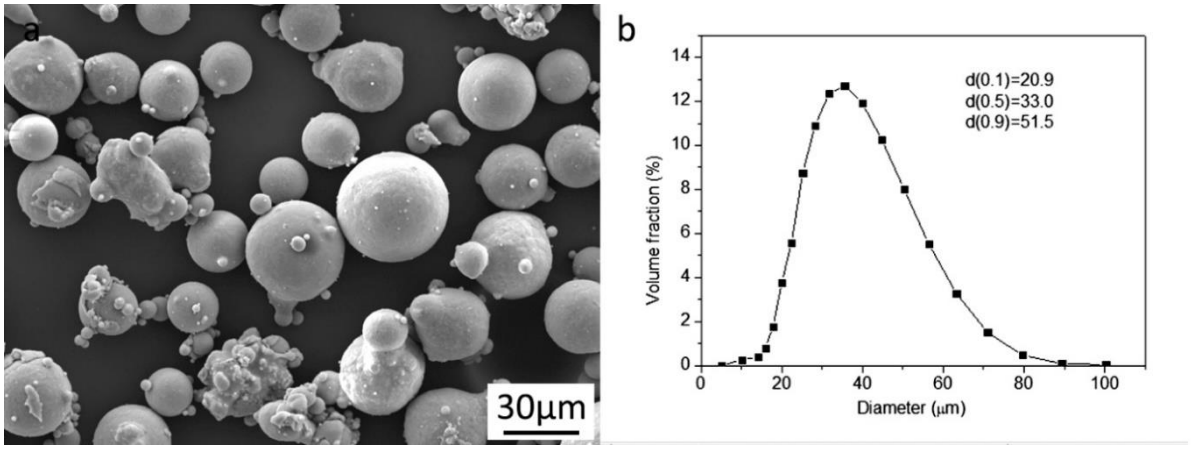

Figure 3.6 (a) SEM photos of Al7075 powder used in experiments (b) the particle size of Al7075 powder used in experiments.

Table 3.1 Operating parameters used for effect analysis of the different robot kinematic parameters.

Group	**Nozzle traverse speed (mm/s)**	**Spray angle (°)**	**Spray distance (mm)**	**Scanning pass***
1	50	50-90	30	20
2	20~ 100	90	30	10
3	50	90	10~45	10

*Scanning pass is the number of times that the nozzle moves along the same track.

3.3.2 Effects of spray angle

The effects of the spray angle of 90°, 80°, 70°,60° and 50° on a single coating profile were investigated in the first test group. The results were measured and shown in Figure 3.7. In practice, the spray angle affects not only the deposition efficiency but also the shape of the coating-profile. It can be noticed that decreasing of spray angle reduces the maximum thickness and influences the profile distribution.

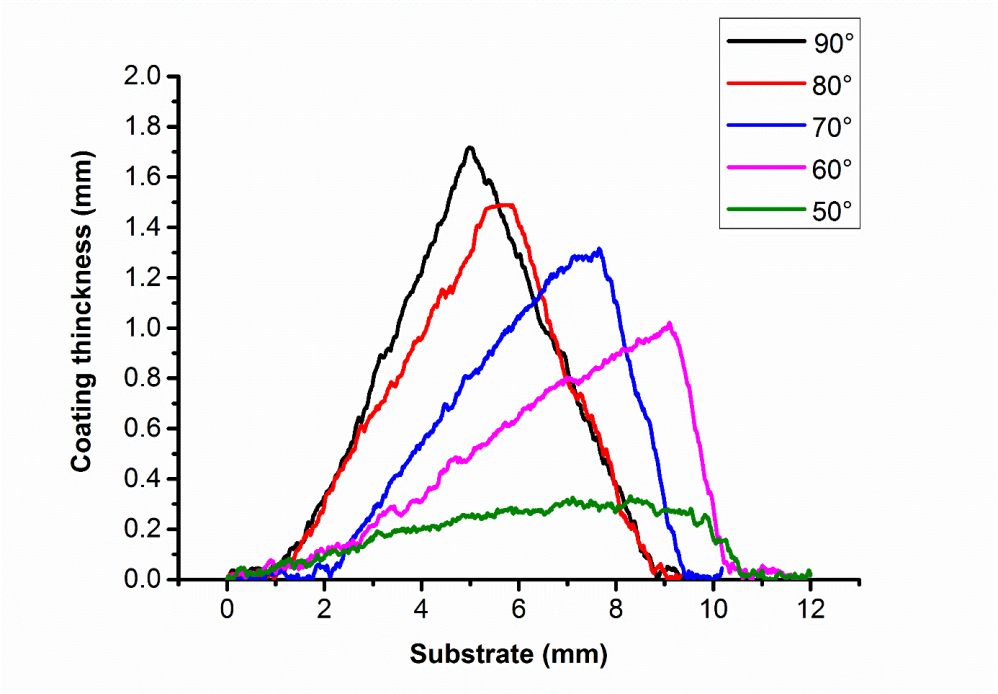

Figure 3.7 Results of coating thickness distribution at spray angle of 90°, 80°, 70°, 60°, 50° respectively.

Then, the weights of the substrate and substrate + coating before and after spraying were measured. The difference between the two measurements is used to calculate the relative deposition efficiency of different spray angles. It is assumed that the relative deposition efficiency is 100% when the spray angle is 90°. The results are given in Figure 3.8. The maximum deposition efficiency can be obtained for a spray angle between 80° and 90°. As for the spray angle between 60° and 80°, a rapid drop of deposition efficiency can be observed because of increased tangential impacting velocity (of the powders) that increases the possibility of particle rebound from the substrate, and decreases thereby the bonding strength between the substrate and the coating. As the spray angle decreases below 60°, the relative deposition efficiency falls down to the minimum value. It can be expected that the deposition efficiency will be zero due to a further decrease of the spray angle. Similar results can be found in Li [23] and Chen [9] reports. In addition, in order to obtain the expression of $\zeta(\theta)$ in Eq 3-1, a polynomial (degree = 4) was used to get a fit function, which was displayed in Figure 3.8.

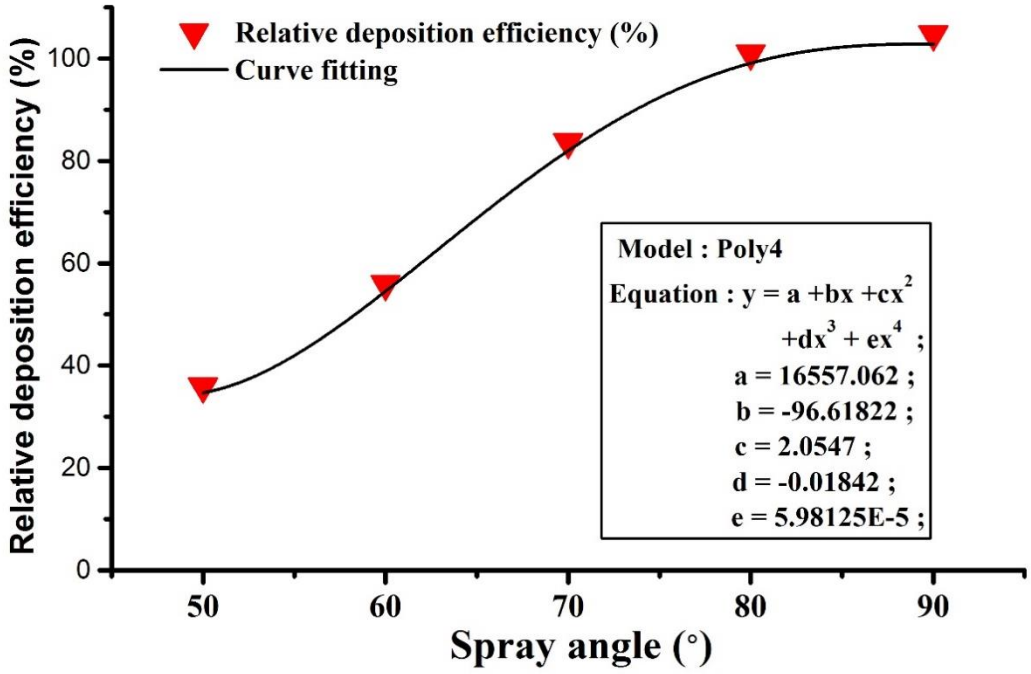

Figure 3.8 Effects of spray angle on weight gain and relative deposition efficiency of 7075 Al coating.

3.3.3 Effects of nozzle traverse speed

The effects of nozzle traverse speed on the maximum coating thickness were studied in the second test group. Previous studies have revealed that the nozzle traverse speed has little effects on deposition efficiency during cold spraying [9]. However, the nozzle traverse speed has a prominent influence on coating thickness. Figure 3.9 shows that the maximum coating thickness decreases with increased nozzle traverse speed, that means less powder was deposited for a higher nozzle traverse speed. This is because, under different nozzle traverse speeds, the amount of particle deposition is different per unit time. In order to obtain the expression of $\zeta(v)$ as in Eq 3-1, it is assumed that the PCF equals to 100% when the nozzle traverse speed is 50 mm/s, and the linear fitting function can be obtained for $\zeta(v)$ (as shown in Figure 3.9).

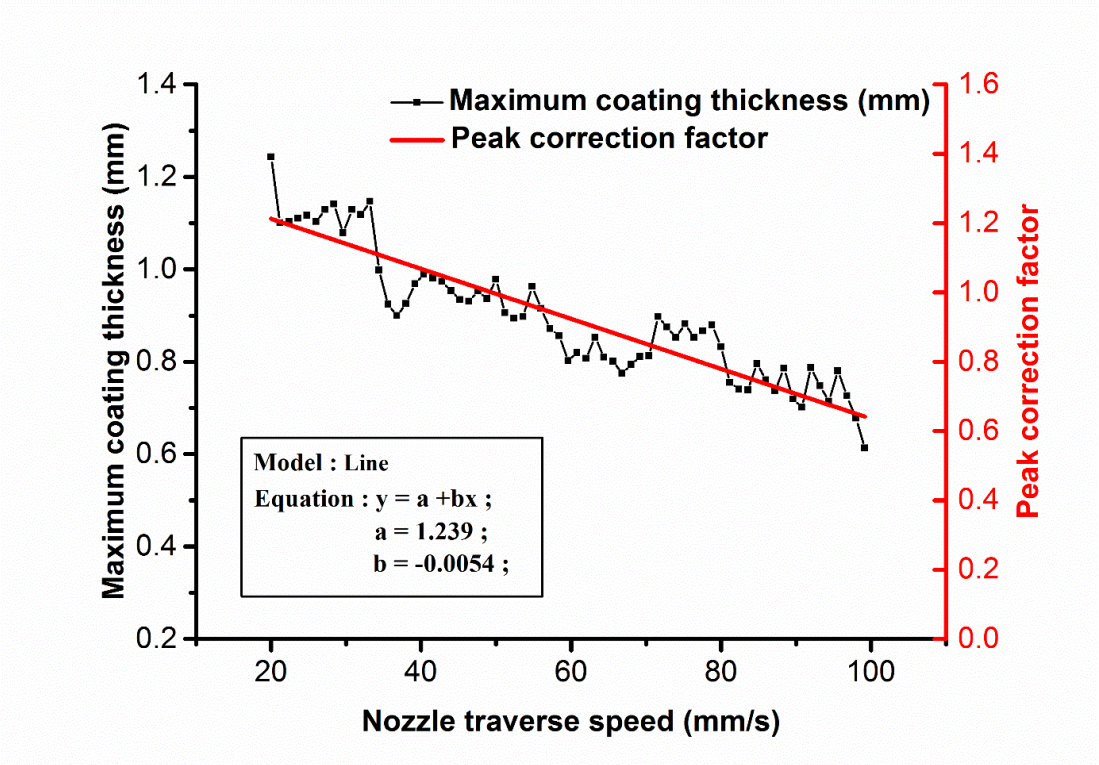

Figure 3.9 Effects of Nozzle traverse speeds (20–100 mm/s) on coating thickness and peak correction factor of Al7075 coating.

3.3.4 Effects spray distance

The effects of the spray distance on a single coating profile were investigated in the third test group. According to the literature [21,24,25], one of the most important factors that affects the coating formation is the critical particle velocity. During the cold spray process, the spray distance cannot be ignored due to the acceleration of the particles between the nozzle outlet and the substrate. Li et al. [26] have also investigated the effects of spray distance on coating deposition property in cold spray. Van Steenkiste et al. [27] reported the decrease of deposition efficiency for Al powder as the spray distance varies from 19 to 38 mm. In this study, the relative deposition efficiency for 7075Al powder changes from 10 to 45 mm. It was determined that the spray distance of 30 mm corresponded to a DE of 100% (Figure 3.10). The deposition efficiency raises as the spray distance increases and then is reduced. This phenomenon can be explained by the behavior of particle acceleration under different spray distances. In addition, a model of cubic was used to get a fit function as ζ (s) to explain the variation of particle velocity depending

on the spray distance (Figure 3.10).

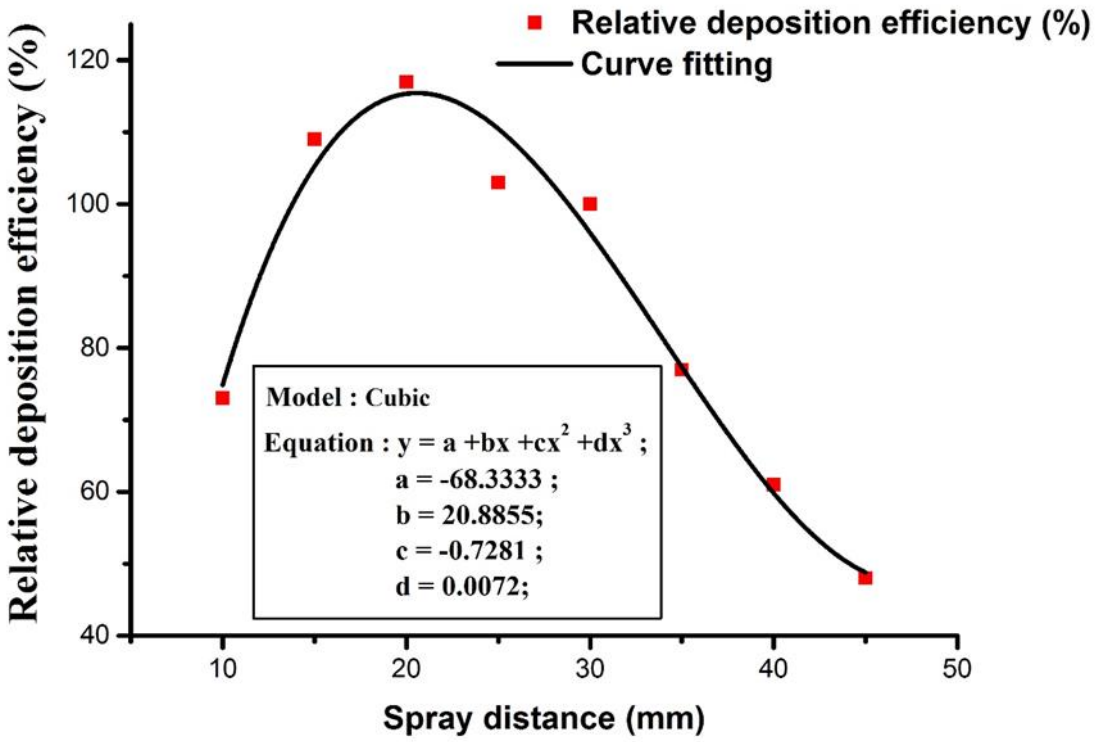

Figure 3.10 Effects of spray distance (from 10 to 45 mm) on coating thickness and relative deposition efficiency of 7075Al coating.

3.4 Evaluation of coating thickness by ProfileKit

As mentioned in Chapter 1, the add-in software package TST developed RobotStudio™ aims to provide a complete solution for the robotic cold spray process [17]. TST consists of four modules: PathKit, ProfileKit, MonitorKit and KinemaKit. Among these modules, PathKit enables the creation of robotic trajectories according to the geometry of workpiece; ProfileKit module is developed for the purpose of the coating deposition simulation; MonitorKit monitors the speed and trajectory of the robot; KinemaKit is used to optimize the kinematics parameters during the spraying process by collecting and analyzing various signal data of the robot's motion. Meanwhile, the functions of TST are constantly being updated and improved.

In this study, the developed 3D geometric coating thickness model is integrated to

ProfileKit. Compared with previous work [9,11], the evolving geometric 3D model is used instead of the numerical simulation so that it can be used for coating simulations with shadow effects. The Gaussian model is improved by introducing the robot kinematic data such as spray angle, real-time nozzle traverse speed and spray distance. The visualized operation effect can intuitively and quickly understand the coating thickness and its whole distribution. In the following sections, the simulation application and its process will be introduced. Both numerical and experimental verifications were carried out to validate its reliability.

3.4.1 3D Coating thickness simulation under RobotStudio™

As mentioned in the previous chapter, RobotStudio™ is a powerful off-line programming software that enables very realistic simulations on robot motion. It makes use real configuration files and robotic programs identical to those used on the spray shop. RobotStudio™ not only has a wealth of features available to users but also provides the interface to develop customized applications. Therefore, it is possible to develop an application program to simulate the deposition of coatings and the distribution of coating- thickness in the framework of RobotStudio™. In this study, an add-in program was developed in C# (programming language of Microsoft™ Company) and the data exchange with RobotStudio™ is based on API functions provided by RobotStudio™[28]. The user interface (UI) of the coating simulation application shown in Figure 3.11 consists of four panels that refer to different operation steps, including basic parameters setting, coating thickness simulation and measurement. It is available for users to focus on coating-thickness calculation and simulation in cold spraying.

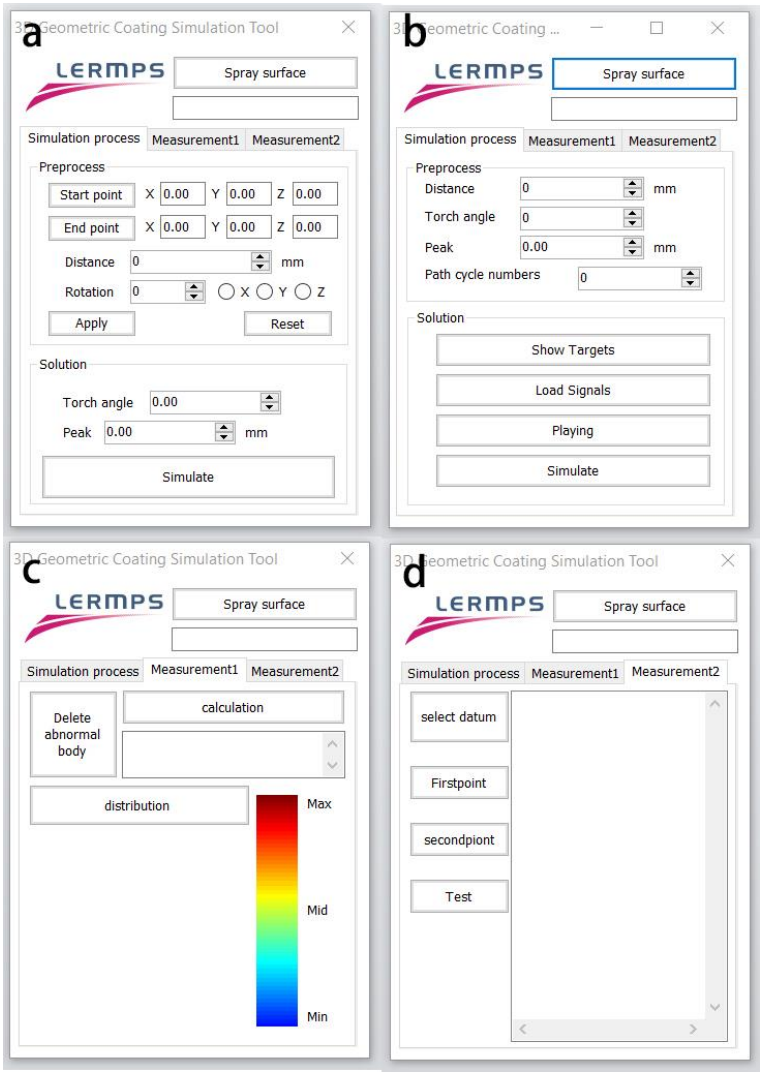

Figure 3.11 The user interface:(a) for basic parameters setting and coating simulation; (b) for coating simulation base on the real robot kinematic data; (c) for measuring the coating thickness; (d) for measuring the coating thickness.

A general coating thickness simulation process is displayed in Figure 3.12. First of all, a corresponding CAD file of the component is needed in the process of coating simulation. The formats of CAD models such as IGES, STL, STEP, ACIS, and ASCII are available in Robotstudio™. After a calibration of the component position and the TCP, the robotic trajectory is generated according to the operating parameters including spray angle, nozzle traverse speed, projection spray distance, scanning step and so on. Here, PathKit of TST can be used to generate trajectories on the surface of workpieces with different kinds of geometric shapes, including the rectangular surface, circular surface, curved surface, rotation of a workpiece. Figure 3.12 (a) is

a simple zigzag path created on a flat substrate.

After that, the corresponding robot path program will be created and run. During the robot path simulation in RobotStudio™, the speed, the position as well as the orientation of the nozzle will change with the robot movement (Figure 3.12 (b)). These signals can be recorded to generate discrete points on the path for coating thickness simulation. However, the virtual Robotic controller system in RobotStudio™ collects the data every 24 ms. The distance in between two collected points is the product of nozzle traverse speed and time step. Table 3.2 listed the distance in between two discrete points under different TCP speeds. Thus, an appropriate distance is significant for coating simulation, that is, because a large distance gives rise to a less accurate outcome and a small one leads to excessive calculation. In this study, the distance between two consecutive points for calculation should not be larger than σ (the standard deviation of coating coating-profile). Therefore, it is necessary to interpolate a certain number of points between two adjacent points if their distance is greater than σ. Figure 3.12 (b) shows discrete points consisting of remaining points and interpolation points after calculation. Finally, according to these discrete points, a 3D coating distribution model can be generated on the surface of the substrate (Figure 3.12 (d)).

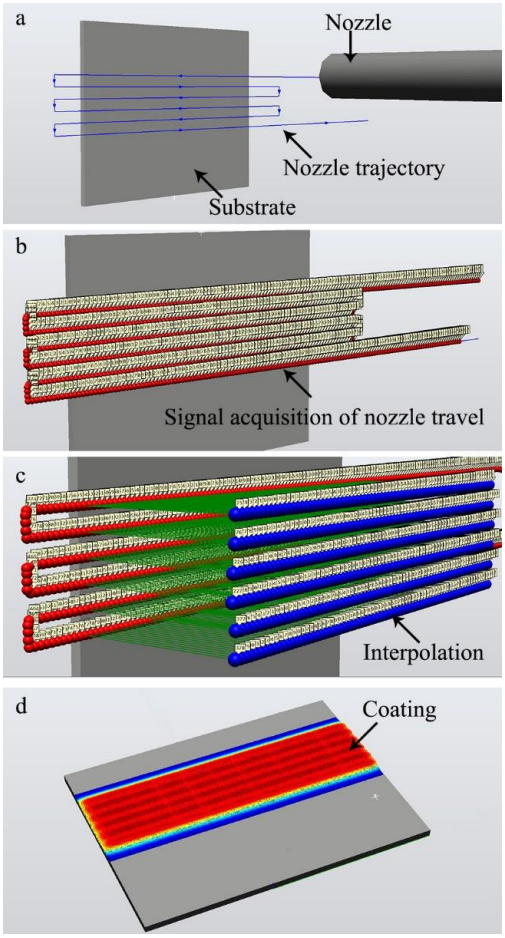

Figure 3.12 Coating thickness simulation in RobotStudio™. (a) Generation of trajectory; (b) Signal of nozzle travel; (c) target points for coating thickness simulation; (d) Coating thickness distribution.

Table 3.2 Distance between two discrete points under different TCP speeds.

TCP speed (mm/s)	**Distance between two discrete points (mm)**
1000	24
800	19.2
500	12
200	4.8
100	2.4
50	1.2
20	0.48

For the coating thickness measuring process, two ways are provided to characterize the thickness of the simulated coating. By selecting the measurement position, the coating thickness,

which is the shortest distance between the measurement position and the substrate, will be automatically calculated and displayed in the graphical virtual environment (Figure 3.13 (a)). The thickness of the coating is represented by colors and its range is demonstrated by a color bar. The second way is to use a plane with an optional direction to intersect the coating and obtain the cross-sectional profile (Figure 3.13 (b)). After that, the distance from each point on the cross-sectional profile to the substrate is calculated and exported as a text file for further processes, such as data processing and drawing charts, etc.

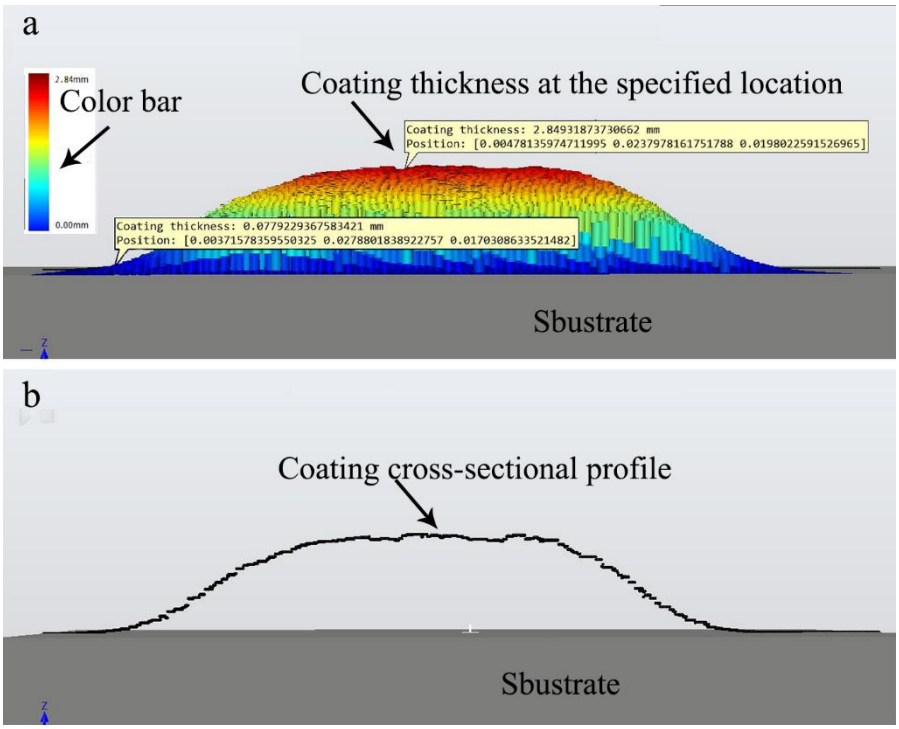

Figure 3.13 Calculate and measure coating thickness. (a) coating thickness at the specified location; (b) coating cross-sectional profile.

3.4.2 Experimental evaluation

In order to evaluate the predictive capabilities of this newly developed approach, both simulation and experimental investigations were carried out in this study. The pure 7075Al powder (Figure 3.6) was used as feedstock to coat Al substrates made of different shapes. One is a plate (84×63×3 mm) to verify the thickness model on flat geometries and the other is a workpiece with three grooves to test the shadow effect on this model. High-pressure

compressed argon with a temperature of 550 °C and a pressure of 2.8 MPa was used as propellant gas. Other operating parameters are listed in Table 3.3. In the simulation, the single coating profile model is generated by deciding each variable in Eq.3-1. The values have been obtained through corresponding experiments. After that, the simulation was carried out with the real configuration files, robotic programs and robot kinematic parameters identical to those used on the spray system. The detailed results were presented in the following paragraphs.

Table 3.3 Operating parameter details used for experiments.

Substrate	**Nozzle traverse speed (mm/s)**	**Spray angle (°)**	**Spray distance (mm)**	**Scanning step (mm)**	**Scanning pass**
Flat	50	90	30	3.8	10
Complex	50	50	30	None	20`

3.4.2.1 Experiment on a flat surface

For the experimental verification on a flat surface, the experiment was performed with the same robot program under the same kinematics parameters as predefined in the simulation (Figure 3.12). The simple zigzag path was created. The spray nozzle was always perpendicular to the surface of the substrate through the entire path. The nozzle traverse speed and the spray distance were set 50 mm/s and 30 mm respectively. In order to make the coating in the cross-sectional direction easier to observe and to compare, a larger scanning step of 3.8 mm was used. Finally, the experimental result is in good agreement with the simulation as shown in Figure 3.14. It is obvious that stripes between two tracks can be observed from both experimental and simulation results due to the large scanning step. It also illustrated that a good deposition uniformity can be achieved by specifying a scanning step of the corrected distribution, that was also reported by Cai [11] and Chen [9] for pure 5056 Al powders.

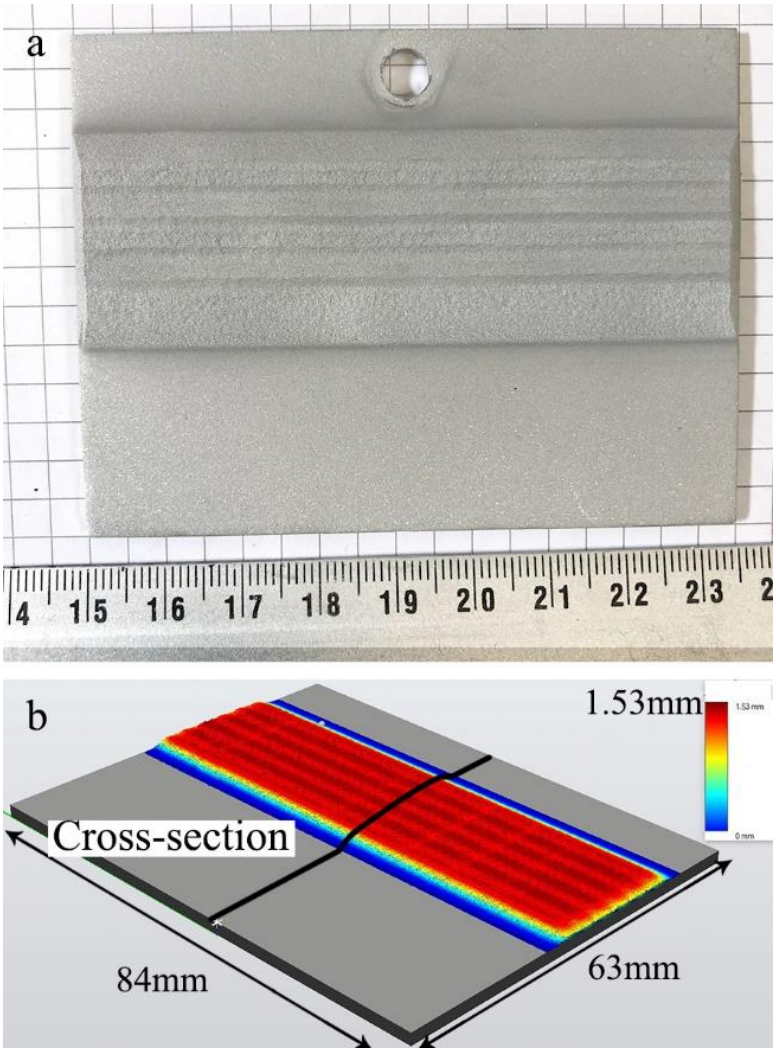

Figure 3.14 Experimental result; (b) simulation result.

The coating thickness obtained by experiment and simulation were compared. The cross-section in the middle of the experimental coating was measured by using a profiler. The second coating thickness measuring method illustrated above was used to determine the results of the cross-section shown in Figure 3.14 (b). The obtained data were used to make the chart. Finally, the cross-sectional comparison of coating thickness distribution is displayed on Figure 3.15. It is found that the experimental result is in good agreement with the simulation. In addition, the results of the error analysis are shown in Table 3.4 and indicates that the simulated coating profile well fits with the experimental data, and the average relative error is 6.85%.

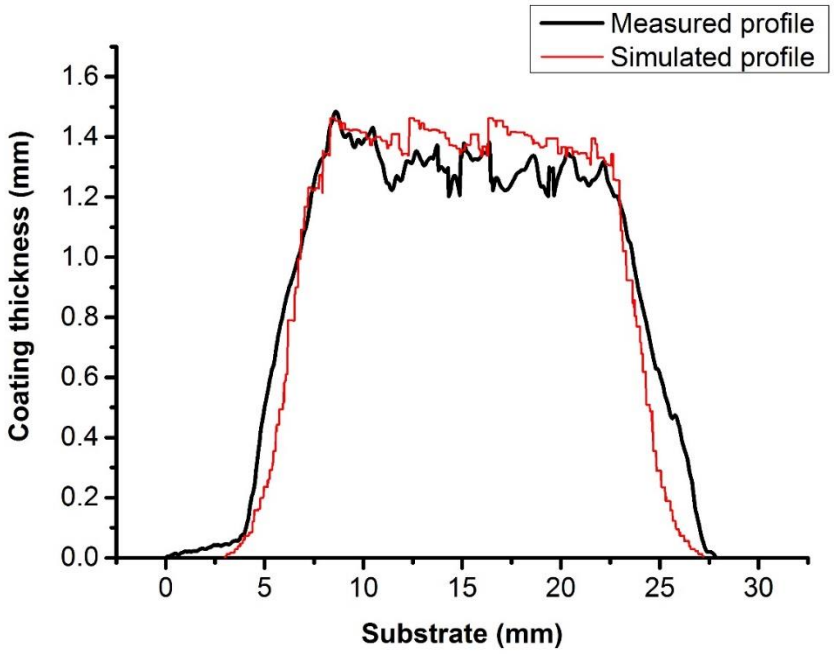

Figure 3.15 Comparison of experimental and simulation results of coating thickness.

Table 3.4 Average and standard deviation of coating thickness, as well as absolute and relative error of simulated results with experimental ones.

	Average coating thickness (mm)	**Standard deviation (mm)**	**Average absolute error (mm)**	**Average relative error (%)**
Experiment	1.298	0.056	0.089	6.85
Simulation	1.387	0.044		

3.4.2.2 Experiment on a part with a shadow effect

As shown in Figure 3.16, the geometric model of the workpiece presents three zones with different groove shapes. The depth of the grooves and the slope of the side walls are different: the first one is 5 mm deep and 68-degree slope; the second one is 10 mm deep and 79-degree slope and the third one is 15 mm deep and 82-degree slope. In the experiment, the objective is to measure the coating thickness in each zone under the spray angle of 50° and spray distance

of 30 mm. The spray path used for deposition is shown in red in Figure 3.17 (a). The nozzle reciprocated up and down along the red path. In order to illustrate the effect of different zones on the distribution of coatings during spraying, more details were shown in Figure 3.17 (b). The trajectory of the nozzle was indicated as purple balls named targets. Red lines were the direction for spraying, and also the centerline of the nozzle. The shortest distance of target-substrate was 30 mm in the direction of the red line. The change of the distance truly affects the coating deposition efficiency as mentioned above. White balls were the intersections centerline/substrate. It is sure that there will be coating deposition only in the intersection. Green arrows were normal to the intersections. It can easy to found that the angle between the normal and the red line was changed along with the movement of the nozzle, that would lead to different spray angles and different coating depositions.

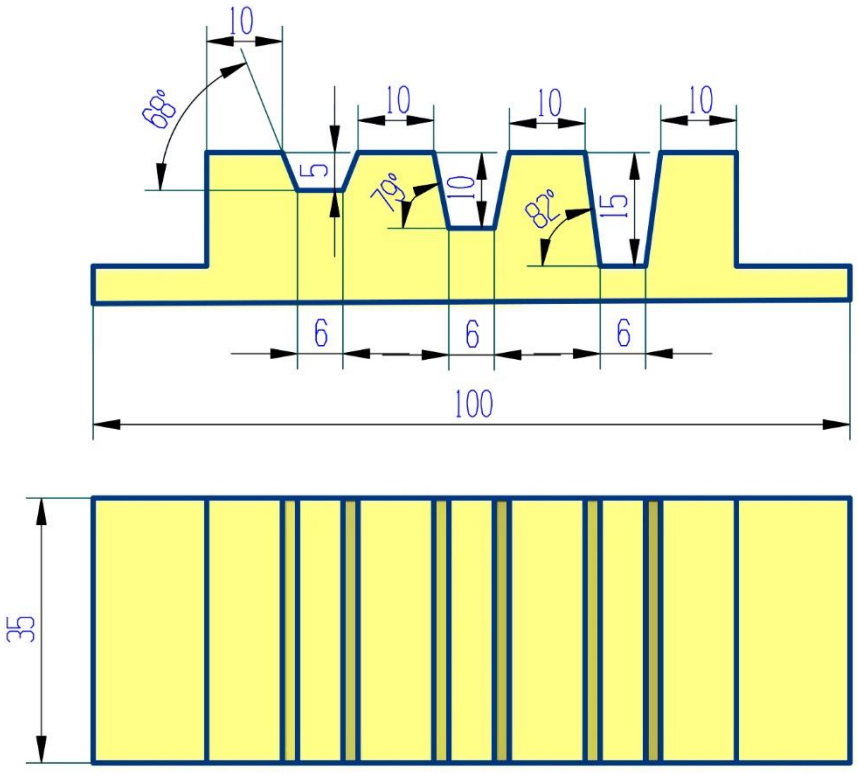

Figure 3.16 The main view and top view of the workpiece with a shadow effect.

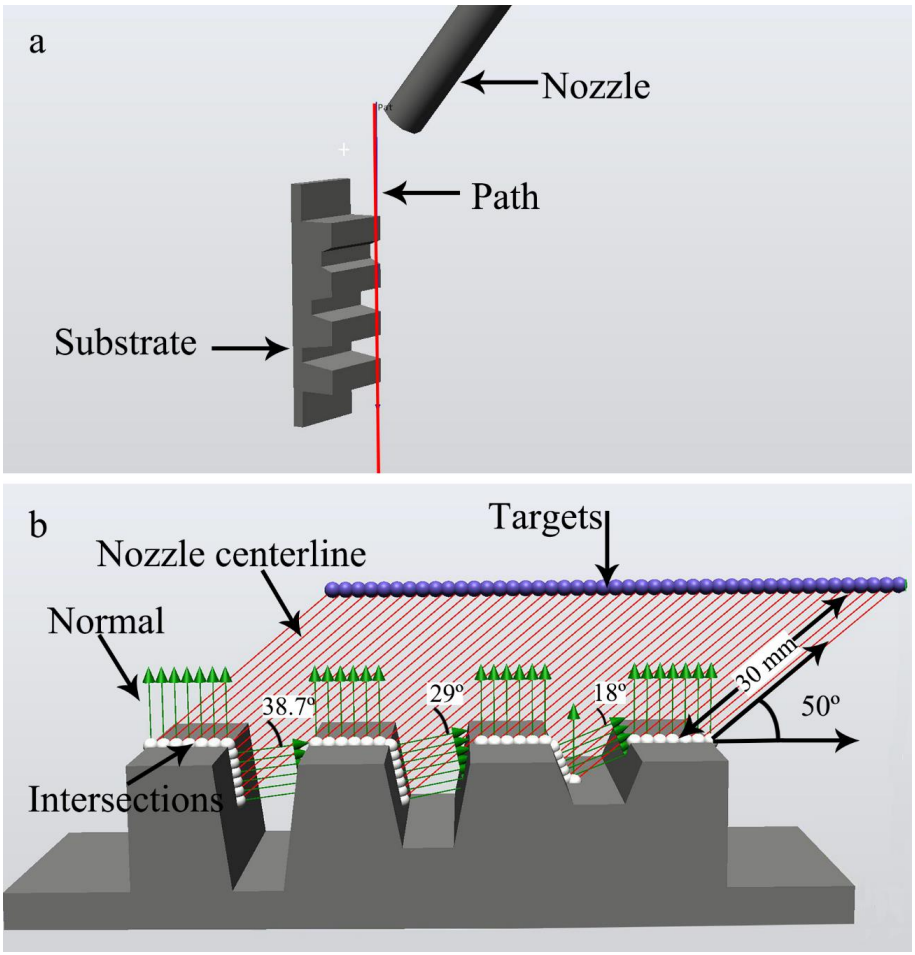

Figure 3.17 (a) Generation of trajectory; (b) target points for coating thickness simulation.

Figure 3.18 (a) and (b) show the results of the experiment and simulation respectively. Each zone was affected by shadow effects under experiment settings. The coating in each zone was different: zone 1 had the largest coating thickness and a triangular-like profile was formed; the lower number of particles was deposited in Zone 3 so the coating thickness was minimum. This was because the spray angle decreased as well as the spray distance increased, and as a result the relative deposition efficiency became smaller. There was no obvious coating on the top surface of the substrate because the deposition efficiency was close to zero. However, the traces washed by the powder particles could be clearly observed. The cross-sectional comparisons of coating thickness distribution in each zone are displayed in Figure 3.19. It is known that the physical influence factors of deposition are very complicated during cold spraying. The parallel multiple passes in a single track will lead to the triangular-like profiles. This is because increasing coating height leads to significant decreasing of deposition efficiency

(more than 35% according to Kotoban's report [29]) due to the diminishing of effective impact angle in between particles and substrate. Obviously, the coating height of zone 1 increased more quickly than other zone owing to its closer spray distance and larger spray angle, that made it the earliest formation of triangular-like profiles (Figure 3.19 (a)). Since the impact of this aspect was not considered in the model used in this article, there were large deviations in the simulated results, especially in zone 1. Finally, Table 3.5 listed the results of the error analysis proving that this method of coating thickness simulation permits convenient prediction of coating thickness in the case of shadow effects. Based on the simulation results, robotic trajectory, operating parameters, and spray strategy can be re-adjusted, like changing the spray angle, setting different nozzle travel speeds, until achieving the desired coating thickness distribution.

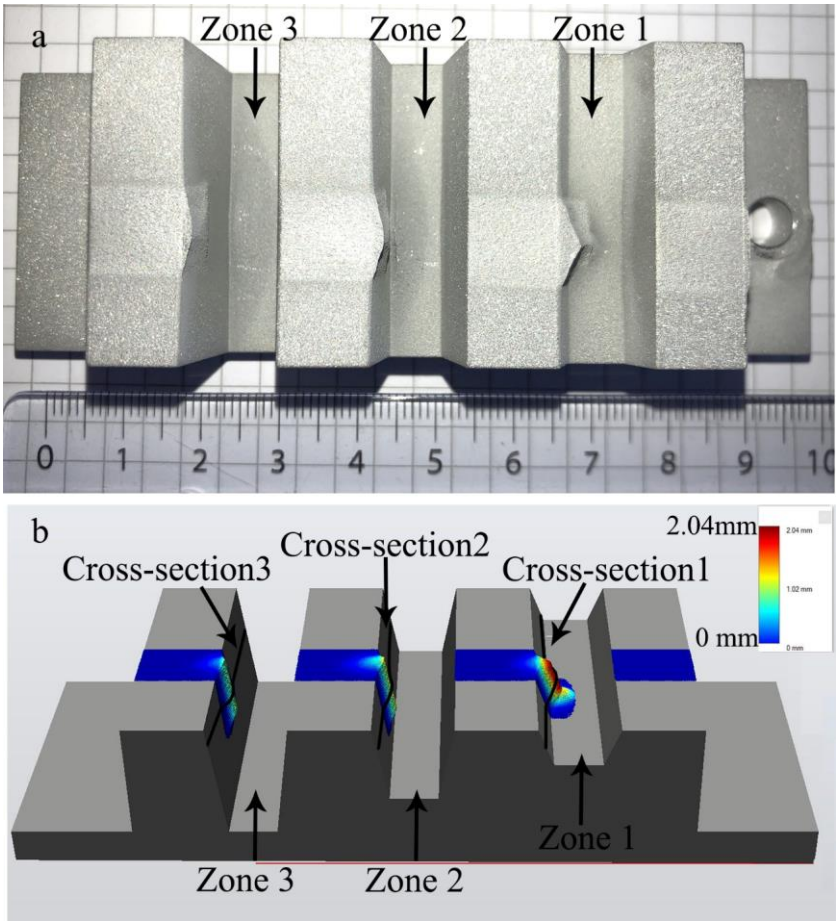

Figure 3.18 (a) Experimental and (b) simulation results of CS deposition on workpiece with shadow effect.

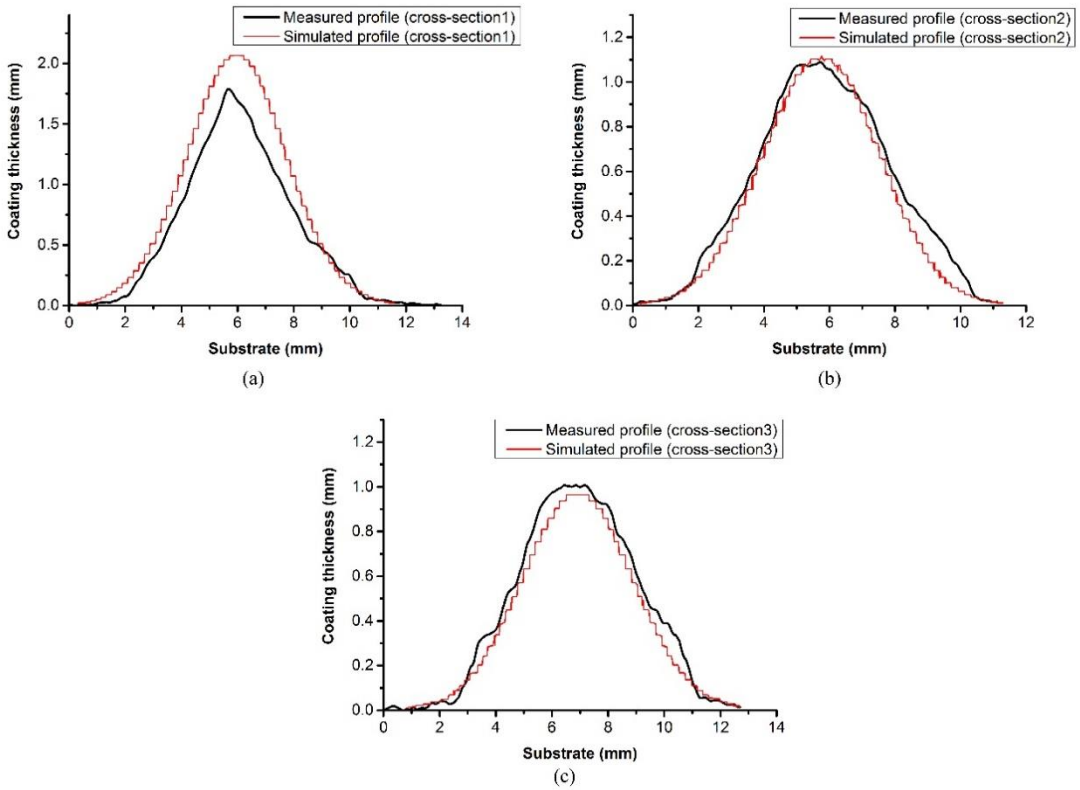

Figure 3.19 Comparison of experimental and simulation results of coating thickness at (a) cross-section 1, (b) cross-section 2 and (c) cross-section 3.

Table 3.5 The absolute and relative error of simulated results compared with experimental ones based on different cross-sections.

Cross-section	**Absolute error (mm)**	**Relative error (%)**
1	0.251	14.03
2	0.025	2.25
3	0.064	6.39

3.5 Conclusion

Nowadays, due to the advantage of low particle temperature, low oxidation, and residual stress, cold spray is considered as an effective additive manufacturing method. In the process of cold spray on complex components, coating thickness is an important indicator to monitor

and control. Although coating quality, coating microstructure and bonding theory of cold spray have been widely studied, the control of the coating thickness and kinematic parameters is rare. In this study, a new approach was developed to simulate coating thickness in cold spraying, especially for the prediction of shadow effects. The experiment result shows that this method can provide acceptable results.

A three-dimensional geometric model of the coating profile based on Gaussian distribution was developed and presented in this chapter. Due to the manipulation of the industrial robot, the coating thickness and quality are directly influenced by the robotic kinematic parameters. Therefore, the coating thickness model considers the relative deposition efficiency resulting from the different robot kinematic parameters. The evolving geometric 3D model can be easily handled with existing programming and geometric modeling tools, that implies the possibility of a wide application without specific simulation codes. In addition, it can offer accurate profile prediction in the robot programming platform that enables the integration of robot programming with simulation to better control the coating process. However, the current research is still located at the profile geometric simulation. In the future, process physical phenomena, e.g. plastic deformation and energy conversion, will be integrated to this model to realize simulation and prediction of coating quality indicators, such as coating porosity. Moreover, it would be applied as an efficient and effective guideline for cold spray additive manufacturing and repairing.

References

[1] V.K. Champagne, The cold spray materials deposition process, Elsevier, 2007.

[2] S. Yin, P. Cavaliere, B. Aldwell, R. Jenkins, H. Liao, W. Li, R. Lupoi, Cold spray additive manufacturing and repair: Fundamentals and applications, Additive Manufacturing. 21 (2018) 628–650.

[3] R.N. Raoelison, C. Verdy, H. Liao, Cold gas dynamic spray additive manufacturing today: Deposit possibilities, technological solutions and viable applications, Materials & Design. 133 (2017) 266–287.

[4] D.Y. Ju, M. Nishida, T. Hanabusa, Simulation of the thermo-mechanical behavior and residual stresses in the spray coating process, Journal of Materials Processing Technology. 92 (1999) 243–250.

[5] J. Liu, Y. Wang, H. Li, S. Costil, R. Bolot, Numerical and experimental analysis of thermal and mechanical behavior of NiCrBSi coatings during the plasma spray process, Journal of Materials Processing Technology. 249 (2017) 471–478.

[6] R. Ghafouri-Azar, J. Mostaghimi, S. Chandra, M. Charmchi, A stochastic model to simulate the formation of a thermal spray coating, Journal of Thermal Spray Technology. 12 (2003) 53–69.

[7] A. Kout, H. Müller, Parameter optimization for spray coating, Advances in Engineering Software. 40 (2009) 1078–1086.

[8] S. Duncan, P. Jones, P. Wellstead, A frequency-domain approach to determining the path separation for spray coating, IEEE Transactions on Automation Science and Engineering. 2 (2005) 233–239.

[9] C. Chen, Y. Xie, C. Verdy, H. Liao, S. Deng, Modelling of coating thickness distribution and its application in offline programming software, Surface and Coatings Technology. 100 (2017) 315–325.

[10] A. Sadovoy, Modeling and offline simulation of thermal spray coating process for gas turbine applications, PhD Thesis, Technische Universität, 2014.

[11] Z. Cai, S. Deng, H. Liao, C. Zeng, G. Montavon, The effect of spray distance and scanning step on the coating thickness uniformity in cold spray process, Journal of Thermal Spray Technology. 23 (2014) 354–362.

[12] T. Wiederkehr, H. Müller, Acquisition and optimization of three-dimensional spray footprint profiles for coating simulations, Journal of Thermal Spray Technology. 22 (2013)

1044–1052.

[13] Z. Djurić, P. Grant, An inverse problem in modelling liquid metal spraying, Applied Mathematical Modelling. 27 (2003) 379–396.

[14] D.A. Stepanenko, Modeling of spraying with time-dependent material feed rate, Applied Mathematical Modelling. 31 (2007) 2564–2576.

[15] A. Hansbo, P. Nylén, Models for the simulation of spray deposition and robot motion optimization in thermal spraying of rotating objects, Surface and Coatings Technology. 122 (1999) 191–201.

[16] C. Chen, Y. Xie, C. Verdy, R. Huang, H. Liao, Z. Ren, S. Deng, Numerical investigation of transient coating build-up and heat transfer in cold spray, Surface and Coatings Technology. 326 (2017) 355–365.

[17] S. Deng, Z. Cai, D. Fang, H. Liao, G. Montavon, Application of robot offline programming in thermal spraying, Surface and Coatings Technology. 206 (2012) 3875–3882.

[18] D.L. Gilmore, R.C. Dykhuizen, R.A. Neiser, M.F. Smith, T.J. Roemer, Particle velocity and deposition efficiency in the cold spray process, Journal of Thermal Spray Technology. 8 (1999) 576–582.

[19] H. Assadi, F. Gärtner, T. Klassen, H. Kreye, Comment on 'Adiabatic shear instability is not necessary for adhesion in cold spray,' Scripta Materialia. 162 (2019) 512–514.

[20] H. Assadi, F. Gärtner, Thorsten Stoltenhoff, Heinrich Kreye, Acta Mater. 51 (2003) 4379–4394.

[21] C.-J. Li, W.-Y. Li, H. Liao, Examination of the critical velocity for deposition of particles in cold spraying, Journal of Thermal Spray Technology. 15 (2006) 212–222.

[22] U. Prisco, Size-dependent distributions of particle velocity and temperature at impact in the cold-gas dynamic-spray process, Journal of Materials Processing Technology. 216 (2015) 302–314.

[23] C.J. Li, W.Y. Li, Y.Y. Wang, H. Fukanuma, Effect of spray angle on deposition characteristics in cold spraying, Thermal Spray. (2003) 91–96.

[24] S. Yin, Q. Liu, H. Liao, X. Wang, Effect of injection pressure on particle acceleration, dispersion and deposition in cold spray, Computational Materials Science. 90 (2014) 7–15.

[25] J.P. Campbell, A. Astarita, A. Viscusi, G.C. Saha, Investigation of strain-hardening characteristics of cold-sprayed Al–Al2O3 coatings: a combined nanoindentation and expanding cavity models approach, Surface Engineering. (2019) 1–10.

[26] W.-Y. Li, C. Zhang, X.P. Guo, G. Zhang, H.L. Liao, C.-J. Li, C. Coddet, Effect of standoff distance on coating deposition characteristics in cold spraying, Materials & Design.

29 (2008) 297–304.

[27] T. Van Steenkiste, J.R. Smith, Evaluation of coatings produced via kinetic and cold spray processes, Journal of Thermal Spray Technology. 13 (2004) 274–282.

[28] M.M. Dalvand, S. Nahavandi, Teleoperation of ABB industrial robots, Industrial Robot: An International Journal. (2014).

[29] D. Kotoban, S. Grigoriev, A. Okunkova, A. Sova, Influence of a shape of single track on deposition efficiency of 316L stainless steel powder in cold spray, Surface and Coatings Technology. 309 (2017) 951–958.

Chapter 4

Stable layer-building strategy to enhance cold spray based additive manufacturing

4.1 Introduction and state of the art

As mentioned in the previous chapters, CS form large volume objects with a possibility of a hybrid AM process that uses direct material-removing processes during the CS deposition. However, it also has been noted that CSAM has some disadvantages, such as low spatial resolution and dimensional accuracy. The distribution and velocity of particles in the feedstock jet are uneven[1–3] and results in a particles distribution close to a Gaussian distribution [4,5].

In practice, an axisymmetric de-Laval nozzle is often used to emerge high-speed particles in CS. When the nozzle traverse speed is low or the number of scanning passes is important, a triangular coating profile will be formed and the subsequent deposition of particles will be difficult [3]. As shown in Figure 4.1, continuous spraying makes the single-track profile gradually changed from a thin coating with high deposition efficiency at the beginning (Figure 4.1(a)) to a triangular-like coating with low deposition efficiency (Figure 4.1(b)).

During the spray process, the velocity of particles in the centre of the feedstock jet is generally higher. Furthermore, the absolute number and the size of particles deposited on the centre area of the track are larger than the particles on the edges. As a result, the thickness in the middle will increase significantly and the impact angle of the particles near the centre line gradually decreases. It is well known that particles in cold spraying to reach a critical speed in order to produce plastic deformation to form a coating. Therefore, cold spraying is a process that is sensitive to the spray angle. An impact angle of 90° can achieve maximum deposition efficiency [6]. For particles with smaller spray angle, the velocity component perpendicular to the impact surface will not reach critical velocity, so it will rebound without forming a coating. Therefore, the coating morphology slowly rising in the middle is not conducive to subsequent particles deposition. The impact angle decreases rapidly and the deposition rate sharply decreases, especially for the particles around the centre line [7]. Gradually, only particles in the centre can continue to be deposited by the high-pressure gas. All this difficulty of subsequent particle deposition, the area where particles can be eventually deposited in the middle to continue to be shrunk to the point where it forms a triangular single-track profile [16,26]. Obviously, this characteristic would limit the application of CSAM for shape forming if no spray strategy for processing adaptation is used.

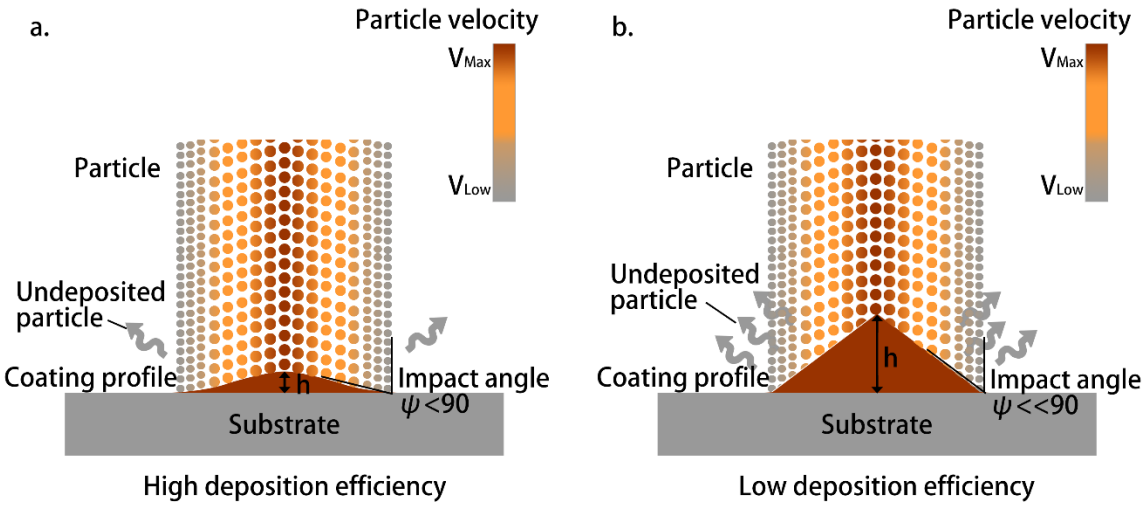

Figure 4.1 Schematic of particle impact conditions in cases with (a) high deposition efficiency phase and (b) low deposition efficiency phase

In AM process benchmarking, local deposition of thick and vertical walls is always required to show the capability of forming complex components with diverse geometries. In order to build a thick and vertical wall without edge milling, J. Pattison et al. [8] proposed a strategy of triangular-tessellation. The process is to tilt the nozzle by a 4/5-axis system so that the current coating is sprayed perpendicularly onto the inclined surface of the previous track. However, they did not give any details on how the nozzle should be tilted. Although their method can form 3D volumes, the control of the process is difficult and it has limitations in forming complex 3D near-net-shapes with acceptable accuracy. This also conflicts with the basic principle of AM where the volume forming is by layers deposition. Moreover, by using this method, a typical triangular-like shape should be generated before tilting the nozzle (Figure 4.2). The particle impact conditions are not optimal in this case. Firstly, the typical triangular-like morphology influences overall deposition efficiency [3]. Such conditions can be attributed to the impact angle decrease as mentioned above. It has been proved that the optimal impact angle in cold spraying is 90° [9–11]. If the impact angle decreases, the deposition efficiency drops sharply. Secondly, high and sharp profiles can cause a tangential component of particle impact velocity that may generate tensile forces and reduces the total contact areas and bonding strength between the particles and the previously sprayed coating or substrate [9]. The porosity would also become greater [6,11]. Considering all the above-mentioned problems, this triangular-tessellation technique may not be a good solution for shape forming to obtain high-

quality objects.

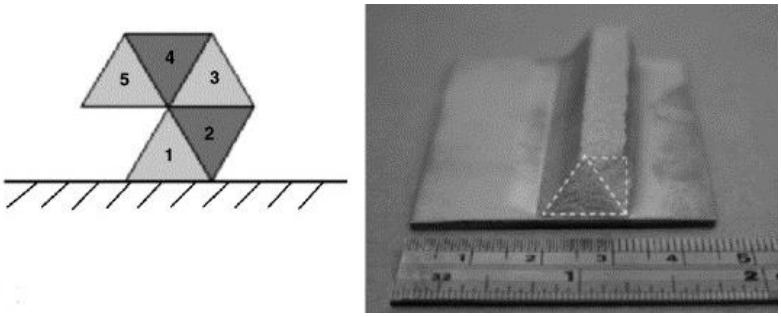

Figure 4.2 Schematic of the triangular-tessellation strategy proposed by J. Pattison [16]

To solve the problems of CS for shape forming and realize easy process control, this chapter proposes a novel spray strategy that enables to form freeform 3D objects with acceptable precision. In view of the characteristic of CS deposition, three parameters are proposed to adjust the coating morphology in order to avoid forming triangular-like deposits. The parameters are the deflection angles θ, the offsets s, and the retreat distance d. They are illustrated in details in the section below. Through the developed CS simulation model mentioned in Chapter 3, the different combinations of these parameters were studied, and it is found that their settings play a key role in determining the layer geometry, and thus the component building process.

To compare with existing spray-coating strategies for additive forming, this chapter also adopts the widely used benchmarking test shape, thick and vertical walls, to demonstrate the performance of the proposed new spray strategy. When additively building the walls or other thick coatings, the effective coating area can be fully covered without edge loss.

4.2 Stable layer-building method for CSAM

Generally speaking, the volume forming in AM depends on the layer by layer formation [12]. The realisation of a stable and controllable layer is the key to obtain the object with the desired shape and accuracy. Starting with the deposition of simple coatings and ending with the fabrication of more complex components, it is always necessary to deposit thick and vertical walls as elementary geometry. In the process of structural design, many complex structures can be formed by a combination of various elementary geometries.

As mentioned, during the cold spray process, the pre-set spray parameters are generally

kept constant during the spray process, while the growth of the coating is only affected by the kinematic parameters such as the nozzle scanning speed, the spray angle and the spray distance. These parameters are directly controlled by industrial robots. The high performance of industrial robots ensures the high precision, high repeatability and high flexibility of these parameters. Therefore, it is required to develop a method that can realize stable and controllable spraying to make CS a real layer-by-layer AM process.

In the following section, a stable layer-building strategy for CSAM will be introduced. Before that, four groups of single-track spraying experiments were carried out. One of the purposes is to reveal the relationship between operating parameters and as-sprayed coatings. Different parameters affect the shape and the height of the single track deposited by CS. Based on the results analysis, we could propose a special spray strategy for creating thick and vertical walls. Another purpose is to complete the specific numerical model of the coating profile that would be used in CSAM simulation. A certain powder/substrate material and spray parameters are necessary for fitting the specific Gaussian profile.

4.2.1 Cold spray single-track analysis

4.2.1.1 Experimental setup

Experiments were carried out under the proposed CSAM system framework (as presented in Chapter 2). The nozzle has a circular cross-section with an approximate expansion ratio of 8.3 and a divergent section length of 130 mm. The dimension details are displayed in Figure 4.3. During cold spraying process, the nozzle was cooled by a water circulation system to avoid nozzle overheating and clogging. Due to the long response time of controlling spray parameters such as gas temperature, powder feed rate, etc., the experiments focused only on kinematic parameters which can be rapidly changed and controlled by the robot. Therefore, the variable parameters depended on different numbers of scanning pass, different nozzle traverse speeds, and different spray angles.

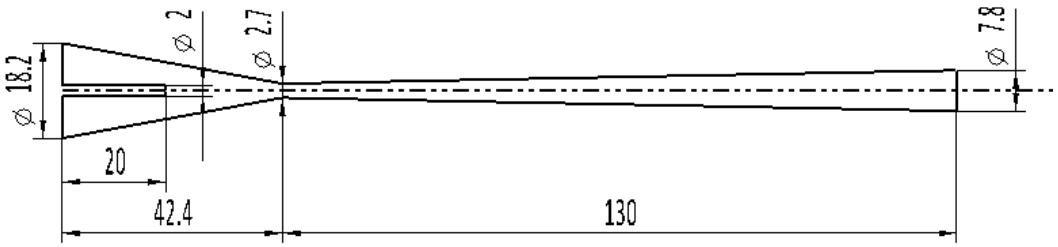

Figure 4.3 Geometry diagram of axisymmetric de-Laval nozzle.

A pure Cu powder with near-spherical morphology are deposited on Al substrates. The diameter range of powder is in between 10 and 45 μm (average size of 26 μm). Figure 4.4 shows the morphology and size distribution of the pure Cu powder. High-pressure air was supplied as propellant gas at a temperature of 500°C and a pressure of 3 MPa, and also as powder carrier gas. The morphology of deposition was measured by a 3D profiler (LJ-V7060, Keyence, Japan). More detailed descriptions of the operating parameters are listed in Table 4.1.

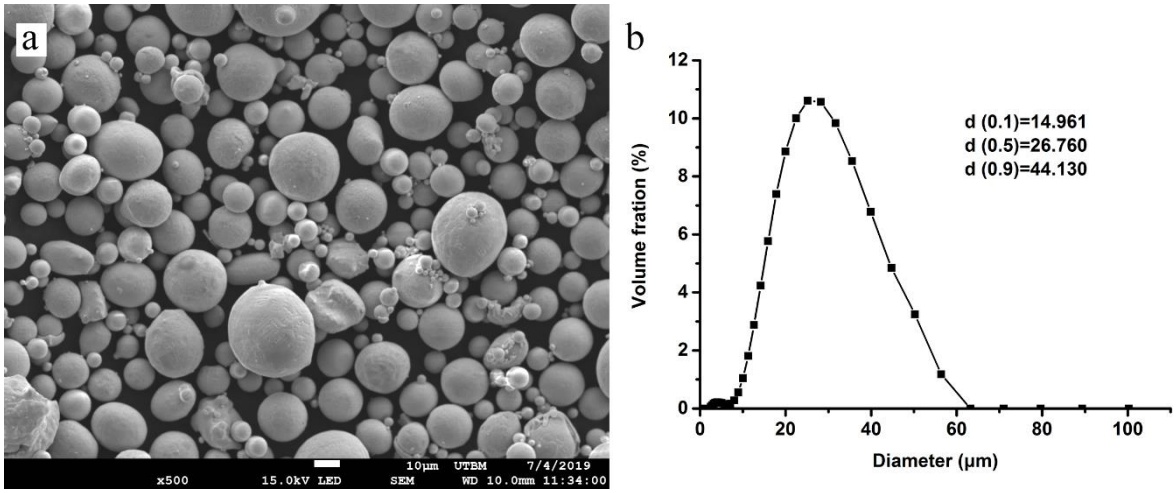

Figure 4.4 SEM image of pure Cu powder used in experiments

Table 4.1 Detailed description of operating parameters.

Group	**Nozzle traverse speed (mm/s)**	**Spray angle (°)**	**Powder feeding rate (g/min)**	**Spray distance (mm)**	**Number of scanning passes**
1	100	90	24	30	1~20
2	20, 50, 100, 200	90	24	30	10
3	100	50, 60, 70, 80, 90	24	30	20

4.2.1.2 Effects of number of scanning passes

The effects of the number of scanning pass on CS single-track profiles were investigated by the first test group. The number of scanning pass increased from 1 to 20 passes while the other parameters were kept constant. The results were measured and shown in Figure 4.5.

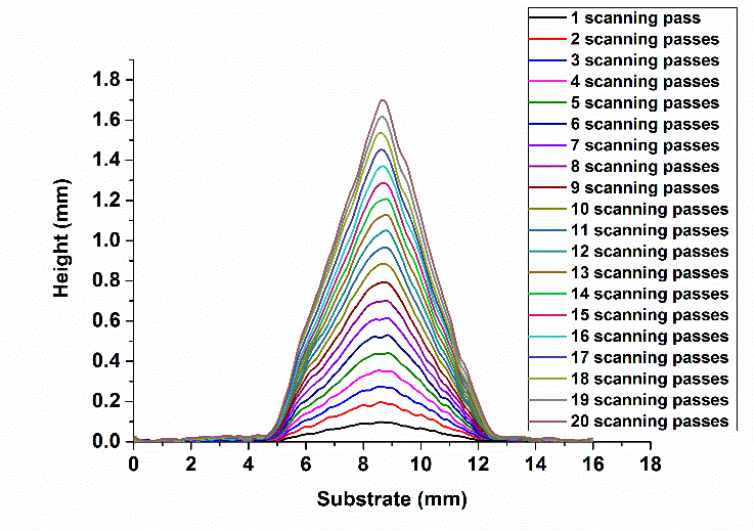

Figure 4.5 Profiles of the single tracks deposited at different numbers of nozzle pass measured by the 3D profiler.

It was found that the coating got thicker constantly and the shape of the single track became a triangle gradually when the number of scanning passes increased. The height of the coating changed from 0.8mm under 1 scanning pass to 16.8mm after 20 scanning passes. Although the height of the coating could gradually increase as the number of scans increase, only the part of the coating in the middle grew. Moreover, this part was getting closer and closer to the middle, and finally, a sharp triangle was formed.

The relative deposition efficiency of different scan passes was evaluated by calculating the area enclosed by each contour line using definite integral. It is supposed that the relative deposition efficiency of the coating is 100% when the number of scanning passes is 1. Figure 4.6 shows the calculation results. It was found that the deposition efficiency decreased as the number of scanning passes increased. When the number of scans is increased to 13, the deposition efficiency is reduced by half.

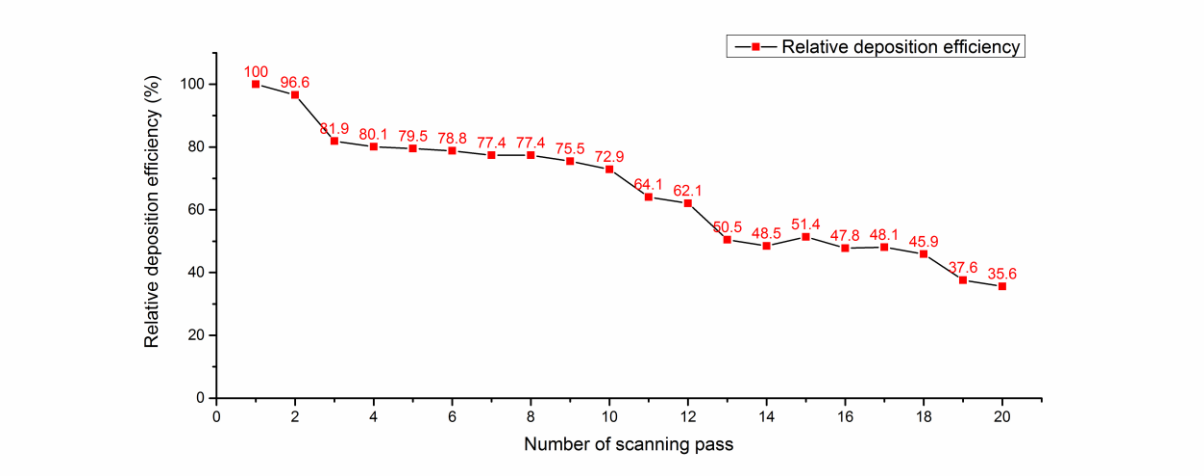

Figure 4.6 Effects of the number of scanning pass on relative deposition efficiency.

4.2.1.3 Effects of nozzle traverse speed

The effects of the nozzle traverse speed on CS single-track profiles were investigated by the second test group. The nozzle traverse speed was set to 20mm/s, 50mm/s, 100mm/s and 200mm/s while the other parameters were kept constant. The results were measured and shown in Figure 4.7. Different nozzle movement speeds can significantly change the height of the deposits, and lower movement speed will cause the coating thickness to increase and become triangular faster. The relative deposition ratio of different nozzle traverse speeds was calculated. It is supposed that the relative deposition ratio is 100% when the nozzle traverse speed is 20mm/s. Figure 4.8 shows the calculation results. Obviously, the nozzle traverse speed has the same effect on the CSed single track as the number of scanning passes. When the nozzle traverse speed is low, a triangular coating profile will be formed and the subsequent deposition of particles will be difficult.

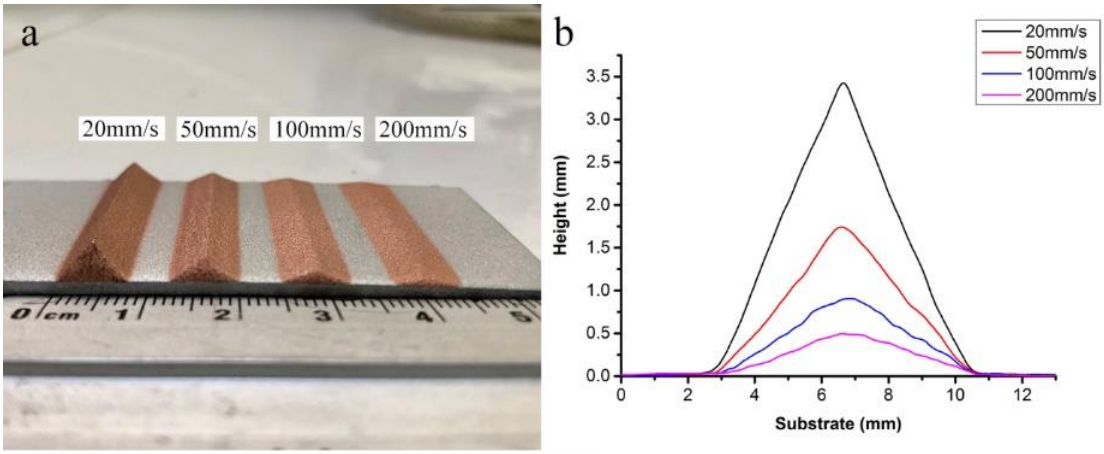

Figure 4.7 (a) Single tracks deposited at different nozzle traverse speed (b) Profiles of single

tracks measured by the 3D profiler.

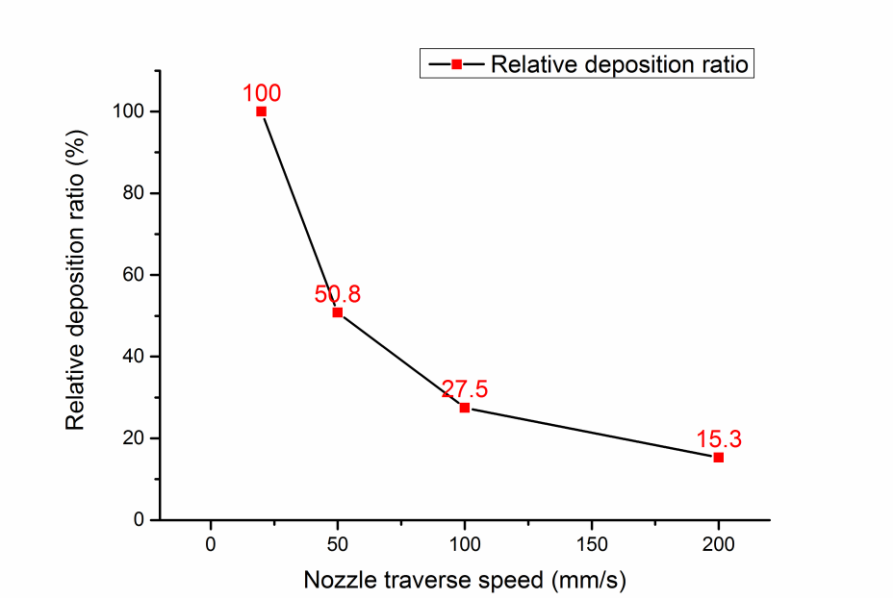

Figure 4.8 Effects of the nozzle traverse speed on relative deposition ratio.

4.2.1.4 Effects of spray angle

The effects of the spray angle of 90°, 80°, 70°,60° and 50° on a single coating profile were investigated by the third test group. The results were measured and shown in Figure 4.9. It is assumed that the relative deposition efficiency is 100% when the spray angle is 90°. Then the relative deposition efficiency of different spray angles was calculated and showed in Figure 4.10. Obviously, the spray angle affects not only the deposition efficiency but also the shape of the coating-profile. Decreasing of spray angle reduces the maximum thickness and influences the profile asymmetry, shifting the centre of gravity of the sprayed coatings in the direction of the incoming particles.

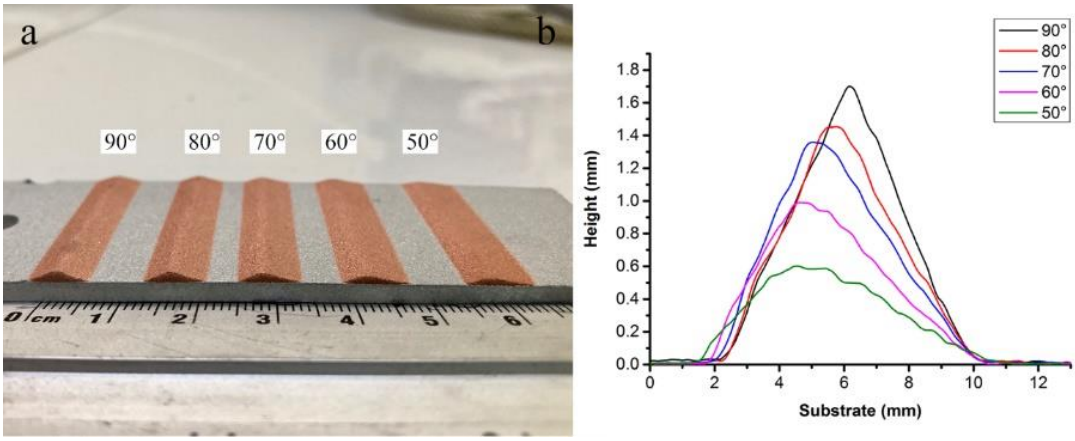

Figure 4.9 (a) Single tracks deposited at different spray angles (b) Profiles of the single tracks measured by the 3D profiler.

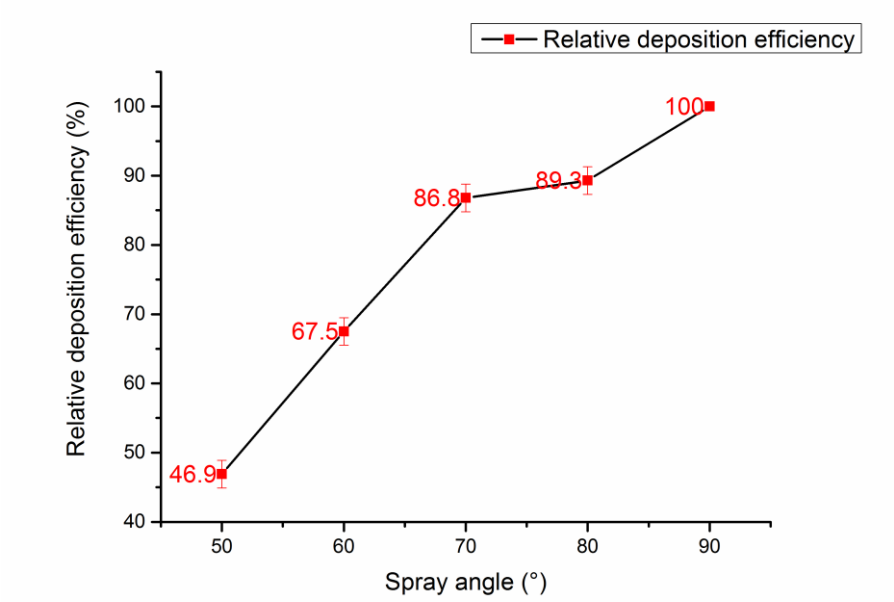

Figure 4.10 Effects of the nozzle traverse speed on relative deposition efficiency.

From the preliminary experiments, it can be seen that the kinematic parameters are the main factors affecting the coating morphology in CS, that are directly controlled by the industrial robots. The deposits are bound to become triangular-like when the axisymmetric nozzle is used to spray continuously. If the kinematic parameters are not changed when spraying on the same regions, the particle impact condition will be worse. Therefore, to make CS a real additive manufacturing technology in the strict sense, it is important to avoid the tendency of triangular-like forming.

An effective solution should be considered to ensure that the deposits can stably grow. Actually, if the height of deposits is low, then the impacting surface could be considered flat.

Also, the impact surface can be kept flat by adjusting the kinematic parameters (such as spray angle) for every layer to avoid coating height increase (in the middle zone), so that the deposits can grow up layer by layer. The detail of the proposed spray strategy will be presented in the following part.

4.2.2 Spray strategy

Generally, cold spraying jet can be regarded as a set of continuous random variables. According to the central limit theorem, the averages of random variables can be considered Gaussian distributed when the amount of variable is sufficiently large. Many research reports have used Gaussian based numerical modeling to study the feature of spray deposits [4,13–15], as done in our previous work [5]. And it is proved to be feasible and reliable. As we all know, the Gaussian curve is a standard curve in the normal distribution. Figure 4.11 shows a normal Gaussian curve; μ is the centre position of the peak and σ is the standard deviation. The values less than σ away from the mean account for 68.27% of the set, while the remaining portion is relatively low. It is conceivable that the main weight of a single CS deposited coating is concentrated in the central area.

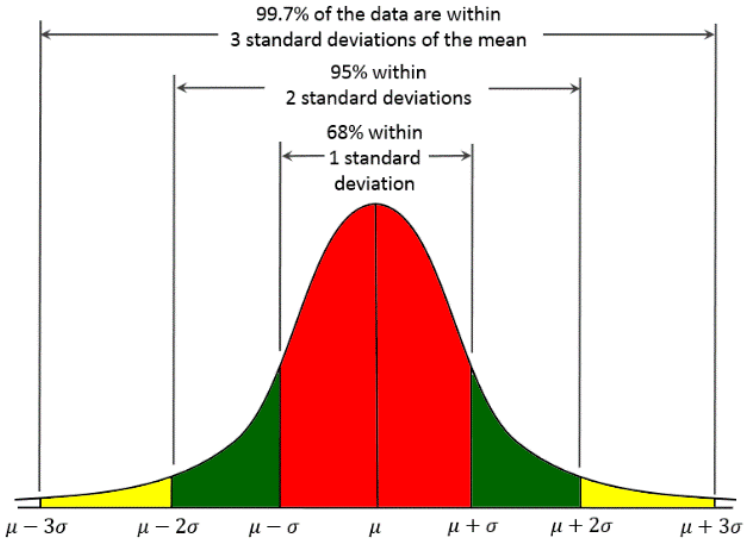

Figure 4.11 Gaussian curve.

In order to obtain a more uniform coating, it is necessary to make mass distribution gradually concentrated on both sides. According to the above analysis, spray angles can change the symmetry, shifting the centre of gravity of the sprayed coatings in the direction of the incoming particles. Hence, the mass distribution of the layer can be uniformed by tilting the

nozzle. Unlike the triangular-tessellation strategy, this spray strategy does not make triangular-like deposits before tilting the nozzle. The inclined spray manner is to compensate for the thickness and weight difference in between the middle and side of the deposit.

Based on the above discussion, three main parameters were proposed to control the shape of deposits. As shown in Figure 4.12, θ is the deflection angle in order to replenish particle depositions at the edge; s is the offset that can adjust the track width in horizon; d is the value that adjusts the retreat distance of the nozzle according to the layer's growth in height.

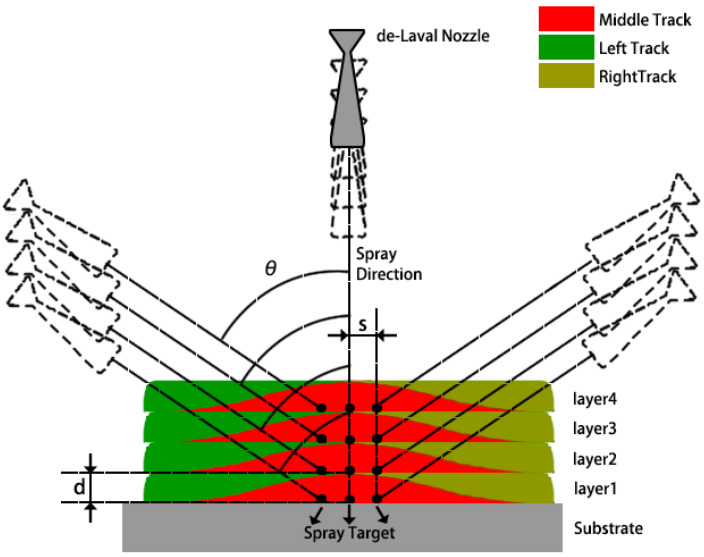

Figure 4.12 Schematic of CSAM spray strategy for thick and vertical walls.

It can ensure that the spray distance between the top layer and the nozzle exit is consistent during spraying. The coating profile in perpendicular spray cases is a Gaussian distribution (shown with red blocks), while the coating profile in off-normal spray cases has no longer a normal Gaussian distribution (the left track with green block, the right track with yellow block). Every layer is composed of a first track in the middle, a second track on the left, and a third one on the right. The first track should be controlled to avoid a triangular-like profile in the middle before performing the left and the right track. After spraying the left and the right track, the current layer could be formed as a flat surface before the next cycle.

In this way, the single layer can steadily rise in a track-by-track manner without appearing to have defective triangular-like depositions. Meanwhile, this spray strategy also appropriates to fabricate large bricks or a thick coating (Figure 4.13). The surface of the prescribed area is sprayed in a perpendicular manner by specifying a scanning step of the corrected distribution.

Then the edges are sprayed by tilting the nozzle to compensate for the edge loss. It can be found that the volume is formed layer after layer using this spray strategy, which implements the basic principles of AM. This strategy can avoid triangular-like depositions. Moreover, with the application of high-performance industrial robot, this spraying strategy can be easily realized. There is no doubted that the parameters used in this strategy can be easily controlled and repeated with high accuracy and flexibility.

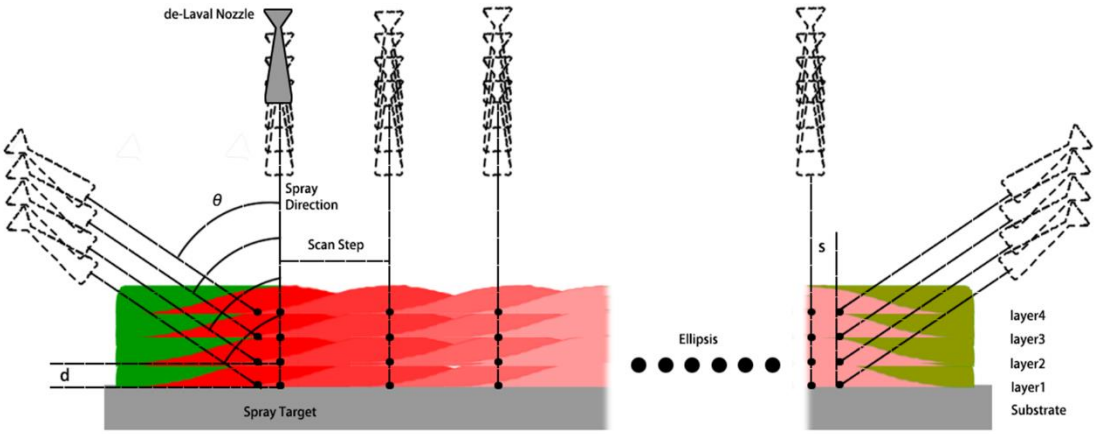

Figure 4.13 Schematic of CSAM spray strategy for large blocks or thick coatings.

In the following sections, both simulation and experiment based on the proposed spray strategy will be introduced. They verify the proposed spraying strategy as pre-spraying application, that is, before the final building results are known. Simulation can obtain an instructive spraying parameter, reducing trial and error experiments. The deposit under the current spray strategy can be observed more clearly.

4.3 Simulation verification

4.3.1 Simulation process

In Chapter 3, a three-dimensional geometric model of the coating profile based on Gaussian distribution was developed for simulating coating thickness in CS. A brief description of the simulation methodology is as follows. Firstly, the three-dimensional geometric model is represented by a Gaussian approximation function. This function considers the effect of spray parameters and kinematic parameters on the deposition efficiency. Secondly, an algorithm couples the model with real robotic trajectories to simulate coating deposition in

RobotStudio™ (ABB). Finally, the simulation results are presented in the graphical virtual environment.

In this work, the 3D coating thickness model was created based on the copper (powder)/ aluminum(substrate) material system and CS system that were illustrated in Section 4.2.1.1. The detail of the creation process can refer to the content of Chapter 3. In order to verify the spraying strategy proposed above and to find the optimal combination/setting of parameters to reduce trial and error physical experiments, different parameters-based simulations were carried out. Table 4.2 gives a detail of parameters used in the simulation.

Table 4.2 Parameters used in simulation.

Group	**Deflection angle θ (°)**	**Offset distance s (mm)**	**Nozzle retreat distance d (mm)**
4	30	0, σ, 2σ, 3σ, 4σ	-
5	10, 20, 30, 40	2σ	-
6	30	2σ	0, Layer thickness

In the current simulation procedure, the first track is generated under normal parameters (in case of perpendicular spray), as shown in Figure 4.14a. It is a typical Gaussian profile. Then the left track (Figure 4.14b) is obtained by tilting the angle θ and by offsetting the distance s to the left side. Thirdly, the right track is also created by the tilting angle θ and the offsetting distance s to the other side (Figure 4.14c). The coating created by such operations can be considered as one layer. Then, the subsequent layers will be created on top of the previous layer following the same procedure. It was observed that the profile topography may change due to different parameters, and it was found that the flatness and verticality of the formed profile are closely related to the combination of these parameters, while these two attributes are exactly the criteria for judging the quality of the control and for reducing the post-machining to achieve net shape.

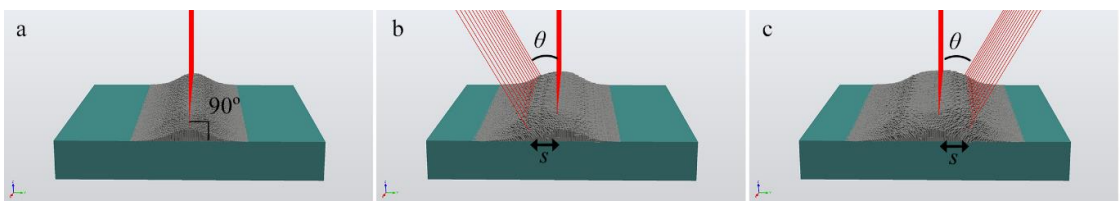

Figure 4.14 Schematic of simulation operation.

4.3.2 Simulation results and discussions

4.3.2.1 Effects of the offset distance *s*

Figure 4.15 shows the results when the deflection angle is 30º (θ=30º) and only the offset distance s is changed (see group 4 in Table 4.2). Figure 4.15 a1–a5 show the first track, which is a typical Gaussian distribution coating profile. Figure 4.15 b1–b5 show the second track superposed on the first one with different offset distance *s* of 0 mm, σ mm, 2σ mm, 3σ mm and 4σ mm, respectively. Figure 4.15 c1–c5 show the third track accumulated on the other side with the offset distance *s* of 0 mm, σ mm, 2σ mm, 3σ mm and 4σ mm, respectively. Figure 4.15 d1–d5 illustrate the deposit results in colour, which correspond to Figure 4.15 c1–c5, respectively, and their ranges are indicated by a colour bar.

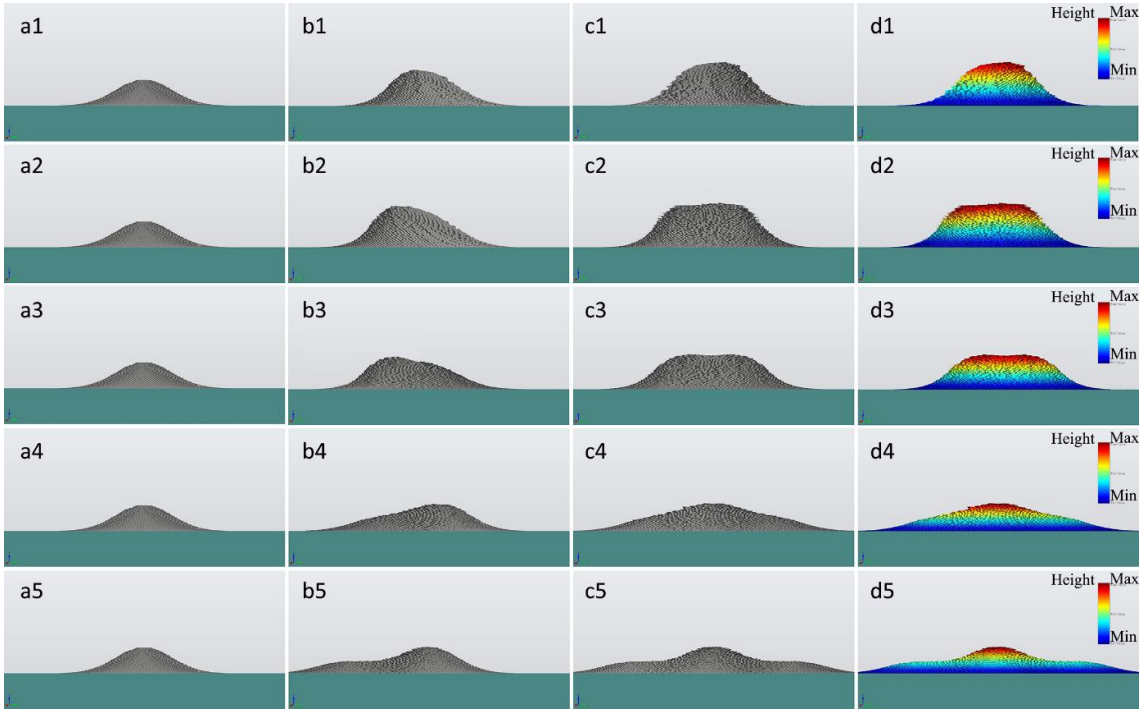

Figure 4.15 Lateral view of spray strategy simulation in a situation where the deflection angle was 30º (θ=30º), and the offset distance *s* changed.

It can be found that the mass distribution gradually concentrated on both sides during the compensation of the deposits on both left and right sides based on the first deposition. But when the value of *s* is larger than three standard deviations, the peaks of mass appear again on both sides of the first track. It also can be found that the flatness of the top of the deposits changed. The flatness in the case of *s*=σ mm and *s*= 2σ mm (Figure 4.15 d2 and Figure 4.15 d3

respectively) is better than the other cases. In case of s=3σ mm and s= 4σ mm (Figure 4.15 d4 and Figure 4.15 d5 respectively), the deposits almost had not flat top.

Moreover, the cross-section of each deposit was measured and shown in Figure 4.16. The height of each case of deposits was about 1.18mm, 0.97mm, 0.72mm,0.71mm, and 0.7mm, which corresponded to the offset distance s of 0 mm, σ mm, 2σ mm, 3σ mm and 4σ mm, respectively. The width of the track increased from 12mm to16mm as the offset distance increased from 0 mm to 4σ mm. Therefore, according to the final results, it can be concluded that as s increases, the width of track increases, while the flatness increases initially and then decreases.

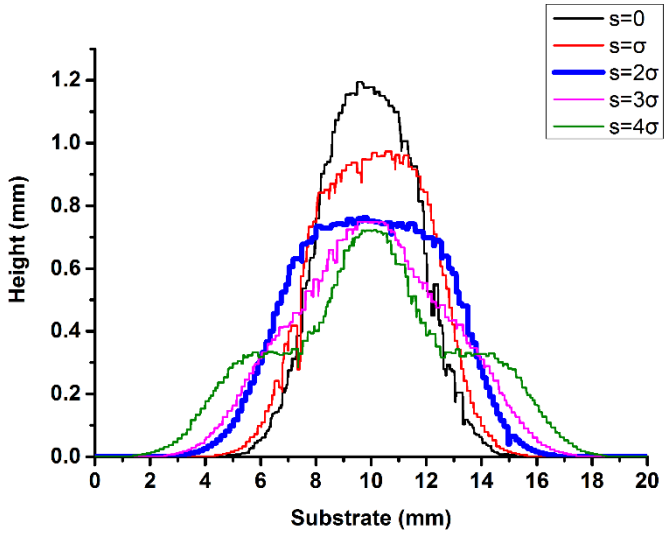

Figure 4.16 The cross-sectional profile based on the simulation in Figure 4.15.

4.3.2.2 Effects of the deflection angle θ

Figure 4.17 shows the simulation results in a case where the offset distance s is fixed at 2σ and the deflection angle is changed (see group 5 in Table 4.2). Figure 4.17 a1–a5 show the first track. Figure. 4.17 b1–b4 show the second track when the deflection angle θ is 10º, 20º, 30º, and 40º, respectively. Figure 4.17 c1–c4 show the third track by the deflection angle θ of 10º, 20º, 30º, 40º, respectively. Figure 4.17 d1–d4 show the results represented in colour corresponding to Figure.4.17 c1–c4, respectively.

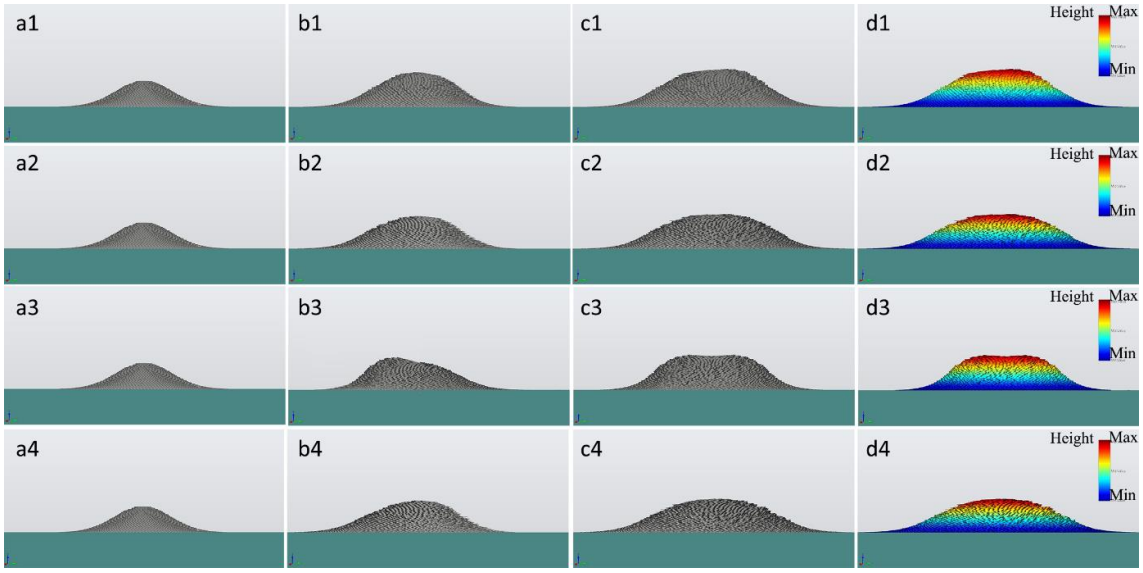

Figure 4.17 Lateral view of spray strategy simulation in a situation where the offset distance was 2σ (s=2σ), and the deflection angle θ changed.

It can be found that the mass distribution changed during the compensation of the deposits on the left and right sides based on the first deposition. The deflection angle effected this change. The flatness of the top of the deposits also changed, but not so much. It seems that a better flattop emerged when the deflection angle was 30º.

Figure 4.18 shows the cross-section of each deposit. The height of deposits was about 0.98mm, 0.91mm, 0.72mm, and 0.68mm respectively, which corresponded to the deflection angle of 0º, 20º, 30º, and 40º. However, increasing θ means a reduction of the spray angle, which will reduce the deposition efficiency. Table 4. 3 lists the relative deposition efficiency of the deposits under different deflection angles. Here it was assumed that the relative deposition efficiency is 100% when the deflection angle is 90°. It was found that the deposition efficiency decreased as the deflection angle increased. When the deflection angle is 40º, the mass is concentrated in the middle zone and the flatness is decreased. According to the final results, it can be concluded that as θ increases, flatness initially increases and then decreases. However, θ cannot be too large because it will significantly reduce the deposition efficiency.

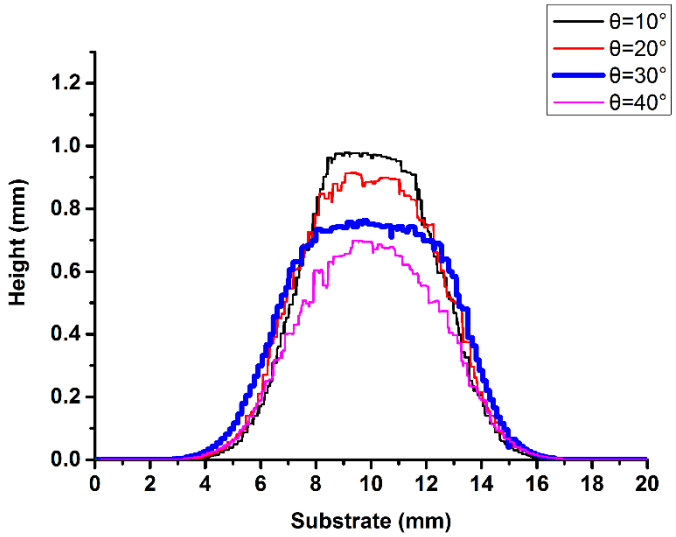

Figure 4.18 The cross-sectional profile based on the simulation results in Figure 4.17.

Table 4.3 The relative deposition efficiency of the different deflection angle in simulation.

***θ* (°)**	**relative deposition efficiency (%)**
10	100
20	98.7±0.5
30	87.2±0.5
40	78.5±0.5

4.3.2.3 Effects of the value of nozzle retreat *d*

Figure 4.19 shows the comparison between the cases with and without appending d (the value of nozzle retreat distance) - (see group 6 in Table 4.2). The value of d equals the height of the layer. Figure 4.19 a1 and a2 show the first layer, which is formed at a deflection angle of 30 º and an offset distance of 2σ mm. Figure 4.19 b1 and b2 show the first + second layers. However, the result in Figure 4.19 b2 was obtained by appending d, and these of Figure 4.19 b1 without appending d. It can be found that the flatness decreases without appending d while the other case can obtain the desired flatness. After spraying the third layer, the deposit in Figure 4.19 d2 can be kept flat while the deposits in Figure 4.19 d2 become uneven. After spraying the third layer, it can be seen that the result with d (Figure 4.19 d2) is conducive to subsequent deposition due to a large flat surface. But the deposits without retreat distance d (Figure 4.19 d1) become convex again.

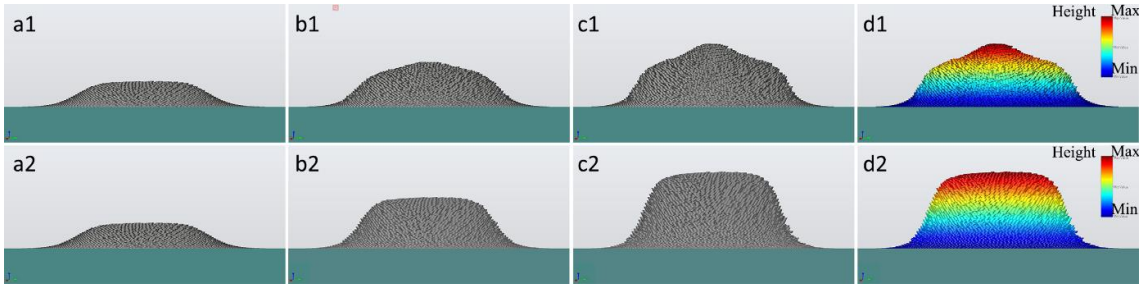

Figure 4.19 Comparison results between appending *d* (the value of nozzle retreat) and without it.

The cross-section of each deposit was measured and shown in Figure 4.20. The height and the flatness of deposits with *d* was better than that in case of without *d*. Therefore, the value of nozzle retreat can ensure the required flatness and the stable growth of the deposits.

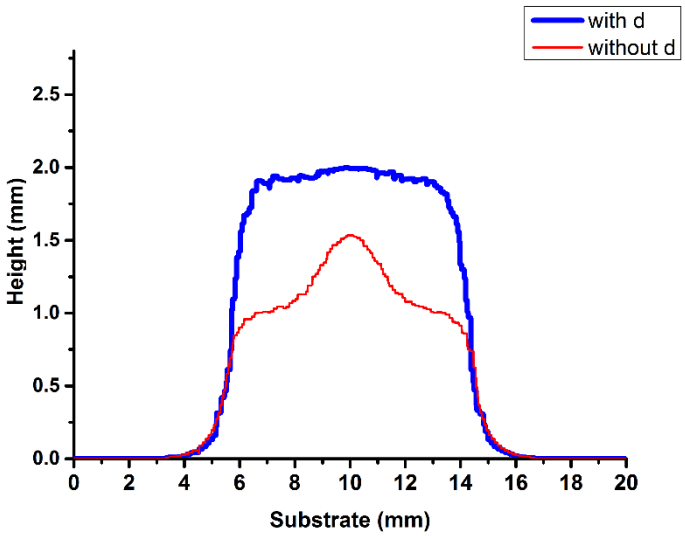

Figure 4.20 The cross-sectional profile based on the simulation results in Figure 4.19.

4.4 Experimental verification.

4.4.1 Experimental setup

The experimental verification was carried out with the same system used in section 4.2.1. In the proposed CSAM system, the spray gun is fixed at an appropriate position while the substrate or the formed part attaches to the robot's end-effector. The robot arm performs not only the relative movement in between the substrate and the spray nozzle, but also the displacement of the formed part in between cold spraying process and coating thickness

measuring process. The nozzle relative traverse speed was defined as 100 mm/s. The spray distance was kept at 30 mm. The pure Cu powder (the same powder as shown in Figure 4.4) with a feeding rate of 24 g/min was used to deposit on Al substrates. The temperature and the pressure of the compressed air were 500°C and 3 MPa, respectively. The parameters of the spraying strategy were set as in the simulation (Table 4.2). The morphology of deposits was measured online by the 3D profiler.

4.4.2 Experimental results and discussion

Experiments of the proposed spray strategy were carried out in the manner of fixing the spray gun. Figure 4.21 shows the deposits profile curves measured by the 3D profiler with a deflection angle of 30º (θ=30º), and the offset distance of 0 mm, σ mm, 2σ mm, 3σ mm, 4σ mm, respectively. They were indicated by lines of different colours. It was found that when s was 0 mm and σ mm, the deposits profile tended to become triangular-like, even though their thickness were larger than the other cases; when *s* was 3σ mm, 4σ mm, the efficiency was dissatisfying; when *s* was 2σ mm, the deposits had a flat top surface and good efficiency.

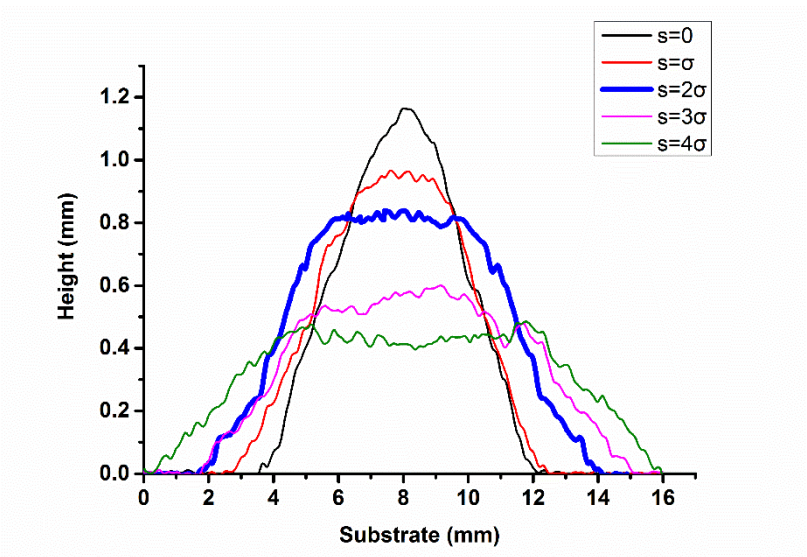

Figure 4.21 Experiment results at the deflection angle of 30º (θ = 30º), and the offset distance was 0 mm, σ mm, 2 σ mm, 3 σ mm, 4 σ mm, respectively (*s* = was 0 mm, σ mm, 2 σ mm, 3 σ mm, 4 σ mm).

Figure 4.22 shows the results with an offset distance of 2σ mm and deflection angles of 10º, 20º, 30º, and 40º. The relative deposition was measured and shown in Table 4.4. Similarly, the relative deposition efficiency was assumed as 100% when the deflection angle was 90°.

Obviously, when θ was 40º, the deposition efficiency was low, while the deposits with the deflection angles of 10º and 20º tended to form triangles. Conclusively, these profiles proved that the value of deflection angle and offset distance significantly affect the flatness and the efficiency of the deposits.

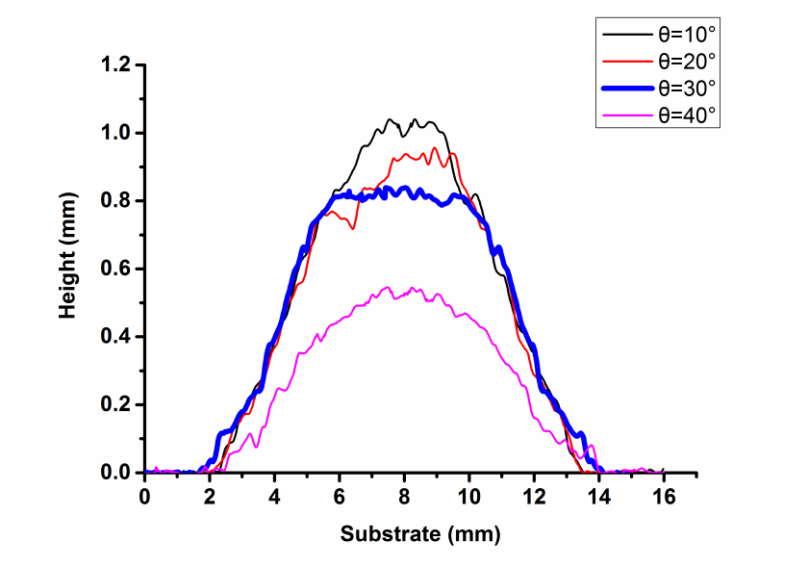

Figure 4.22 Experiment results at the offset distance of 2 σ mm (s= 2 σ mm), and the deflection angle was 10º, 20º, 30º, 40º, respectively (θ =10º, 20º, 30º, 40º).

Table 4.4 The relative deposition efficiency of the different deflection angle in the experiment.

θ (º)	relative deposition efficiency (%)
10	100
20	94.5±0.5
30	93.5±0.5
40	55.7±0.5

Figure 4.23 illustrates the results of multiple layers obtained from real-time online measuring. The value of nozzle retreat distance was set to 0.4 mm in order to make the deposits grow stably in the preconceived manner. Figure 4.23a illustrates cross-section image of pure Copper-aluminum samples produced by the spray strategy with the axisymmetric de-Laval nozzle, taken by optical microscopy.

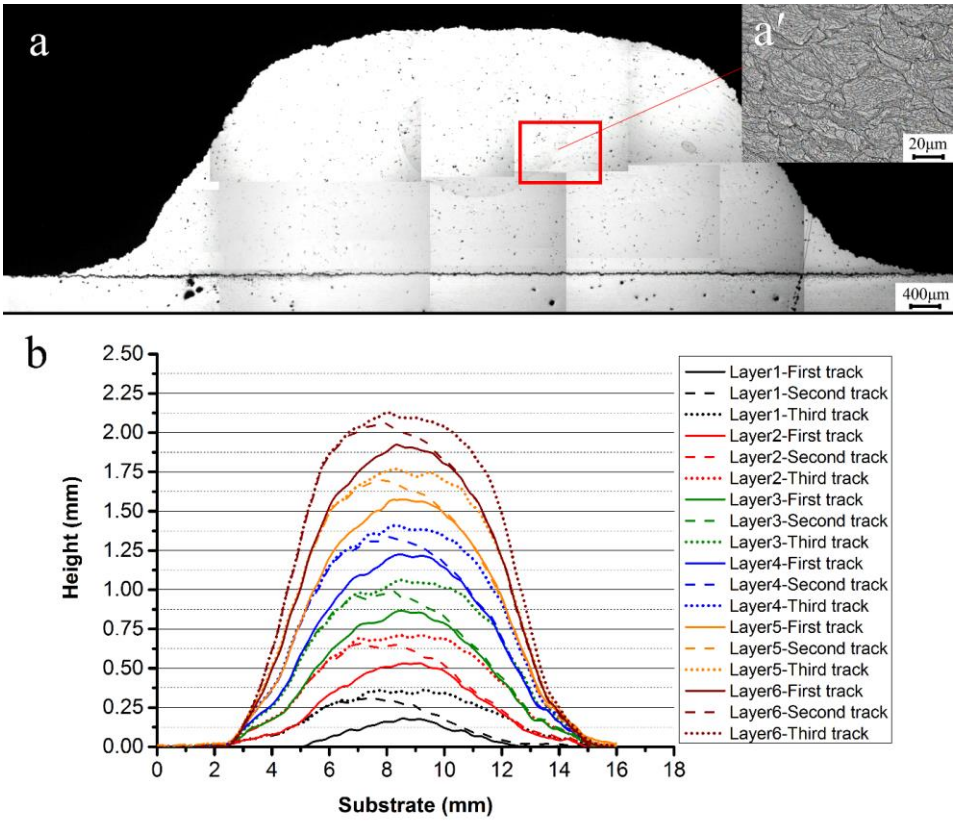

Figure 4.23 (a) Cross-sectional view sprayed track using optical microscope; (a′) Optical micrograph of coatings; (b) Each sprayed track morphology measured by a 3D profiler.

It can be observed that the profile is not a typical CS triangular-like, and the upper surface has a substantially large and flat area, which created quite favourable conditions for the subsequent deposition of particles. The coating was dense and had not obvious cracks. The partial enlargement view showed the sample etched that reveals the particle/particle boundaries (as shown in Figure 4.23a′). The particles appear to be tightly bonded. There were some pores in the coating and the porosity was calculated to about 0.4% using imaging software (ImageJ). Figure 4.23b shows the results of each sprayed track measured by the 3D profiler. Lines of different colours are used to distinguish the profile of different tracks. The growth of the coating in the processing can be observed. The deposits could basically be formed in the preconceived manner, as confirmed by the simulation in the previous section. It is obvious that layer-by-layer deposition permits the coating to stably grow without forming triangular morphology.

Moreover, this spray strategy can be applied to build blocks or thick coatings on prescribed areas without edge losses. Figure 4.24 shows thick coatings on the prescribed area. It can be seen that the normal spray strategy leads to edge losses. This means that during the coating formation, the area of the upper surface shrinks (more than 34% in this case). While the same

coating was sprayed by performing this strategy, the borders were compensated without edge losses. The coating grew layer by layer, and the effective area reached nearly 100%.

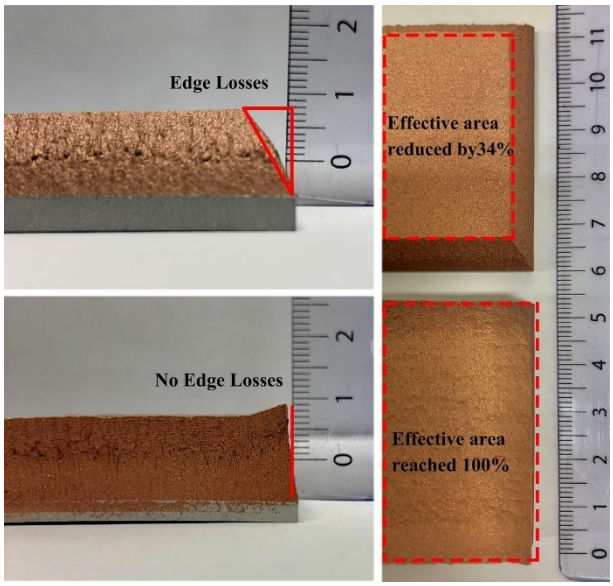

Figure 4.24 Creation of thick coatings.

Finally, based on the presented spray strategy, different shaped samples were created successfully. As Figure 4.25 illustrates, thick and vertical walls could be built on both a flat surface (Figure 4.25a, b, and c) and on a curved surface (Figure 4.25d). It proved that this method can be used for shape control and production of more complex components in cold spray additive manufacturing.

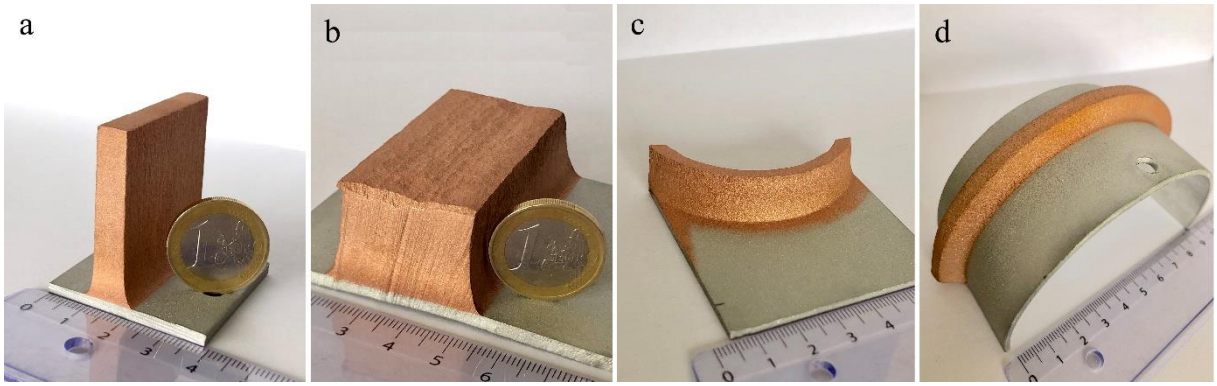

Figure 4.25 (a) a thick and vertical wall was created on a flat surface; (b) a block was created on a flat surface; (c) a thick and vertical curved wall was created on a flat surface; (d) a thick and vertical wall was created on a curved surface.

4.5 Conclusion

Nowadays, both industrial and academic communities are paying more and more attention to CSAM, especially for the direct manufacturing of soft metal components. A stable layer-by-layer building strategy and capability of CS is a key preliminary step for forming complex 3D shapes in an additive way. This study focused on the spray strategy with consideration of both kinematic factors and coating characteristics of CS to develop a stable layer-building strategy. Here, three main parameters were proposed to control the shape of deposits. They were deflection angle θ, offset distance s and nozzle retreat distance d. In the current framework of CSAM system, these parameters were controlled directly by the high-performance industrial robot, which permitted the process to be easily controlled, repeated, and followed. Numerical simulation and physical benchmarking case study results validate the proposed method and imply that more complex 3D geometries can be built via the use of this proposed layer-building strategy and sophisticated coating scanning path. It was found that the combination of controlling different parameters played a key role in determining the layer geometry, and thus the component built-up process. Future work will further investigate the impact of nozzle shape and size on the layer building and the development of a multi-axis robotic tool-path planning strategy for building complex 3D curved layers or freeform 3D objects in near-net-shape with the proposed layer-building method.

References

[1] D.L. Gilmore, R.C. Dykhuizen, R.A. Neiser, M.F. Smith, T.J. Roemer, Particle velocity and deposition efficiency in the cold spray process, Journal of Thermal Spray Technology. 8 (1999) 576–582.

[2] A.P. Alkhimov, V.F. Kosarev, S.V. Klinkov, The features of cold spray nozzle design, Journal of Thermal Spray Technology. 10 (2001) 375–381.

[3] D. Kotoban, S. Grigoriev, A. Okunkova, A. Sova, Influence of a shape of single track on deposition efficiency of 316L stainless steel powder in cold spray, Surface and Coatings Technology. 309 (2017) 951–958.

[4] C. Chen, Y. Xie, C. Verdy, H. Liao, S. Deng, Modelling of coating thickness distribution and its application in offline programming software, Surface and Coatings Technology. 100 (2017) 315–325.

[5] H. Wu, X. Xie, M. Liu, C. Chen, H. Liao, Y. Zhang, S. Deng, A new approach to simulate coating thickness in cold spray, Surface and Coatings Technology. 382 (2020) 125151.

[6] C.J. Li, W.Y. Li, Y.Y. Wang, H. Fukanuma, Effect of spray angle on deposition characteristics in cold spraying, Thermal Spray. (2003) 91–96.

[7] C.-J. Li, W.-Y. Li, H. Liao, Examination of the critical velocity for deposition of particles in cold spraying, Journal of Thermal Spray Technology. 15 (2006) 212–222.

[8] J. Pattison, S. Celotto, R. Morgan, M. Bray, W. O'neill, Cold gas dynamic manufacturing: A non-thermal approach to freeform fabrication, International Journal of Machine Tools and Manufacture. 47 (2007) 627–634.

[9] W.-Y. Li, S. Yin, X.-F. Wang, Numerical investigations of the effect of oblique impact on particle deformation in cold spraying by the SPH method, Applied Surface Science. 256 (2010) 3725–3734.

[10] S. Yin, X. Wang, W. Li, B. Xu, Numerical Study on the Effect of Substrate Angle on Particle Impact Velocity and Normal Velocity Component in Cold Gas Dynamic Spraying Based on CFD, J Therm Spray Tech. 19 (2010) 1155–1162. doi:10.1007/s11666-010-9510-3.

[11] K. Binder, J. Gottschalk, M. Kollenda, F. Gärtner, T. Klassen, Influence of impact angle and gas temperature on mechanical properties of titanium cold spray deposits, Journal of Thermal Spray Technology. 20 (2011) 234–242.

[12] I. Gibson, D.W. Rosen, B. Stucker, Additive manufacturing technologies, Springer, 2014.

[13] Z. Cai, S. Deng, H. Liao, C. Zeng, G. Montavon, The effect of spray distance and scanning step on the coating thickness uniformity in cold spray process, Journal of Thermal Spray Technology. 23 (2014) 354–362.

[14] M.M. Fasching, F.B. Prinz, L.E. Weiss, Planning robotic trajectories for thermal spray shape deposition, Journal of Thermal Spray Technology. 2 (1993) 45–57.

[15] C. Chen, Y. Xie, C. Verdy, R. Huang, H. Liao, Z. Ren, S. Deng, Numerical investigation of transient coating build-up and heat transfer in cold spray, Surface and Coatings Technology. 326 (2017) 355–365.

Chapter 5

Conclusion and prospects

5.1 Conclusion

With the continuous development of CS technology and the expansion of application fields, CS has been widely used to prepare various functional coatings on components surface, to restore damaged metal components, or to fabricate freestanding 3D metal components. Nowadays, CS has drawn more and more attention in its ability in AM. Many advantages make it uniquely competitive among AM technologies. In particular, the application of high-performance industrial robots improves the accuracy and ability of CS so that it can complete more and more complex tasks. The latest developments in the CSAM industry require more new methods and processes to improve its manufacturing accuracy, flexibility and reliability, to be more competitive. Therefore, the work of this thesis aims to research new process implementation to enhance CS based AM. The system framework, building strategy and method proposed in this thesis can become a model for the CSAM industry in the future. The details of the conclusion are listed as below.

Firstly, a concept of modular system was used in this study to design and implement a new CSAM framework. In this study, the new CSAM system was developed based on the conventional CS system. At the same time, various technology and application were integrated into the current system as different modules to enhance the ability of entire system. According to the different applications and purposes, the conventional CSAM system is divided into five modules: Spray module, Robot module, In-situ measurement module, Inter-process module and Post-process module. The physical and functional relationships between the key elements of the entire system were discussed in detail. Spray module is used for adding materials; Robot module is used to achieve various movements and the connection between modules; In-situ measurement module is for online monitoring and measurement; Inter-process module is a complementary module allowing materials removing and enhancement; Post-pross module is used to obtain the final product including heat-treatment, post-machining, test, etc. This physical and functional modularity is an indispensable necessity to promote a hybrid AM process.

Secondly, a new approach was developed to simulate coating process in CS. Here, a three-dimensional geometric model based on Gaussian distribution was developed to simulate the CS coating profile. This model considered the relative deposition efficiency resulting from the different robot kinematic parameters. Afterwards, the 3D geometric coating thickness model was integrated into the off-line programming software RobotStudio™ as a module in the

software TST, which implied the possibility of a wide application without specific simulation codes and offering accurate profile prediction. Both numerical and experimental verifications proved that the proposed method has a reliable prediction accuracy in practice, especially in coating thickness prediction including shadow effects.

Finally, based on the designed CSAM system framework, a stable layer-building strategy was proposed to enhance the forming ability of CSAM. Normally, the stable layer-by-layer building is the key function for forming complex 3D shapes in an additive manner. The proposed spray strategy considered both kinematic factors and coating characteristics. Three main parameters were pointed out to control the shape of deposits. They are the deflection angle θ, the offset distance s and the nozzle retreat distance d, which make the robot easier to control and help to repeat the process. Afterwards, based on the developed 3D geometric coating thickness model, a series of simulation verification was carried out according to the combination of different parameters. It was found that the combination of controlling different parameters played a key role in determining the layer geometry, and thus the component built-up process. Moreover, the experiments of layer built benchmarking test objects have satisfactory shape accuracy, which implied that the proposed method makes CS a real and ready to use layer-by-layer AM process for 3D shape forming.

5.2 Prospects

In this work, a new CSAM system framework was proposed for the implementation of a new process to enhance CS based AM. However, to fully exert the potential of CSAM, efforts are still required to integrate more technologies. Future research will focus on the improvements for each component of the framework and on the development of more spray strategies for CSAM. One of the ideas is to combine this system with conventional machining techniques. When the monitored deposits no longer meet the expectations, the milling cutter will permit desirable accuracy and reliable shape control.

The 3D geometric coating thickness model was developed and integrated into the ProfileKit of TST for the purpose of CS deposition process simulation based on kinematic data. However, some improvements should be made to optimize and enhance the functions of the software. Firstly, the code in the program as well as the algorithm should be further optimised to improve its computing performance and accuracy. Secondly, current research is still located at the profile geometric simulation. In the future, process physical phenomena, e.g. plastic

deformation and energy conversion, will be integrated in this model to realize simulation and prediction for coating quality indicators, such as coating porosity.

As for the stable layer-building method for CSAM, more efforts should be made to study the properties and reliability of the 3D volumes it creates, such as the porosity, the microstructure, the bonding strength, etc. Future work will also further investigate the impact of nozzle shape and size on the layer building, and the development of a multi-axis robotic tool-path planning strategy for building complex 3D curved layers or freeform 3D objects in near-net-shape with the proposed layer-building method.

Annexes

Annex Computer graphics: topology and 3D geometric transformations

Computer graphics is the branch of computer science that deals with generating images with the aid of computers. Some topics in computer graphics include user interface design, image visualization, computational geometry, 3D modeling, image rendering, etc. In this study, the coating thickness model is created by a series of computer graphic processing methods. Thus, it is of great importance to investigate the basics of topology and quaternions in 3D modeling.

1. Model topology

Generally, model topology refers to the spatial relationship between various entities of the model in computer graphics. This study adopts the model topology elements under RobotStudio™ framework. Figure 6.1 shows the relationship of its topology elements, which is based on the definition of the boundary representation of a 3D ACIS Modeler (ACIS). These elements are implemented in ACIS using the C++ classes Part, Body, Shell, Face, Loop, Wire, Coedge, Edge and Vertex. Each of these classes is derived from the Entity class. In order to better understand this relationship, Figure 6.2 illustrates an example of the topology on a 3D geometry. The specific definition and inheritance relation of each class are described as follows.

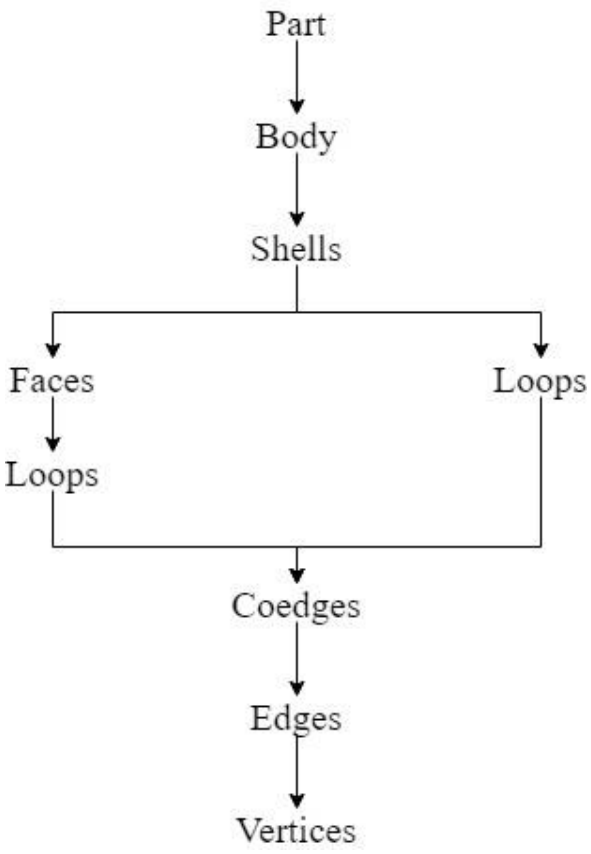

Figure 0.1 Model topology.

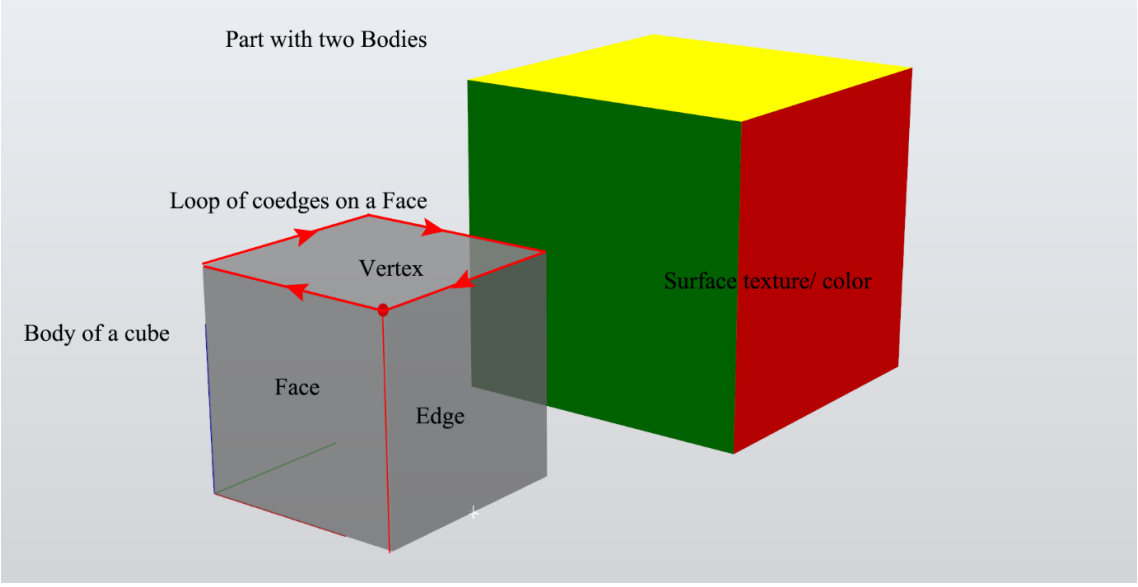

Figure 0.2 Schematic diagram of model topology.

A Part is a container for bodies and can hold zero or more bodies. It also contains an orientation. Several bodies can be composited into one body via the Boolean algorithm (such

as intersect, subtract and union).

A Body is a shape + its pose, which is typically a single 3D solid or a 2D surface, but it can also be several disjoint lumps treated as one body. It is the highest-level object in the geometric model. Bodies consist of one or several shells.

A Shell is a set of connected Faces and Wires. It is normally the outside of a solid Body, but it can also be the inside of a hollow Body.

A Face is a bounded portion of a single geometric surface, which refers the two-dimensional analog of a Body. The boundary is represented by one or more Loops or Edges. Each Face is simply connected, implying that one can traverse from any point on the interior of the Face to any other point on the interior of the Face without crossing the boundary of the Face. In general, it is not meaningful to distinguish exterior and interior Loops of Edges, though for certain surface types this may be possible and some algorithms may do so.

A Loop is a set of connected Coedges. Normally it has no start or end points.

A wire is a collection of Edges that are connected to each other, without being attached to a Face. Wires may represent abstract items, such as profiles, construction lines and center lines, or idealizations of rod or beam-like objects or internal passages. They are also commonly used to form wire frames to form solid-bounding Shells.

A Coedge is closely related to an edge. A Coedge stores its relationships with adjacent edges and with superior owning entities. (In some contexts, the Coedge may be viewed as the use of an edge by a Face or Wire.) The data structures formed by these relationships (stored as pointers) and their interpretation depend upon the nature of the owning entity. A Coedge can be accessed through a Wire or a Loop in a Face, which is based on the model geometry.

An Edge is bounded by one or more vertices, referring to one Vertex at each end. Edges are closely related to Coedges, which allows the Edge to occur in more than one Face, thus makes it possible to create solids.

A Vertex refers to a point in object space, and is the corner of either a Face or a Wire.

In addition, the appearance of a surface can be specified in the 3D graphics. As shown in Figure 6.2, special texture image or color can be applied to surfaces in the 3D view.

2. 3D geometric transformations

In computer graphics, Transformations are fundamental to working with 3D scenes. 3D geometric transformation mainly involves translation, rotation and scaling. Generally, 4×4 homogenous matrices H are widely used to describe the 3D geometric transformation. Its form is as follows:

$$H = \begin{bmatrix} a_{11} & a_{12} & a_{13} & \vdots & b_{14} \\ a_{21} & a_{22} & a_{23} & \vdots & b_{24} \\ a_{31} & a_{32} & a_{33} & \vdots & b_{34} \\ \cdots & \cdots & \cdots & \cdots & \cdots \\ c_{41} & c_{42} & c_{43} & \vdots & d_{44} \end{bmatrix} = \begin{bmatrix} A & \vdots & B \\ \cdots & \cdots & \cdots \\ C & \vdots & D \end{bmatrix} \qquad \text{Eq.6-1}$$

where [A] is for scaling, rotation transformations, [B] is for translation transformation, [C] is for projection transformation, and [D] is for overall scaling transformation. Here, we shall discuss translation, rotation, and scaling only.

- Translation

As described by the linear transformation theory, a position P= (x, y, z) in 3D space can be translated to a location P'= (x', y', z') by adding a translation vector T= (tx, ty, tz) (As shown in Figure 6.3 and described by Eq.6-2).

$$P' = T \cdot P = \begin{bmatrix} x' \\ y' \\ z' \\ 1 \end{bmatrix} = \begin{bmatrix} 1 & 0 & 0 & t_x \\ 0 & 1 & 0 & t_y \\ 0 & 0 & 1 & t_z \\ 0 & 0 & 0 & 1 \end{bmatrix} \cdot \begin{bmatrix} x \\ y \\ z \\ 1 \end{bmatrix} \qquad \text{Eq.6-2}$$

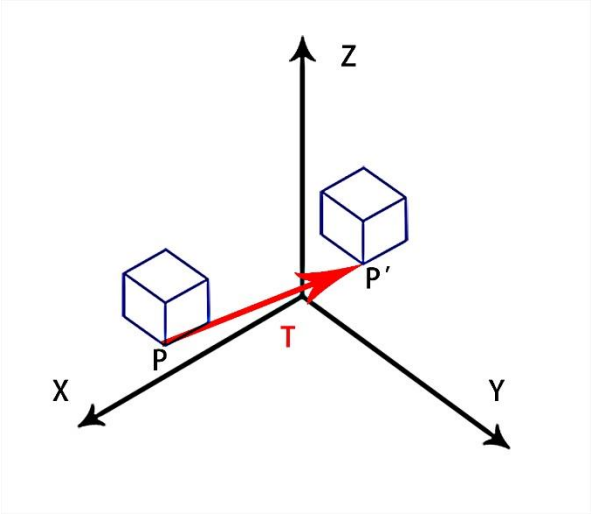

Figure 0.3 Shifting the position of a three-dimensional object using translation vector T.

- Rotation

As shown in Figure 6.4, an object in space can either rotate about the x-axis, the y-axis or the z-axis. When rotating about the z-axis, only coordinates of x and y will change and the z-coordinate will be the same. In effect, it is exactly a rotation about the origin in the xy-plane. Therefore, the relationship in which P is rotated with an angle α around the z-axis to become P'zz (Eq.6-3) can be described as follows:

$$p'_{zz} = Rz \cdot P = \begin{bmatrix} x' \\ y' \\ z' \\ 1 \end{bmatrix} = \begin{bmatrix} \cos\alpha & -\sin\alpha & 0 & 0 \\ \sin\alpha & \cos\alpha & 0 & 0 \\ 0 & 0 & 1 & 0 \\ 0 & 0 & 0 & 1 \end{bmatrix} \cdot \begin{bmatrix} x \\ y \\ z \\ 1 \end{bmatrix} \qquad \text{Eq.6-3}$$

Based on the same idea, rotating with an angle α around the x-axis and y-axis are the following respectively (Eq.6-4 and Eq.6-5):

$$p'_{xx} = Rx \cdot P = \begin{bmatrix} x' \\ y' \\ z' \\ 1 \end{bmatrix} = \begin{bmatrix} 1 & 0 & 0 & 0 \\ 0 & \cos\alpha & -\sin\alpha & 0 \\ 0 & \sin\alpha & \cos\alpha & 0 \\ 0 & 0 & 0 & 1 \end{bmatrix} \cdot \begin{bmatrix} x \\ y \\ z \\ 1 \end{bmatrix} \qquad \text{Eq.6-4}$$

$$p'_{yy} = Ry \cdot P = \begin{bmatrix} x' \\ y' \\ z' \\ 1 \end{bmatrix} = \begin{bmatrix} \cos\alpha & 0 & \sin\alpha & 0 \\ 0 & 1 & 0 & 0 \\ -\sin\alpha & 0 & \cos\alpha & 0 \\ 0 & 0 & 0 & 1 \end{bmatrix} \cdot \begin{bmatrix} x \\ y \\ z \\ 1 \end{bmatrix} \qquad \text{Eq.6-5}$$

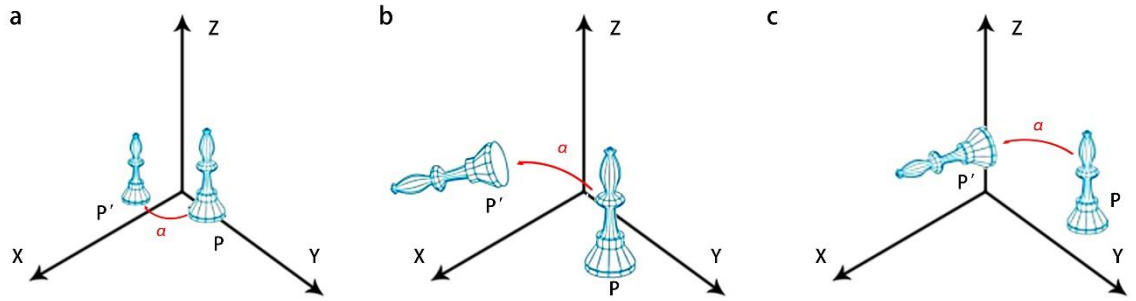

Figure 0.4 (a) Rotation of an object around the z axis; (b) Rotation of an object around the x axis; (c) Rotation of an object around the y axis.

- Scaling

In computer graphics, an object can change its size by using scaling transformation. In the scaling process, the dimensions of the object can either expand or compress. Scaling can be achieved by multiplying the original coordinates of the object with the scaling factor to get the desired result, and the positive or negative scale factors represent enlargement or shrinking of the object, respectively. Figure 6.5 shows the effect of 3D scaling. The matrix expression for the scaling transformation of a position P = (x, y, z) relative to coordinate origin can be written as follows (Eq 6-6):

$$p' = S \cdot P = \begin{bmatrix} x' \\ y' \\ z' \\ 1 \end{bmatrix} = \begin{bmatrix} s_x \cdot x \\ s_y \cdot y \\ s_z \cdot z \\ 1 \end{bmatrix} = \begin{bmatrix} s_x & 0 & 0 & 0 \\ 0 & s_y & 0 & 0 \\ 0 & 0 & s_z & 0 \\ 0 & 0 & 0 & 1 \end{bmatrix} \begin{bmatrix} x \\ y \\ z \\ 1 \end{bmatrix} \quad \text{Eq.6-6}$$

where the sx, sy, sz are the scale factors in each direction.

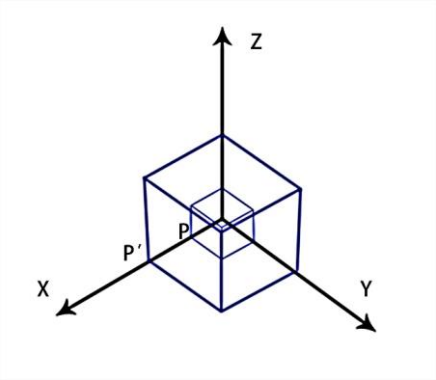

Figure 0.5 Scaling objects relative to the original point.

Generally, an object requires to scale relative to a selected fixed point (xf, yf, zf). In this case, the object should be moved to the original point before being scaled and returned to the previous position after scaling (as shown in Figure 6.6). So, the linear transformation of displacement T should also be multiplied in order to scale the object according to the selected fixed point as presented in Eq 6-7.

$$p' = T \cdot S \cdot T \cdot P = \begin{bmatrix} 1 & 0 & 0 & x_f \\ 0 & 1 & 0 & y_f \\ 0 & 0 & 1 & z_f \\ 0 & 0 & 0 & 1 \end{bmatrix} \begin{bmatrix} s_x & 0 & 0 & 0 \\ 0 & s_y & 0 & 0 \\ 0 & 0 & s_z & 0 \\ 0 & 0 & 0 & 1 \end{bmatrix} \begin{bmatrix} 1 & 0 & 0 & -x_f \\ 0 & 1 & 0 & -y_f \\ 0 & 0 & 1 & -z_f \\ 0 & 0 & 0 & 1 \end{bmatrix} \begin{bmatrix} x \\ y \\ z \\ 1 \end{bmatrix} \quad \text{Eq.6-7}$$

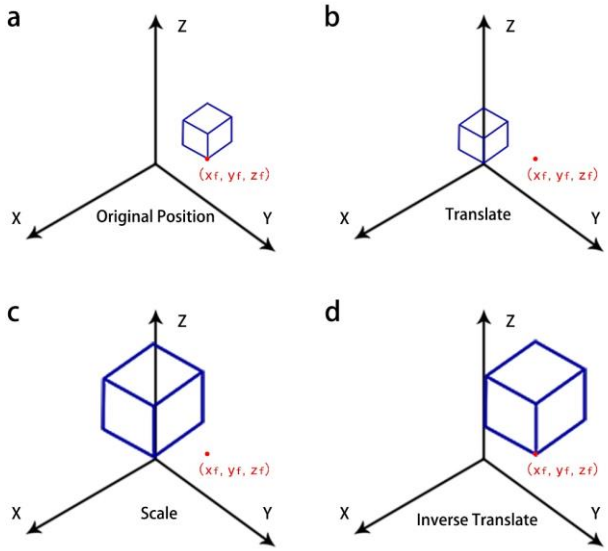

Figure 0.6 Scaling objects relative to a selected fixed point (xf, yf, zf).

Titre : Modélisation et Planification de Processus pour la Fabrication Additive Basé Robotique-Projection à Froid

Mots clés : La fabrication additive à froid ; robot; cadre modulaire; stratégie de projection; simulation de processus; programmation hors ligne.

Résumé : La projection à froid (Cold spray, CS) est une technologie de dépôt de revêtement à l'état solide qui a récemment été appliquée comme processus de fabrication additive (Additive manufacturing, AM) pour fabriquer des composants individuels. Ce procédé potentiel attire de plus en plus de l'attention en raison de ses avantages : efficacité de formage élevée, basse température de travail et absence de changement de phase des matériaux. Ces avantages peuvent permettre à la projection à froid de former des objets de grand volume pour devenir un procédé de fabrication additive efficace. De nos jours, de nouvelles avancées dans la fabrication additive à froid (Cold spray additive manufacturing, CSAM) nécessitent de nouvelles implémentations de processus pour améliorer la précision et la flexibilité de fabrication. Par conséquent, le but de cette étude est d'améliorer la méthode additive utilisant la projection à froid grâce à la modélisation et à la planification du processus robotique CS. Le travail de cette thèse se compose en trois parties.

Premièrement, des efforts ont été consacrés à la conception et à la mise en œuvre d'un nouveau cadre pour la technique CSAM. Dans cette partie, un concept de système modulaire est présenté. Ici, le système CSAM actuel est décomposé en différents modules afin de comprendre les relations physiques et fonctionnelles entre les éléments clés de l'ensemble du système. Cette modularité physique et fonctionnelle est une nécessité indispensable pour promouvoir les processus AM hybrides. De nouveaux modules, tels que le module de mesure in-situ, le module inter-processus peuvent être intégrés pour offrir plus de possibilités au processus CS conventionnel. Il est révélé que la modularité du système est adaptée pour révolutionner la méthode et technique CSAM. On peut voir que pour exploiter pleinement le potentiel de cette approche, des efforts sont encore nécessaires pour intégrer et coordonner davantage de technologies à l'aide du cadre modulaire proposé.

Deuxièmement, une nouvelle approche est présentée pour simuler le dépôt. Ici, un modèle géométrique tridimensionnel du profil de revêtement basé sur la distribution gaussienne est développé. Le modèle est combiné avec la trajectoire du robot et les paramètres de traitement pour simuler l'évolution des dépôts. En outre, il peut offrir une prédiction précise du profil dans la plate-forme de programmation hors ligne du robot, en particulier dans le cas des effets d'ombre, ce qui permet l'intégration de la programmation du robot avec la simulation pour mieux contrôler le processus de revêtement. Les résultats des vérifications numériques et expérimentales montrent que cette méthode proposée a une bonne précision de prédiction.

Enfin, par rapport à la stratégie actuelle de formation de volume basée sur le volume (par exemple, une méthode basée sur la tessellation), cette étude propose une nouvelle stratégie qui prend en compte les caractéristiques et les paramètres cinématiques de la projection à froid pour améliorer la construction de couches stables pour l'obtention de forme 3D. La simulation et les expériences sont menées pour la vérification de la méthode. Les essais comparatives créés par couches ont une meilleure précision de forme que celle des méthodes existantes. Cela implique que la méthode proposée fait de la projection à froid un processus additif efficace pour la création additive de formes 3D.

Title: Process Modeling and Planning for Robotic Cold spray based Additive Manufacturing

Keywords: Cold spray additive manufacturing; robot; modular framework; spray strategy; process simulation; offline programming.

Abstract: Cold spray (CS) is a solid-state coating deposition technology that has recently been applied an additive manufacturing (AM) process to fabricate individual components. This potential AM process is attracting more and more attention because of its advantages: high-forming efficiency, low temperature, and no phase changing of materials. These advantages make CS able to form large-volume objects to become an efficient and effective AM process. Nowadays, new advances in cold spray additive manufacturing (CSAM) call for new process implementation to improve the manufacturing accuracy and flexibility. Therefore, the purpose of this study is to enhance CS-based AM through the modeling and planning of the robotic CS process. The work of this thesis consists of three parts.

Firstly, efforts have been dedicated to design and implement a new framework for CSAM. In this part, a concept of modular system is presented. Here, the current CSAM system is decomposed into different modules in order to understand the physical and functional relationships in between the key elements of the entire system. This physical and functional modularity is an indispensable necessity to promote hybrid AM processes. New modules, such as in-situ measurement module, inter-process module can be integrated into the framework to bring more possibilities to the conventional CS process. It is revealed that system modularity is suitable to revolutionize the CSAM method and conduction. To fully exert the potential of CSAM, efforts are still required to integrate and coordinate more technologies with the help of the proposed modular framework.

Secondly, a novel approach is presented to simulate the CS deposition. Here, a three-dimensional geometric model of the coating profile based on Gaussian distribution is developed. The model is combined with robot trajectory and processing parameters to simulate the evolving CS deposits. In addition, it can offer accurate profile prediction in the robot off-line programming platform, especially in case of shadow effects, which enables the integration of robot programming with simulation to better control the coating process. The results of both numerical and experimental verifications show that this proposed method has a good prediction accuracy for practice.

At last, compared with the current bulk-based volume-forming strategy (e.g. a tessellation-based method), this study proposes a new spray strategy that considers the characteristics and kinematic parameters of cold spray to enhance stable layer building for 3D shape forming. Both simulation and experiments are conducted for method verification. Layer built benchmarking test objects have better shape accuracy than that of existing methods. This implies that the proposed method makes CS a real and layer-by-layer ready AM process for 3D shape forming.

Université Bourgogne Franche-Comté
32, avenue de l'Observatoire
25000 Besançon